LIPID ALTERATIONS IN EXCITOTOXIC BRAIN INJURY

HE XIN

(MSc)

Supervisor: Associate Professor Ong Wei Yi

A THESIS SUBMITTED FOR THE DEGREE OF

DOCTOR OF PHILOSOPHY

DEPARTMENT OF ANATOMY

YONG LOO LIN SCHOOL OF MEDICINE

NATIONAL UNIVERSITY OF SINGAPORE

2006

ACKNOWLEDGMENTS

I wish to express my deepest appreciation and heartfelt thanks to my supervisor, **Associate Professor Ong Wei Yi**, Department of Anatomy, National University of Singapore, for suggesting this study topic, and for his constant and patient guidance and encouragement throughout the course of the study. He has not only introduced me to an entirely new basic research field but also has been a role model for hardwork and commitment to research. His deep and sustained interest, immense patience and stimulating discussions have been most invaluable in the accomplishment of this thesis.

I am very grateful to **Professor Ling Eng Ang**, Head, Department of Anatomy, National University of Singapore, for his constant encouragement, kindness and unfailing support to execute this research. I am greatly indebted to **Assistant Professor Andrew M. Jenner**, Department of Biochemistry, National University of Singapore, for strong guidance in cholesterol and oxysterol analysis, and all-round expertise and opinions helped me through many problems. My deep indebtedness goes to **Assistant Professor Markus R. Wenk**, Department of Biochemistry, National University of Singapore, for his invaluable suggestions and friendly help during this study. I thank **Ranbaxy Malaysia Sdn Bhd** for generous supply of lovastatin, and **Professor David W. Russell**, Department of Molecular Genetics, University of Texas Southwestern Medical Center, USA, for

generous gift of cholesterol 24-hydroxylase antibody and helpful comments on the manuscript.

I must also acknowledge my gratitude to **Mrs Ng Geok Lan** and **Mrs Yong Eng Siang** for their excellent technical assistance; **Miss Chan Yee Gek** and **Mdm Wu Ya Jun** for Electron Microscopy work; **Mr Yick Tuck Yong** for his constant assistance in computer work; **Mr Lim Beng Hock** for looking after the experimental animals; **Mdm Ang Lye Gek Carolyne** and **Mdm Teo Li Ching Violet** for their secretarial assistance.

I sincerely thank my co-worker **Miss Guan Xue Li**, Department of Biochemistry, National University of Singapore, for her invaluable help in sphingolipid analysis. I would like to thank all other staff members and my fellow honous and postgraduate students at Department of Anatomy who help me in one-way or another.

A major credit also goes to my parents, my brother and my husband, **Mr. Li Quan Sheng,** for their full and endless support for my study.

Last , but not least, my many thanks are due to the National University of Singapore for supporting me with a Research Scholarship to bring this study to reality.

This thesis is dedicated to

my beloved family

TABLE OF CONTENTS

ACKNOWLEDGEMENTS …….. I

TABLE OF CONTENTS…….. IV

PUBLICATIONS…….. XI

ABBREVIATIONS……..XIII

SUMMARY…….. XVII

CHAPTER I INTRODUCTION …….. 1

1. General introduction.....2

2. Cell lipids……..…….. 3

2. 1. Phospholipids…….. 3

2. 1. 1. Structure and functions.....3

2. 1 .2. Phospholipids in the brain.....4

2. 1. 3 Phospholipids in neurological disorders.....7

2. 2. Cholesterol……..……..……..…….....9

2. 2. 1. Distribution and functions…….....9

2. 2. 2. Cholesterol in the brain.....12

2. 2. 2. 1. Cholesterol synthesis and elimination in the brain.....12

2. 2. 2. 2. Cholesterol binding/transport proteins in the brain.....15

2. 2. 2. 3. Apolipoprotein D.....17

2. 2 .3. Cholesterol in neurological disorders.....20

2. 3. Ceramide.....22

2. 3. 1. Structure and functions.....22

2. 3. 2. Ceramide generation and metabolism.....24

2. 3. 3. Ceramide in the brain.....27

2. 3. 4. Ceramide in neurological disorders.....29

3. Kainate-induced excitotoxic neuronal injury …….....31

4. Aims of the present study ……..……...……..…….... 34

4. 1. Dysregulation of cholesterol metabolism after kainate injury.....35

4. 2. Dysregulation of ceramide metabolism after kainate injury.....35

4. 3. Effect of apolipoprotein D on the neuronal injury after kainate injury.....36

CHAPTER II EXPRIMENTAL STUDIES ……..38

I. Lovastatin modulates increased cholesterol and oxysterol levels and has a neuroprotective effect on rat hippocampal neurons after kainate injury..39

1. Introduction ……...……..……..40

2. Materials and methods ……..……..……..... 41

2. 1. Animals and intracerebroventricular kainate injection 41

2. 2. Western blots.....……...……...……..…….....42

2. 3. Immunohistochemical analyses...….....43

2. 3. 1. Immunoperoxidase labeling..... 43

2. 3. 2. Quantitation of labeled cells.....44

2. 3. 3. Electron microscopy.....45

2. 3. 4. Double immunofluorescence labeling.....45

2. 4. Hippocampal slice cultures ……..…..... 46

2. 5. Gas chromatographic/mass spectrometric (GC/MS) analysis.....47
2. 5. 1. Kainate and lovastatin treatment.....47
2. 5. 2. Lipid extraction.....49
2. 5. 3. Lipid hydrolysis.....49
2. 5. 4. Cholesterol and oxysterol extraction.....49
2. 5. 5. GC/MS measurement.....50
2. 5. 6. Cholesterol analysis.....51
2. 5. 7. Oxysterol analysis.....51
2. 6. *In vivo* effect of lovastatin on neuronal survival after kainate injury.....52
2. 7. *In vitro* effect of lovastatin on neuronal survival after kainate injury.....53
2. 8. *In vitro* effect of oxysterols on neuronal survival.....54
2. 9. Statistical analysis.....54
3. Results.....55
3. 1. Western blot analysis.....55
3. 2. Immunohistochemical analyses of cholesterol 24-hydroxylase after kainate lesions.....55
3. 2. 1. Light microscopy.....55
3. 2. 2. Electron microscopy.....57
3. 2. 3. Double immunofluorescence labeling.....58
3. 3. GC/MS analysis of cholesterol and oxysterols in the kainate-injected rat hippocampus.....58
3. 4. Effect of lovastatin on cholesterol and oxysterol concentrations after kainate injury.....59

3. 4. 1. *In vivo* analyses.....59

3. 4. 2. *In vitro* analyses.....60

3. 5. Effect of lovastatin on neuronal survival after kainate injury.....60

3. 5. 1. *In vivo* analyses.....60

3. 5. 2. *In vitro* analyses.....61

3. 6. Effect of 24-hydroxycholesterol on neuronal injury.....61

4. Discussion.....62

II. Expression, activity, and role of serine palmitoyltransferase in the rat hippocampus after kainate injury.....68

1. Introduction.....69

2. Materials and methods.....70

2. 1. Animals and intracerebroventricular kainate injection.....71

2. 2. SPT expression by Western blot analyses.....71

2. 3. SPT activity assay.....71

2. 4. SPT immunohistochemistry.....72

2. 4. 1. Immunoperoxidase labeling.....72

2. 4. 2. Double immunofluorescence labeling.....73

2. 4. 3. Electron microscopy.....74

2. 5. Hippocampal slice cultures.....74

2. 6. Electrospray ionization mass spectrometry (ESI-MS).....74

2. 7. Quantitation of cellular injury by microtubule associated protein (MAP2) immunolabeling.....75

2. 8. Quantitation of cellular injury by lactate dehydrogenase (LDH) assay..76
3. Results.....77
3. 1. SPT expression by Western blot analyses.....77
3. 2. SPT activity assay.....77
3. 3. SPT immunohistochemistry.....77
3. 3. 1. Immunoperoxidase labeling.....77
3. 3. 2. Double immunofluorescence labeling.....79
3. 3. 3. Electron microscopy.....79
3. 4. Role of SPT in kainate injury.....79
3. 4. 1. Effect on ceramide and sphingomyelin concentrations.....79
3. 4. 2. Effect on MAP2 immunolabeling.....80
3. 4. 3. Effect on LDH release.....80
4. Discussion.....80

III. Effect of apolipoprotein D on neuronal survival, cholesterol and Lipid oxidation product formation after kainate-induced neuronal injury.....**85**
1. Introduction.....86
2. Materials and methods.....87
2. 1. Hippocampal slice cultures.....87
2. 2. Quantitation of cellular injury by MAP2 immunolabeling.....88
2. 3. Quantitation of cellular injury by LDH assay.....88
2. 4. GC/MS analysis.....88
2. 4. 1. Chemicals.....88

2. 4. 2. Lipid extraction.....89

2. 4. 3. Lipid hydrolysis.....89

2. 4. 4. Mixed anion exchange solid phase extraction.....89

2. 4. 5. Derivatization.....90

2. 4. 6. GC/MS analysis of cholesterol and oxysterols.....91

2. 4. 7. GC/MS analysis of F_2-isoprostanes.....91

2. 5. Statistical analysis.....92

3. Results.....92

3. 1. Effect of apoD on kainate-induced injury.....92

3. 2. Effect of apoD on F_2-isoprostanes, cholesterol, and oxysterol levels in cultured hippocampal slices.....93

3. 3. Effect of apoD on F_2-isoprostanes, cholesterol and oxysterol levels in cultured fibroblasts after hydrogen peroxide treatment.....93

4. Discussion.....94

CHAPTER III CONCLUSION.....98

CHAPTER IV REFERENCES.....104

CHAPTER V TABLE, TABLE CAPTION, FIGURES AND FIGURE LEGENDS.....134

PUBLICATIONS

Various portions of the present study have been published or submitted for publication.

International Refereed Journals

1. He X, Jenner AM, Ong WY, Farooqui AA, Patel SC (2006) Lovastatin Modulates Increased Cholesterol and Oxysterol Levels and Has a Neuroprotective Effect on Rat Hippocampal Neurons After Kainate Injury. J Neuropathol Exp Neurol 5:652-663

2. He X, Guan XL, Ong WY, Farooqui AA, Wenk MR (2007) Increased expression of serine palmitoyltransferase, and role of ceramide biosynthetic activity in neuronal degeneration after kainate treatment. J Neuro Res 85:423-432

3. Guan XL, He X, Ong WY, Yeo WK, Shui G, Wenk MR (2006) Non-targeted profiling of lipids during kainate-induced neuronal injury. FASEB J 20:1152-1161 (GXL and HX contributed equally)

ABBREVIATIONS

ABC	avidin-biotin complex
Acetyl- CoA	acetyl-coenzyme A
ACAT	acyl-coenzyme A: cholesterol acyltransferase
AD	Alzheimer's disease
ALS	amyotrophic lateral sclerosis
AP	alkaline phosphatase
ApoA-I	apolipoprotein A
ApoA-IV	apolipoprotein A-IV
ApoD	apolipoprotein D
ApoE	apolipoprotein E
ApoER2	apolipoprotein E receptor 2
ApoJ	apolipoprotein J
Aβ	amyloid β-peptide
ATP	adenosine triphosphate
BACE1	β-site APP cleaving enzyme 1
BBB	blood brain barrier
B-BFAP	brain fatty acid binding protein
BHT	butylated hydroxytoluene
BLG	beta-lactoglobulin
BSTFA	N,O-bis(trimethylsilyl)trifluoroacetamide
CA	cornu amonis
CA1	hippocampal cornu amonis area 1

CA3	hippocampal cornu amonis area 3
Cer	ceramide
Chol	cholesterol
CNS	central nervous system
DAB	3, 3'-diaminobenzidine tetrahydrochloride
DIPEA	N,N-diisopropylethylamine
DNA	deoxyribonucleic acid
EM	electron microscope
ESI/MS	electrospray ionization mass spectrometry
ER	endoplasmic reticulum
FA	Fatty acid
FAN	factor associated with NSmase activation
GC/MS	Gas chromatography/mass spectrometry
GFAP	glial fibrillary acidic protein
GluRs	glutamate receptors
H_2O_2	hydrogen peroxide
HCl	hydrochloric acid
HD	Huntington's disease
HDL	high density lipoprotein
H-FABP	heart fatty acid binding protei
HMG-CoA	3-hydroxy-3-methylglutaryl coenzyme A
HNE	hydroxynonenal
HRP	horseradish peroxidase

IHC	immunohistochemistry
JNK	jun kinase
KA	kainic acid
kDa	kilodalton
LCAT	lecithin cholesterol acyltransferase
LDH	lactate dehydrogenase
LDL	low-density lipoprotein
LDL-R	low-density lipoprotein receptor
LPA	lysophospholipases
LRP	low density lipoprotein receptor-related protein
MAX	Mixed Anion Exchange
MW	molecular weight
NGF	nerve growth factor
NPC	Niemann–Pick disease type C
PAGE	polyacrylamide gels
PBS	phosphate buffered saline
PBS-Tx	phosphate buffered saline containing 0.1% Triton X
PC	phosphatidylcholine
PD	Parkinson's disease
PE	phosphatidylethanolamine
PFBBr	pentafluorobenzylbromide
PG	glycerol glycerophospholipid
PI	phosphoinositide

PKC	protein kinase C
PLA	phospholipase
PP	phospholipid
PS	phosphatidylserine
PVDF	polyvinylidene difluoride
RER	rough endoplasmic reticulum
RNA	ribonucleic acid
SCP-2	sterol carrier protein-2
SCP-X	sterol carrier protein-X
SDS	sodium dodecyl sulfate
SER	smooth endoplasmic reticulum
SK	sphingosine kinase
Sph	sphingosine
SMase	sphingomyelinase
SPT	serine palmitoyltransferase
S1P	sphingosine 1-phosphate
TBS	Tris buffered saline
TCR	T cell receptor
TEM	transmission electron microscope
TEMED	N,N,N,N -tetramethyl-ethylenediamine
TMCS	trimethylchlorosilane
VLDL	very low-density lipoprotein
VLDL-R	very low-density lipoprotein receptor

SUMMARY

Lipids are necessary components of all cell membranes and are important both as structural elements and as modulators of cell fluidity. Several lipid molecular species are present in cells, including various types of phospholipids, cholesterols and sphingolipids. Lipids are especially important in the central nervous system (CNS). Homeostasis of membrane lipids in neurons and myelin is essential to prevent the loss of synaptic plasticity, cell death and neurodegeneration. Because membrane lipids are so important as structural components in the CNS, changes in brain lipid levels due to their increased or decreased synthesis or metabolism may result in homeostatic dysregulation and ultimately neurodegeneration. This is important because neurodegeneration is a characteristic component of all dementias. Inhibition of dysregulated lipid metabolism may confer neuroprotection. This study used a kainate-induced neurodegenerative model and suggests that dysregulation of two important membrane lipids, cholesterol and ceramide, may lead to or accelerate neurodegeneration and therefore may be important in the pathogenesis of neurodegenerative diseases. The results also indicate the neuroprotective effect of a lipid binding protein, apolipoprotein D (apoD).

The first part of the present study was carried out to elucidate alterations in metabolism of cholesterol, a key lipid component of the cell membrane, after neuronal injury induced by the excitotoxin, kainate. Increased immunolabeling of the oxysterol biosynthetic enzyme, cholesterol 24-hydroxylase, was observed in

the rat hippocampus after kainate lesions. This was accompanied by increased levels of cholesterol, 24-hydroxycholesterol (product of cholesterol 24-hydroxylase enzymatic activity) and 7-ketocholesterol in homogenates of the degenerating hippocampus, as detected by gas chromatography / mass spectrometry (GC/MS). Hippocampi from rats or organotypic slices that had been treated with kainate plus lovastatin showed significantly lower levels of cholesterol, 24-hydroxycholesterol, and 7-ketocholesterol, compared to those treated with kainate only. Lovastatin also modulated hippocampal neuronal loss after kainate treatment, *in vivo* and *in vitro*. The level of 24-hydroxycholesterol detected *in vivo* after kainate treatment (> 50 μM) was found to be neurotoxic in hippocampal slice cultures. The above results suggest that increased brain cholesterol biosynthesis and oxysterol formation play a role in propagation of neuronal death after kainate injury and brain permeable statins such as lovastatin could have a neuroprotective effect by limiting the levels of oxysterols in brain areas undergoing neurodegeneration.

The second part of the study focused on changes in metabolism of ceramide, another major lipid component of the cell membrane, after kainate-induced neuronal injury. Ceramide is involved in many cellular events including apoptosis, growth arrest, differentiation, senescence, mediating an immune response, oxidative stress responses, and nitric oxide signaling. An increase in ceramide species has recently been demonstrated by lipidomic analysis of the rat hippocampus after kainate-induced excitotoxic injury. In addition, increased expression of serine palmitoyltransferase (SPT), the first enzyme in the ceramide

biosynthetic pathway was observed in reactive astrocytes of the hippocampus after kainate injections. The increase in enzyme expression was paralleled by increased SPT enzyme activity in the hippocampus at two week post-kainate injection. *In vitro* studies showed that treatment of hippocampal slice cultures with SPT inhibitor ISP-1 (myriocin) or L-cycloserine modulated increases in 16:0, 18:0 and 20:0 ceramide species and partially reduced kainate-induced cell death. The above findings indicate a role of SPT in ceramide increase after kainate injury. They also suggest that increased SPT activity and biosynthetic ceramide might contribute to neuronal injury after kainate excitotoxicity.

The third part of this study was carried out to examine potential effects of a lipid binding protein, apoD on neuronal survival after kainate injury. ApoD belongs to the lipocalin superfamily of transporter proteins that carry various small hydrophobic ligands, such as arachidonic acid and cholesterol. A marked increase of apoD has been shown in the rat hippocampus after neuronal injury induced by kainate. Addition of purified human apoD to kainate treated hippocampal slice cultures resulted in reduction in neuronal death, and modulation of increased arachidonic oxidation product (F_2-isoprostane), cholesterol, and cholesterol oxidation product (24-hydroxycholesterol and 7-ketocholesterol) levels in the kainate treated slices. The results showed that the neuroprotective effect of apoD may be due to its ability to bind arachidonic acid, thus resulting in reduction of lipid peroxidation products, and its ability to prevent the formation of neurotoxic cholesterol oxidation products by regulating the cholesterol metabolism. Fibroblasts from apoD knockout mice showed increased

F_2-isoprostane and 7-ketocholesterol levels after hydrogen peroxide induced oxidative stress, suggesting that this lipocalin may be an important antioxidant protein in the brain.

Taken together, the above findings indicate that deleterious changes in lipid homeostasis and signaling may be a key factor in the onset and progression of pathologies of the brain. They also provide clues to the development of pharmaceutical strategies to treat neurodegenerative disorders by regulating the lipid metabolism, in which cholesterol and ceramide metabolic enzyme, and apoD may play important roles.

CHAPTER I

INTRODUCTION

1. General introduction

Lipids are important for the brain, as it contains the second highest concentration of lipids exceeded only by adipose tissue (Adibhatla et al. 2006). Besides this quantitative importance, lipids in the brain show bewildering diversity (Wenk 2005). A large number of proteins are associated with synaptic membranes. In addition, a number of key enzymes involved in the metabolism of lipids have been discovered and characterized in nerve terminals (Cremona and De Camilli 2001).

The majority of cellular lipids are organized in membranes (van Meer 2001). This is a fluid patchwork of lipid and protein molecules in constant motion. Carbohydrates attached to the proteins and phospholipids form glycoproteins and glycolipids (Alberts et al. 1994). The most abundant membrane lipids are the phospholipids (PPs). In addition, sphingolipids form a static, solid membrane, which is fluidized by cholesterol (reviewed in Fahy et al. 2005).

Functional responses of ion channels, synaptic function and cellular signaling cascades may be affected by the lipid composition of the cell membrane. It has been suggested that neuronal cell function can be modified to meet physiologic demand through appropriate alterations in the type, nature and organization of lipids in specific cell membrane compartments (reviewed in Gross et al. 2005).

Deleterious changes in lipid homeostasis are viewed as important factors in the pathogenesis of many neurological disorders such as Alzheimer's disease (AD) (Cutler et al. 2004b), Parkinson's disease (PD) (Sharon et al. 2003),

Niemann–Pick disease type C disease (NPC) (Sturley et al. 2004), and cerebral ischemic injury (Farooqui et al. 2004; Rao et al. 2000; Nakane et al 2000).

2. Cell lipids

2. 1. Phospholipids

2. 1. 1. Structure and functions

Phospholipids are composed of a glycerol (3 carbon chain) backbone with fatty acids esterified at the *sn*-1 and *sn*-2 positions (Fig. 1). The fatty acids can vary in length from 14 to 22 carbons and can have from 0 to 6 double bonds (Schiller et al. 2004). The *sn*-3 position has a phosphate group attached to a polar head group (Fig. 1). The amphiphilic nature of phospholipids, owing to the polar head group and non-polar fatty acid tails, causes them to come together as a bilayer (reviewed in Peterson and Cummings 2006). There are several groups of phospholipids based on the polar head group: choline glycerophospholipids (PC), ethanolamine glycerophospholipids (PE), inositol glycerophospholipids (PI), glycerol glycerophospholipids (PG) or serine glycerophospholipids (PS) (Paltauf 1994; Farooqui et al. 2000a). The cell membrane has an asymmetrical distribution of phospholipids. The outer leaflet is mainly composed of PC while PE and PS are the primary phospholipids found in the inner cytosolic membrane (Bevers et al.1998). Besides the above glycerophospholipids, membranes also contain plasmalogens (PlsC and PlsE), which are glycerophospholipids of neural membranes containing vinyl ether bonds (Farooqui and Horrocks 2001).

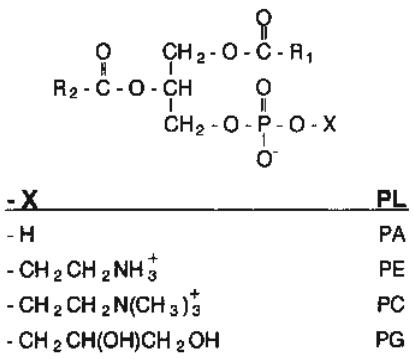

Figure 1. Basic structure of phospholipids. Consists of a glycerol backbone with fatty acids (R1 and R2) linked at the *sn*-1 and *sn*-2 positions. Various polar head groups (X) link to the phosphate group at the *sn*-3 position (Peterson and Cummings 2006).

Phospholipid bilayer membranes are highly structured, dynamic and penetrated to varying degree by receptors, enzymes, and ion channels. The latter protrude differentially through the membrane or localize predominantly on the intracellular or extracellular membrane surface. The changes in phospholipid metabolism can regulate activities of membrane-bound enzymes, receptors, and ion channels (Farooqui and Horrocks 1985). Different pools of phospholipid molecular species may have different metabolic and physical properties depending upon their localization in different types of cell membranes (Farooqui et al. 2004).

2. 1. 2. Phospholipids in the brain

Brain tissue contains relatively high amounts of phospholipids. Together with cholesterol and glycolipids, they represent 50–60% of the total membrane mass of neural membranes (Farooqui et al. 2000b). Human brain neural membranes contain a variety of phospholipids including PC, PE, PlsE, PS, PI, and sphingomyelin (Horrocks et al. 1981). PC, PlsE, and PE are major

phospholipid components of neural membranes in all regions. This is followed by sphingomyelin, which is most enriched in white matter (Söderberg et al. 1990). Among the membranes of the brain, myelin contains the highest content of phospholipids. The phospholipid composition of myelin is similar to that of white matter and very different from that of grey matter (Farooqui et al. 2004).

Neural membrane phospholipids are predominantly synthesized in the endoplasmic reticulum (ER). Significant synthesis of PC and PI also occurs in Golgi membranes (Farooqui et al. 2000a). Following synthesis, phospholipids are transported to membranes by phospholipid transfer-exchange proteins (Voelker et al. 2003). Neural membrane phospholipids are degraded by receptor-mediated hydrolytic process involving phospholipases (PLA), lysophospholipases (LPA), and lipases (Farooqui 2000b).

The polyunsaturated fatty acids at the *sn*-2 position of phospholipids are susceptible to free radical attack at the α-methylene carbon. The lipid hydroperoxides thus formed are not completely stable *in vivo* and, in the presence of iron, can further decompose to radicals that can propagate the chain reactions started by an initial free radical attack. Lipid hydroperoxides also generate aldehydes that can in turn cross-link enzymes and proteins making them inactive (Farooqui et al. 2000a, Halliwell 1994).

The damage to neural membranes induced by lipid peroxidation can result in the following effects: (a) changes in physicochemical properties of neural membranes (microviscosity) resulting in alterations in the orientation of optimal domains for the interaction of functional membrane proteins such as receptors,

enzymes, and ion-channels; (b) changes in the number of receptors and their affinity for neurotransmitters and drugs; and (c) inhibition of ion pumps resulting in changes in ion homeostasis (Farooqui et al. 2000a).

The presence of peroxidized phospholipids in neural membranes may also produce a membrane-packing defect, making the *sn*-2 ester bond more accessible to the action of PLA_2. The hydrolysis of peroxidized phospholipids results in removal of peroxidized fatty acyl chains, which are reduced and re-esterified. Thus, the action of PLA_2 repairs and restores the physiological physicochemical state of neural membranes (Farooqui et al. 2000a). Healthy neural cells contain tight packing of phospholipids in the outer leaflet. The disruption of phospholipid asymmetry leads to looser phospholipid packing in the outer leaflet, thus allowing Ca^{2+} entry. The alteration in Ca^{2+} homeostasis and its short duration may lead to neuronal degeneration by the activation of PLA_2 (Farooqui et al. 2000b).

The activation of PLA_2 releases arachidonic acid from neural membrane phospholipids and sets in motion an uncontrolled ‘‘arachidonic acid cascade’’. That includes the synthesis and accumulation of prostaglandins, leukotrienes, thromboxanes, and 4-hydroxy-2-nonenal (4-HNE), a peroxidized product of arachidonic acid. High concentration of arachidonic acid has a profound adverse effect on the ATP producing capacity of the brain mitochondria. It uncouples oxidative phosphorylation and induces efflux of Ca^{2+} and K^+ from mitochondria (Katsuki and Okuda 1995). 4-HNE impairs the activities of key metabolic enzymes, including Na^+, K^+-ATPase, glucose-6-phosphate dehydrogenase, and

several kinases. It stimulates stress-activated protein kinases such as c-jun amino terminal kinase (JNK) and p38 mitogen-activated protein kinase (Camandola et al. 2000; Tamagno et al. 2003). The arachidonic acid cascade also potentiates the formation of free radicals and lipid hydroperoxides produced by the action of 12-lipoxygenase. The lipid hydroperoxides are known to inhibit reacylation of phospholipids in neuronal membranes (Zaleska and Wilso 1989). This inhibition may contribute to necrotic cell death in neural cells (Farooqui et al. 2000c).

2. 1. 3. Phospholipids in neurological disorders

Loss of phospholipids and increase in phospholipid-degradation products are known to occur in acute brain trauma and neurodegenerative diseases (Farooqui and Horrocks 1994; Pettegrew et al. 1995). Changes in phospholipids and stimulation of phospholipases have been reported in acute brain disorders such as ischemia, hypoxia, hypoglycemia, spinal cord and brain injuries (Farooqui and Horrocks 1991), excitotoxic models of neurodegeneration (Sandhya et al. 1998), and in chronic neurodegenerative diseases such as AD (Kanfer et al. 1986; Nitsch et al. 1992; Farooqui et al.1990; Farooqui and Horrocks 1991; Prasad et al. 1998), schizophrenia (Gattaz and Brunner 1996; Ross et al. 1999), and Huntington's disease (HD) (Ellison et al. 1987).

Phospholipid degradation in brain tissue results in a decrease in content of essential phospholipids in neuronal and glial cell membranes, and an accumulation of free fatty acids, prostaglandins, lysophospholipids, and lipid

peroxides (Prasad et al. 1998). High concentrations of these metabolites may alter the physicochemical properties of neuronal and glial cell membranes and loss of ionic gradients due to alterations in the conformation and function of transmembrane ion-channels, inflammation, and oxidative stress. All these processes, along with compromised metabolism, may contribute to irreversible neural cell injury (Farooqui and Horrocks 1994; Farooqui et al. 1997; Farooqui et al. 2000b).

In ischemic injury, the glutamate-mediated neurodegeneration may be rapid (in days) because of the sudden lack of oxygen, quick drop in ATP, and alterations in ion homeostasis. Ischemic injury results in a huge increase in the levels of free fatty acids and a marked decrease in the phospholipid content of neural membranes. This is due to the stimulation of PLA_2 (Edgar et al. 1982; Rordorf et al. 1991).

In chronic neurodegenerative diseases such as AD, oxygen, nutrients, and ATP are available to the nerve cells and ionic homeostasis is maintained to a limited extent. Thus the resulting neural cell injury takes several years to develop (Farooqui and Horrocks 1991; 1994). Neural membranes of AD patients is not only accompanied by increased PLA_2 activities in different regions of AD brain compared to age matched controls (Stephenson et al. 1996; 1999), but also by the elevation of phospholipid degradation metabolites. This increase in phospholipid metabolites correlates with pathologic markers of AD such as neurofibrillary tangles and senile plaques (Pettegrew 1989). The aldehydic product of arachidonic acid metabolism, 4-HNE, co-localizes with intraneuronal

neurofibrillary tangles and has been suggested to contribute to the cytoskeletal derangement found in AD. Alterations in phospholipid metabolism may be closely associated with the loss of synapses and neurons in AD (Farooqui and Horrocks 1994; Prasad et al. 1998).

2. 2. Cholesterol

2. 2. 1. Distribution and functions

Cholesterol is a sterol (a combination of steroid and alcohol) found in the cell membrane of all body tissues. It makes the membrane's fluidity- degree of viscosity - stable over wider temperature. It is a constituent of the myelin sheath in nerves and present in all plasma lipoproteins. The requirement for cholesterol is much greater in cells dividing or growing rapidly than in those in a resting state. It is a component of lipid rafts in the plasma membrane and implicated in cell signalling processes. Cholesterol reduces the permeability of the plasma membrane to proton and sodium ions (Haines 2001). It is also essential for the structure and function of caveolae and clathrin-coated pits, including the caveolae-dependent endocytosis and clathrin-dependent endocytosis (Pichler and Riezman 2004).

Cholesterol plays an important role with respect to the physical structure of the cell membrane. Another important role of cholesterol is its interaction with membrane proteins and this interaction has been described in both neuronal and non-neuronal cells (Krueger and Papadopoulos 1990; Michelangeli 1990). In both erythrocytes (Schroeder et al. 1991) and synaptic plasma membranes

(Wood et al. 1989a), cholesterol accounts for over 40 mol% (40 membrane cholesterol molecules/100 cholesterol molecules in a lipid unit) of total cholesterol lipid. The distribution of cholesterol in the plasma membrane is asymmetric and lateral, and it is usually located in different pools or domains (Schroeder et al. 1988; Wood et al. 1993; Wood et al. 1999). Modification of membrane cholesterol content in different pools or domains can alter membrane fluidity, lipid packing and interdigitation, as well as membrane protein functions (Yeagle 1992).

The brain is the cholesterol-rich organ in the human body (Cook 1958). The central nervous system accounts for only 2% of the whole body mass but contains almost a quarter of the unesterified cholesterol (~ 15 g) present in the whole individual (Dietschy and Turley 2001). Brain cholesterol is found in the plasma membranes of glial cells, in neuronal membranes, and in the myelin sheaths (Spady and Dietschy 1983). Cholesterol is important for the function of this organ as a constituent of myelin and cell membranes, and has also been shown to modulate the stability of microtubules in cultured neurons, as well as neuronal functions such as endocytosis and antigen expression (Fan et al. 2002).

Cholesterol plays an important role in the normal function of the brain. Modification of cholesterol domains can alter the activity of certain intergral proteins, and such domains may be important to neuronal functions, such as ion transport and receptor function. For example, a reduction in the content of cholesterol in the membranes produces a loss in sodium dependent γ-aminobutyric acid (GABA) uptake in synaptic plasma membrane and

synaptosomes (North and Fleischer 1983). The uptake is restored by the addition of cholesterol. The functions of other proteins, including Na^{+}-K^{+} ATPase (Yeagle et al. 1988; Incerpi et al. 1992) and Ca^{2+}-Mg^{2+} ATPase (Cornea and Thomas 1994), are also affected by alterations in the content of membrane cholesterol.

The inner leaflet of synaptic plasma membranes contains over 85% of the total plasma membrane cholesterol (Wood et al. 1990). It is well known that membrane fluidity is inversely correlated with the cholesterol-to-phospholipid ratio and that the increased ratio reduces fluidity. As a result, the inner leaflet that contains almost seven times as many cholesterol levels as those of outer leaflet is markedly less fluid compared to the outer leaflet (Wood et al. 1990). Factors such as ethanol (Schroeder et al. 1988; Wood et al. 1989b) and increasing temperature (Schroeder et al. 1988) have a greater effect on the fluidity of the outer leaflet. *In vivo*, the synaptic plasma membrane cholesterol can also be modified by specific factors (Wood et al. 1999). A mouse model of chronic ethanol consumption showed approximately a two-fold increase in cholesterol in outer leaflet, but no change in total cholesterol compared with control groups (Wood et al. 1989b).

Thus far, little is known about the mechanisms that regulate cholesterol domains and their contribution to neuronal homeostasis. Evidence shows that changes in sterol carrier protein-2 (SCP-2), brain fatty acid binding protein (B-FABP), and heart fatty acid binding protein (H-FABP) in the brain are associated with modification of the transbilayer distribution of cholesterol and fluidity in the synaptic plasma membrane of chronic ethanol consumption mice and aged mice

(Myers-Payne et al. 1996a, b; Pu et al. 1999). In addition, other factors associated with cholesterol metabolism such as apolipoproteins, their receptors, and sphingomyelin could also play a role in regulation of the distribution of cholesterol content in the plasma membrane. This is supported by the observation that the cholesterol level of the outer leaflet is two-times higher in the synaptic plasma membrane of apoE-deficient and low-density lipoprotein receptor (LDL-R) deficient mice than that in controls (Igbavboa et al. 1997). These differences in cholesterol distribution are not accounted for by difference in the total amount of membrane cholesterol.

2. 2. 2. Cholesterol in the brain

2. 2. 2. 1. Cholesterol synthesis and elimination in the brain

A large number of studies have established that there is little uptake of cholesterol from the bloodstream into the brain, and that brain cholesterol is derived mostly from *de novo* synthesis (Fig. 2, Wilson 1970; Kabara 1973; Jurevics and Morell 1995). The brain has a high rate of cholesterol synthesis during late fetal and early neonatal life (Ness et al. 1979; Dietschy et al. 1983; Cavender et al. 1995). This declines rapidly at about the time of weaning, and remains low throughout adulthood (Ness et al. 1979; Dietschy et al. 1983; Spady and Dietschy 1983). The high rate of cholesterol synthesis in early life is essential to ensure normal growth and development of the brain. In patients with Smith-Lemli-Optiz syndrome, an autosomal recessive disorder, a major block in

the terminal step of the cholesterol biosynthesis pathway results in severe mental retardation and multiple birth defects (Tint et al. 1994).

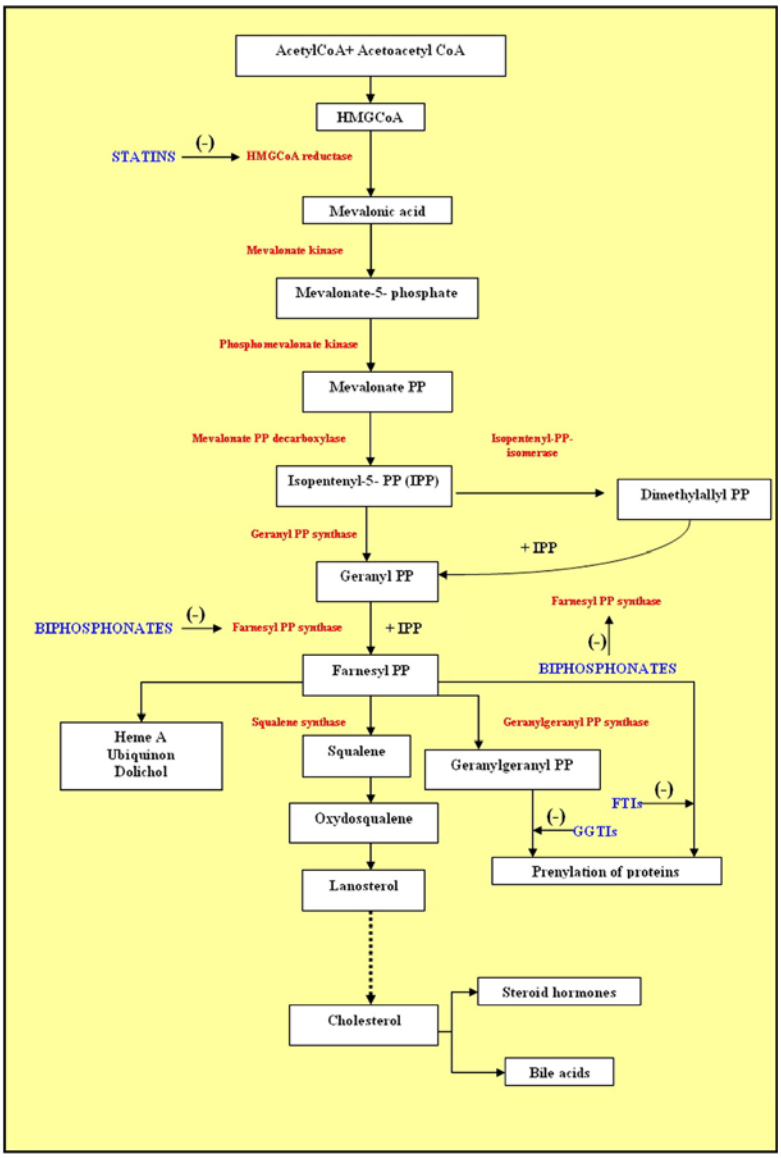

Figure 2. Synthetic and metabolic pathways for cholesterol (Buhaescu and Izzedine 2007)

The rate of cholesterol biosynthesis was reported to be only ~ 0.1% of newly synthesized cholesterol in adult monkey brains. The biosynthetic rates were assessed by measuring the velocity at which [3H] water was incorporated into digitonin-precipitable sterols (DPS) in the intact animal. When expressed as a percentage of total body synthesis, the whole brain of the monkey contained

1% of the [3H] DPS and the liver contained 40% of [3H] DPS (Spady and Dietschy 1983). In humans, therefore it is estimated that only 1-2 mg of cholesterol will be synthesized each day. Nevertheless, a study that measures the absolute rate of cholesterol synthesis in the brain of neonatal rats shows the amount of cholesterol synthesized locally is sufficient to fully account for all the brain cholesterol deposition that occurs during that stage of their development (Jurevics et al. 1997; Turley et al. 1981). Based on *in vitro* experiments, it is expected that the half-life of brain cholesterol in rat brain slices is about 6 months (Andersson et al. 1990).

The highest concentration of cholesterol is found in myelin in the brain. The source of cholesterol for myelination is mainly by local synthesis (Snipes and Suter 1997). *In vitro* studies have confirmed that oligodendrocytes have the ability to synthesize cholesterol from acetoacetate and glucose (Koper et al. 1984). However, it appears that oligodendrocytes may not be the only cell type in the brain that can synthesize cholesterol. An increase of cholesterol esters (Kinney et al. 1994), 24-hydroxycholesterol, and 7-dehydrodesmosterol (Bourre et al. 1990) is observed, even before the time of myelination in the human CNS. It is therefore likely that neurons may be another important cell type that can synthesize cholesterol in the brain. This is supported by the finding in cultured rat sympathetic neurons that the cell bodies of neurons have the ability to synthesize cholesterol. This study also suggests that cholesterol synthesized by neuron cell bodies is sufficient for the elongation of axons (Vance et al.1994).

As mentioned earlier, essentially all of the cholesterol in the brain is derived from local synthesis (Dietschy and Turley 2001). Cholesterol in membranes is held in place primarily with van der Waal's and hydrophobic forces. Cholesterol molecules can easily leave the bilayer membrane and then return. This type of turnover is rapid, but not easily detected. Metabolic turnover is very slow. Brain cholesterol is characterized by a low turnover and little exchange with lipoproteins in the circulation because of the protection of blood-brain barrier (Björkhem et al. 1997). Thus, mechanisms that remove cholesterol from the brain are required for the brain cholesterol homeostasis. Recent evidence suggests that a 24S-hydroxylase mediated mechanism could be the most important mechanism in the elimination of cholesterol in the brain (Björkhem et al. 1999). 80% of the 24S-hydroxycholesterol in the human body is present in the brain, and the concentration of 24S-hydroxycholesterol is 30-1500 times higher in the brain than in any other organs except adrenals (Lütjohann et al. 1996).

A net flux has been demonstrated from the brain into the circulation by measuring the 24S-hydroxycholesterol in the serum samples from the internal jugular vein and the branchial artery in human (Lütjohann et al. 1996). Moreover, the rate of excretion of this compound into the plasma roughly equals the rate of cholesterol synthesis in the adult rat brain (Björkhem et al. 1997). Once the 24S-hydroxycholesterol is synthesized, it is readily secreted across the blood-brain barrier into the circulation (Björkhem et al. 1997) and rapidly taken up and metabolized in the liver (Björkhem et al. 1998).

24S-hydroxylase cDNA has been cloned and the expression of the enzyme in the mouse brain was studied by in situ hybridization and immunohistochemistry (Lund et al. 1999). 24S-hydroxylase is expressed in neurons rather than the cholesterol-laden cells or lipid-rich myelin sheaths. It is expressed in multiple subregions of mouse brain, including the cerebral cortex, hippocampus, dentate gyrus, and thalamus. These results suggest that the 24S-hydroxylase mediated pathway is an important mechanism for elimination of cholesterol from the human brain (Lund et al. 1999).

2. 2. 2. 2. Cholesterol binding/ transport proteins in the brain

Cholesterol transport and the proteins involved in such transport have been extensively studied *in vitro* and in systems outside the brain. In contrast, studies on cholesterol transport in the brain are relatively few. Most of the transport proteins found in brain tissues belong to either intracellular transport proteins or apolipoproteins. At least four families of transport proteins that may be involved in cholesterol trafficking have been reported in the brain.

The first group of intracellular cholesterol transport proteins found in the brain is SCP-2 (van Amerongen et al. 1985; Myers-Payne et al. 1996a). Pro-SCP-2 was detected in brain by immunoblotting (Van Heusden et al. 1990) and was present in pinched off nerve ending or synaptosomes (Myers-Payne et al. 1996a). An *in vitro* binding study reveals that SCP-2 can bind cholesterol with high affinity and it markedly facilitates transfer of cholesterol as well as other molecules, such as oxysterols and phospholipids (Schroeder et al. 1996).

Overexpressing the SCP-2 gene products led to upregulation of many aspects of cholesterol metabolism, including cholesterol uptake (Moncecchi et al. 1996), cellular cholesterol mass, cholesterol esterification (Murphy and Schroeder 1997), cellular cholesteryl ester mass, transfer of plasma membrane cholesterol to ER, and mitochondrial cholesterol oxidation (Yamamoto et al. 1991). However, thus far, the function role of SCP-2 in the brain has not been determined. Evidence shows that cholesterol is synthesized only in the cell body and transported to the axon by some unidentified mechanism in cultured sympathetic neurons (Vance et al. 1994). The isolation of SCP-2 from neurons suggests that it may be part of such a transport mechanism.

The second group of intracellular cholesterol transport proteins found in the brain is caveolin (Cameron et al. 1997; Ikezu et al. 1998). Caveolins belongs to a multimember family and caveolin 1, 2, 3 have been identified in brain endothelial cells and astrocytes (Cameron et al. 1997; Ikezu et al. 1998). Their functions are thought to be involved in the transport of cholesterol from ER to the plasma membrane (Smart et al.1996).

The third group of intracellular cholesterol transport proteins isolated from the brain is the fatty acid binding family. Two members of the family, H-FABP and B-FABP, are found in synaptosomes (Myers-Payne et al. 1996b). Interestingly, these proteins inhibit intermembrane sterol transfer *in vitro* instead of binding cholesterol (Pu et al. 1998).

The last group of cholesterol transport proteins reported in the brain is apolipoproteins. This family includes apolipoprotein A-I (apoA-I) (Harr et al. 1996),

apolipoprotein A-IV (apoA-IV), apolipoprotein E (apoE) (Pitas et al. 1987; Harr et al. 1996), apolipoprotein J (apoJ) (Harr et al. 1996), and apolipoprotein D (apoD) (Suresh et al. 1998). These apolipoproteins, which are the primary means of cholesterol trafficking systemically, are believed to be capable to bind cholesterol, esterified cholesterol, phospholipids, and triglycerides (Harr et al. 1996).

Among all the apolipoproteins found in the brain, apoE has been intensely studied as a result of the association between the apoE4 allele and AD (Poirier et al. 1993; Strittmatter et al. 1993; 1996). This apolipoprotein is thought to be synthesized in astrocytes and released to deliver cholesterol to other cells in the brain (Pitas et al. 1987). The released apoE enriched lipoproteins can bind to cells expressing the low-density lipoprotein receptor (LDL-R), VLDL receptor (VLDL-R), the low density lipoprotein receptor-related protein (LRP), and the apoE receptor 2 (apoER2). These receptors were observed in astrocytes, pial cells (Pitas et al. 1987; Wolf et al. 1992) and neurons (Poirier et al. 1993; Wolf et al. 1992; Christie et al. 1996; Narita et al. 1997). Besides apoE, there is increasing attention on the role of an atypical apolipoprotein, apoD, in the brain.

2. 2. 2. 3. Apolipoprotein D

Apolipoprotein D (apoD), a member of the lipocalin superfamily of ligand transporters, has also been shown to localize in the brain (Peitsch and Boguski 1990). ApoD was first isolated and partially characterized from plasma high density lipoproteins (HDL) in 1973 (McConathy and Alaupovic 1973). Human apoD cDNA was cloned and sequenced, and immunoreactive apoD was

expressed by cultured cells transfected with the clone cDNA (Drayna et al. 1986). Translation of the *apoD* gene sequence predicts a 169-amino acid mature protein preceded by a 20-residue hydrophobic leader peptide (Drayna et al. 1987). As a member of lipocalin protein family, apoD has three characteristic conserved sequence motifs, the kernel lipocalins. Unlike typical apolipoproteins, which feature an amphipathic α-helical structure that mediates noncovalent interaction with lipids, the tertiary structure of apoD is characterized by eight antiparallel β-sheets (Peitsch and Boguski 1990), which form a ligand-binding pocket. The functional role of apoD is thought to be a transporter for several small hydrophobic molecules including cholesterol (Drayna et al. 1986), progesterone (Lea 1988; Balbin et al. 1990), porphyrins (Peitsch and Boguski 1990), and arachidonic acid (Morais et al. 1995).

ApoD showed high binding affinity to cholesterol (Patel et al. 1997). This is thought to have a physiological role in cholesterol transport. Such binding could allow translocation of cholesterol between domains of high and low concentrations of the sterols that are known to exist within cellular membranes (Patel et al. 1997). ApoD could also form a complex with lecithin cholesterol acyltransferase (LCAT). An increase in the cholesteryl esterification activity of LCAT is observed in presence of apoD and the formation of an apoD–LCAT complex appears to have a stabilizing effect on LCAT (Kostner and Steyer 1988). Thus, by increasing cholesterol esterification by LCAT, apoD could indirectly promote reverse cholesterol transport (Drayna et al. 1986). ApoD metabolism has been shown to interact with that of cholesterol. In mouse astrocytes, apoD

expression is induced by 25-hydroxycholesterol and apoD is secreted associated with lipids (Ong et al. 1997).

Arachidonic acid is a potential physiological ligand with highest affinity for apoD (Morais-Cabral et al. 1995). ApoD could be implicated in the transport of arachidonic acid and play an important role in cellular regulation. Through its association with LCAT, apoD could also modulate the metabolism of arachidonic acid in lipoproteins by controlling the conversion of arachidonic acid (active form) into cholesteryl esters (inactive form) (Morais-Cabral et al. 1995).

The apoD gene is expressed in many tissues, with high levels of expression in spleen, testes and brain (Drayna et al. 1986). In a study on the cellular localization of apoD mRNA in the rhesus monkey brain by in situ hybridization (Smith et al. 1990), strong hybridization was observed in a number of cells within the subarachnoid space, as well as in a population of perivascular cells surrounding small vessels penetrating from the surface of the brain. Similar results have been observed in human brain by immunocytochemistry (Navarro et al. 1998). ApoD immunoreactivity is found in neuroglial cells, pial cells and perivascular cells, in the white matter (Boyles et al. 1990a; Smith et al. 1990; Patel et al. 1995; Navarro et al. 1998). ApoD is secreted in the CNS by oligodendrocytes and astrocytes, and has been postulated to participate in reinnervation of damaged neurons (Patel et al. 1995; Boyles et al. 1990b).

ApoD may participate in CNS maintenance and repair. Elevated apoD expression is present after experimental brain injury (Ong et al. 1997; Montpied et al. 1999, Franz et al. 1999; Terrisse et al. 1999), and in neurological disorders

such as AD (Terrisse et al. 1998; Thomas et al. 2003), NPC disease (Suresh et al. 1998), and prion disease (Dandoy-Dron et al. 1998). Increased apoD expression could be linked to the ability of apoD to function as a transporter of sterols, steroids, arachidonic acid or a still unidentified ligand in the brain that is implicated in tissue repair following injury (Rassart et al. 1998).

2. 2. 3. Cholesterol in neurological disorders

There is considerable turnover of cholesterol in neurons and glia during brain growth, neuronal repair and remodeling (Dietschy and Turley 2001). Abnormalities in cholesterol metabolism have also been reported to play a role in the pathophysiology of AD (Eckert et al. 2000). The evidence for such an association is the epidemiological data indicating a relationship between the apoE4 allele and the occurrence of AD (Strittmatter and Roses 1996; Sparks 1997). Production of Aβ appears to play a central role in the pathophysiology of AD. The β-secretase pathway is critical to the amyloid hypothesis because it generates Aβ. APP is first cleaved by β-secretase and then by the γ-secretase complex to yield Aβ. A critical reason that Aβ production is sensitive to cholesterol levels is because the activity of β- and γ-secretase complexes is dependent on cholesterol metabolism. Both β- and γ-secretase complexes reside in cholesterol-rich membrane domains within the membrane. β-Secretase appears to be particularly sensitive to membrane cholesterol content and is located in lipid rafts. Reducing cellular cholesterol appears to inhibit β-secretase activity (Cordy et al. 2003; Fassbender et al. 2001). γ-Secretase is an aspartyl

protease complex composed of the four core components APH-1, nicastrin (NCT), presenilin (PS), and PEN-2 (Capell et al. 2005), and also resides in cholesterol-rich membrane domains and the cleavage has also been shown to be affected by cholesterol content (Wahrle et al. 2002).

Cholesterol content is slightly but significantly increased in frontal cortex gray matter of AD patients with the apoE4 allele (Sparks 1997). However, another study concluded that brain cholesterol content may be lower in AD patients than that in non-demented subjects. The cholesterol to phospholipid ratio is decreased by 30% in the temporal gyrus, but not in the cerebellum, of the autopsied brains from AD patients compared to control brains (Mason et al. 1992). The reduction in the cholesterol to phospholipid ratio is likely attributed to a reduction of cholesterol content since the phospholipid to protein ratio is similar in brains from AD patients and control subjects. Platelet membrane of AD patients has been found to be more fluid than control membranes and this difference in fluidity may be resulted from a reduction in membrane cholesterol of AD patients (Zubenko et al. 1987).

Several studies have indicated that the amount of 24-hydroxycholesterol is higher in plasma and cerebrospinal fluid of AD patients than in unaffected individuals (Lütjohann et al. 2000; Papassotiropoulos et al. 2002; Schonknecht et al. 2002), suggesting that the turnover of cholesterol in the brain is increased during the neurodegenerative changes of AD. In contrast, in other studies the amount of 24-hydroxycholesterol in plasma was found to be lower in advanced AD patients, and also in a murine model of AD, than in controls (Bretillon et al.

2000; Heverin et al. 2004). It is possible that an increased plasma level of 24-hydroxycholesterol reflects ongoing neurodegeneration and/or demyelination, whereas a decrease in the amount of plasma 24-hydroxycholesterol reflects a selective loss of the population of neurons that express cholesterol 24-hydroxylase (Björkhem and Meaney 2004). Thus, a reduction in cholesterol levels in the brains of AD patients might be the result, rather than the cause, of the enhanced neurodegeneration.

2. 3. Ceramide

2. 3. 1. Structure and functions

Besides phospholipids and cholesterol, another major group of lipids, sphingolipids, have long been regarded as structural and inert components of cell membranes. Sphingolipids comprise around 3% of the cell membrane. They are derivatives of long-chain bases and display a great structural diversity and complexity (Hakomori 1981).

A key sphingolipid is ceramide. The latter is comprised of a sphingosine backbone and fatty acid joined in an amide bond. The sphingosine base in ceramides is typically D-*erythro*-1, 3-dihydroxy-2-amino-14-octadecene (C18:1). Minor additional forms include C20:1 (mainly in brain), 1,3,4-trihydroxy-2-amino-hexadecanol (phytosphingosine) and D-*erythro*-1,3-dihydroxy-2-amino-4,14-octadecadiene. The fatty acid chain length of ceramide can vary from 2 to 28 carbons, although C16 to C24 ceramides are most abundant in mammalian cells. These fatty acids are usually saturated or monounsaturated, and sometimes may

contain a hydroxyl group at the C2 position (α-hydroxy fatty acid) or on the terminal C atom (Cremesti et al. 2002). All sphingolipids contain ceramide as the basic hydrophilic component. They derive from ceramide through biosynthetic pathways that modify primarily the 1-hydroxyl position of the ceramide backbone (Spiegel and Merrill 1996). This hydroxyl group can serve as an acceptor for glucose in the first step of glycosphingolipid synthesis or as a phosphocholine acceptor to yield sphingomyelin. Conversely, in catabolic pathways, ceramide is most commonly cleaved at the amide bond to yield sphingosine and a fatty acid (Perry and Hannun 1998).

Ceramide is known to function within the cell membrane in both microdomain coalescence and receptor clustering (Bollinger et al. 2005), and is involved in many cellular events including apoptosis, growth arrest, differentiation, senescence, mediating an immune response, oxidative stress responses, and nitric oxide signaling (Kolesnick and Hannun 1999; Hannun and Obeid 2002; Pettus et al. 2002).

Several targets for ceramide action have been identified. They include kinases, phosphatases, proteases and various transcription factors including AP1, NF-κB, and IL-6 (Kolesnick and Kronke 1998; Ohanian and Ohanian 2001). Ceramide also interacts with cholesterol to form microdomains (caveolae) and lipid rafts (Simons and Toomre 2000; van Meer and Lisman 2002). These microdomains and lipid rafts have been implicated in the modulation of signal transduction, cell adhesion, and function of ion channels (Bock et al. 2003).

Ceramide can interact with phospholipids to alter the physicochemical properties of neural membranes (Farooqui et al. 2004). These interactions are important because they constitute the physicochemical basis of several processes of potential physiological significance, namely the ceramide-dependent increase in membrane permeability, transbilayer lipid motion, and lateral segregation of ceramide-enriched domains (Montes et al. 2002; Carrer and Maggio 1999; Ruiz-Arguello et al. 1998). In the brain, other important effects of ceramide in hippocampal neurons include modulation of ion currents, neurotransmitter release and synaptic transmission (Furukawa and Mattson 1998; Yang 2000).

2. 3. 2. Ceramide generation and metabolism

Ceramide can be generated in cells by *de novo* synthesis or sphingomyelin hydrolysis. *De novo* synthesis of ceramide occurs in cytosolic face of the ER (Mandon et al. 1992) and in mitochondria (Bionda et al. 2004; Shimeno et al. 1998) and begins with the condensation of serine and palmitoyl-CoA to form 3-ketosphinganine as catalyzed by serine palmitoyltransferase (SPT). SPT is the first and rate-limiting enzyme in the pathway (Merrill et al. 1989; Merrill and Wang 1986; Perry et al. 2000). 3-Ketosphinganine is then reduced to form sphinganine, which is acylated to generate dihydroceramide. The acylation of sphinganine to form dihydroceramide is catalyzed by ceramide synthase. A trans double bond is then introduced at the 4–5 position to generate ceramide. Alternately, this pathway may reutilize sphingosine released by sequential

degradation of more complex sphingolipids for ceramide synthesis. Recent evidence suggests that exogenous, cell-penetrant, short chain ceramides recycle into long chain ceramides via this pathway (Ogretmen et al. 2002).

SPT consists of heterodimers of 53-kDa regulatory SPT1 and catalytic 63-kDa SPT2 subunits and binds to the ER (Hanada et al. 1997; Hanada 2003). Ceramide synthase can utilize both sphingosine and sphinganine as substrates, and thus, ceramide can be directly generated from sphingosine and a fatty acyl-CoA. Ceramide synthase has been localized to the ER (Michel and van Echten-Deckert 1997), mitochondrial outer and inner membranes (Bionda et al. 2004). The enzymes involved in the *de novo* synthesis of cellular ceramide are principally localized within the ER and mitochondria. However, ceramide generated within a specific site may be subsequently transported to other cellular compartments (van Meer and Lisman 2002).

De novo synthesis of ceramide is an important pathway for increasing ceramide levels in response to tumor necrosis factor (TNF), chemotherapeutic agents, and ionizing radiation, resulting in apoptosis as reflected by nuclear morphology and DNA fragmentation (Perry and Hannun 1998). *De novo* production of ceramide is implicated in cell cycle arrest (Lee et al. 1998) and apoptosis (Kolesnick and Kronke 1998; Kroesen et al. 2001; Perry et al. 2000; Perry 2002).

Recent findings have highlighted the importance of the *de novo* synthetic pathway. Reduction of ceramide synthesis by inhibitors of SPT or ceramide synthase attenuates cell death (Edsall et al. 2001; Bieberich et al. 2001;

Korkotian et al. 1999). The disorder known as hereditary sensory neuropathy (HSN) was traced to certain missense mutations in SPT, resulting in increased activity. Subsequent increases in ceramide biosynthesis were proposed to trigger apoptosis in peripheral sensory neurons resulting in the progressive degeneration of dorsal root ganglia and motor neurons in these patients (Dawkins et al. 2001).

Besides *de novo* synthesis, ceramides can also be generated from the sphingomyelin pathway via the sphingomyelin hydrolysis catalyzed by distinct sphingomyelinases (SMase) (Kolesnick and Kronke 1998; Liu et al. 1997). SMases are classified by their pH optima, dependence on cofactors, such as magnesium and zinc, and subcellular location (Okazaki et al. 1989; 1990; Marchesini and Hannun 2004; Levade and Jaffrezou 1999; Samet and Barenholz 1999; Stoffel 1999). Membrane neutral magnesium-dependent SMase (nSMase) and acid SMase (aSMase) are rapidly activated by diverse stress stimuli such as cytokines, antibody receptors steroids, G protein-coupled receptors and cellular stress, resulting in increased ceramide levels over a period of minutes to hours (Hannun et al. 2001; Mathias et al. 1998).

Once generated, ceramide can accumulate in the cell or may be converted into a variety of metabolites (Fig. 3). Phosphorylation by ceramide kinase (Hannun et al. 2001; Mathias et al. 1998) generates ceramide 1-phosphate, while deacylation by either neutral or acid ceramidase (Li et al. 2002) yields sphingosine, which may then be phosphorylated by sphingosine kinases (SKs) to generate S1P. Ceramide can be glycosylated to form complex

glycosphingolipids in the Golgi apparatus or can be used to form sphingomyelin as catalyzed by sphingomyelin synthase (Kolesnick 2002).

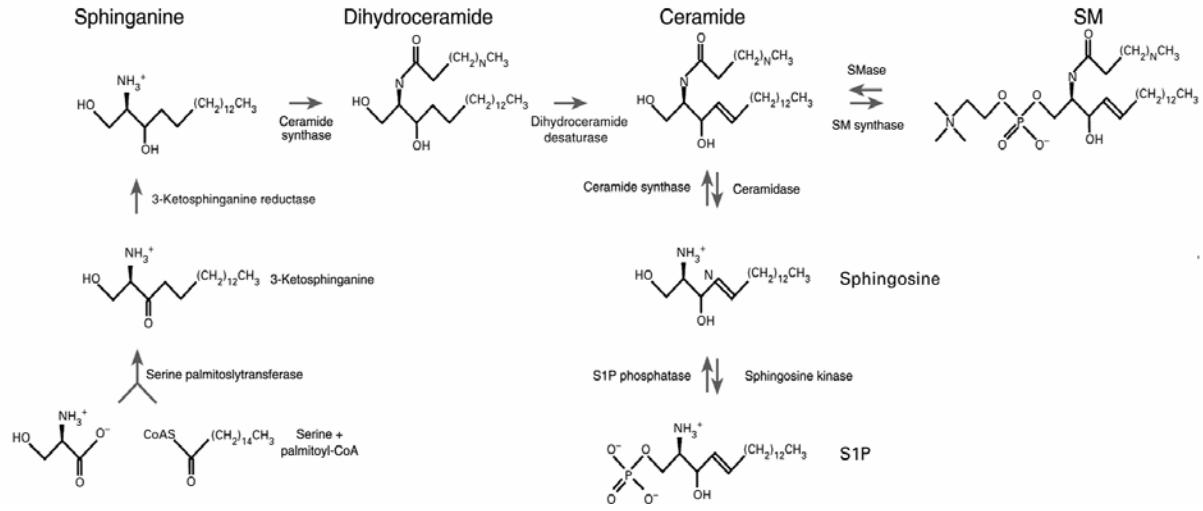

Figure 3. Major synthetic and metabolic pathways for ceramides (Kolesnick 2002)

2. 3. 3. Ceramide in the brain

Both *de novo* and the sphinomyelin breakdown pathway have been shown involved in neuronal ceramide generation. *De novo* ceramide synthesis is involved in regulating various aspects of neuronal development and death. Studies using inhibitors of *de novo* ceramide synthesis (Wang et al. 1991), originally suggested an important role for *de novo* synthesis of ceramide in axonal and dendritic development of hippocampal neurons (Harel and Futerman 1993; Schwarz and Futerman 1998). Similar results were also shown in Purkinje cells (Furuya et al. 1995). Treatment of sensory neurons with the ceramide synthesis inhibitors also inhibits the generation of ceramide and apoptosis induced by suramin (Gill and Windebank 2000).

In neurons, distal axons are rich in nSMase activity but contain almost no aSMase activity, which is concentrated in cell bodies/proximal axons (de Chaves et al. 2000). Consequently, the axonal pool of ceramide responsible for the inhibition of axonal growth in sympathetic neurons is mostly generated by nSMase. NSMase is found at highest levels in brain, and its expression and specific activity rapidly increases in parallel with neuronal maturation during the neonatal period in the rat brain (Spence and Burgess 1978). This suggests that ceramide generated from sphingomyelin by nSMase may contribute to normal neuronal survival, growth and maturation of the CNS. In Neuro2a cells, bioactive ceramide generated in response to retinoic acid (RA) treatment is derived from both *de novo* synthesis and the activity of nSMase (Riboni et al. 1995).

Exogenous ceramide may either protect or kill neurons, depending upon the concentration and experimental paradigm used (Weisner and Dawson 1996a, b; Furuya et al. 1998; Irie and Hirabayashi 1998). The effects of ceramide on hippocampal neuron survival and dendrite outgrowth depend on the developmental neuronal stage and the concentration of ceramide used. At concentrations below 5 μM exogenous ceramide either does not affect survival during the first day in culture (Schwarz and Futerman 1997) or increases cell viability (Mitoma et al. 1998). At concentrations over 5 μM exogenous ceramide given to immature hippocampal neurons causes apoptosis (Mitoma et al. 1998, Schwarz and Futerman 1997). In addition, ceramide concentrations lower than 1 μM protect hippocampal neurons from several insults such as excitotoxicity, $FeSO_4$ and Aβ (Goodman and Mattson 1996). In mature hippocampal neurons

(after 6–7 DIV) even low concentrations of ceramide cause cell death (Mitoma et al. 1998). C6-ceramide (<3 mM) increased cell survival and neurite outgrowth and protected against excitotoxic agents whereas C6-ceramide (>3 mM) induced cell death (Mitoma et al. 1998).

Ceramide-induced apoptosis of cortical neurons is accompanied by caspase 3 and caspase 9 activation (Willaime et al. 2000; Willaime-Morawek et al. 2003). With respect to neurite development and extension, treatment of cortical neurons with ceramide causes rapid neurite retraction and loss of dendritic MAP2 immunoreactivity (Willaime et al. 2000; Willaime-Morawek et al. 2003). Treatment of cerebellar granule cells in culture with exogenous short-chain ceramides causes apoptosis (Colombaioni and Garcia-Gil 2004; Centeno et al. 1998; Toman et al. 2002; Vaudry et al. 2003). Serum/K^+ deprivation or exposure of granule cells to the anticancer agent etoposide leads to accumulation of endogenous ceramide and cerebellar granule cells death (Vaudry et al. 2003). In addition to the activation of apoptosis, C2-ceramide induces rapid and transient activation of cell migration and inhibits neurite outgrowth in immature cerebellar granule cells (Falluel-Morel et al. 2005).

2. 3. 4. Ceramide in neurological disorders

In addition to the effects of cholesterol on AD, substantial depletions of plasmalogen and sulfatide as well as dramatic increases in ceramide are manifested at the earliest clinically recognizable stage of AD. Ceramide elevation in the brain is evident at an early stage in AD patients (Han et al. 2002; Cutler et

al. 2004b; Satoi et al. 2005). The increase of ceramide in AD may result from membrane-associated oxidative stress and might be accompanied by a decrease in sphingomyelin (Cutler et al. 2004b). Alteration of sphingolipid metabolism might be associated with the development of sporadic AD and ceramides have emerged as significant regulators of APP cleavage and Aβ production. Addition of C6- ceramide or nSMase increases Aß generation by regulating β-cleavage through β-site APP cleaving enzyme 1 (BACE1) stabilization but without affecting γ-cleavage of APP in cultured cells expressing APP (Puglielli et al. 2003).

Ceramide has also been identified as a possible second messenger in Aβ-induced death. Treatment of cultured cells with Aβ (Jana et al. 2004; Lee et al. 2004; Cutler et al. 2004b) or intracerebral administration of Aβ to rats (Alessenko et al. 2004) causes ceramide elevation. The apoptotic effects of Aβ are mimicked by exogenous short-chain ceramides (Jana and Pahan 2004; Liu et al. 1998). Aβ-induced activation of nSMase has been demonstrated in human primary neurons, oligodendrocytes and cerebral endothelial cells (Jana and Pahan 2004; Lee et al. 2004; Yang et al. 2004). The mechanisms by which Aβ causes nSMase activation and ceramide accumulation seem to be redox-sensitive and activation of NADPH oxidase and/or regulation of glutathione metabolism (Jana and Pahan 2004). Ceramide elevation is accompanied by an increase in the peroxidation product 4-HNE and is prevented by the antioxidant α-tocopherol (Cutler et al. 2004b).

Recent finding has shown that overproduction of ceramide may be involved in neuronal death in HIV-associated dementia patients (Haughey et al.

2004). Sphingolipid deregulation is more pronounced in HIV-associated dementia patients with an apoE4 genotype, who have worse prognoses (Cutler et al. 2004a).

Elevated levels of ceramide have also been detected in the brain after cerebral ischemia (Herr et al. 1999; Kubota et al. 1996; Nakane et al. 2000; Takahashi et al. 2004; Ohtani et al. 2004) and status epilepticus (Mikati et al. 2003). A previous study demonstrated that ceramide is released *in vivo* in the post-ischemic rat brain. Maximal generation of ceramide occurs during the early phase of reperfusion and is mediated by enhanced aSMase activity as found by the use of a neuroblastoma cell line in an *in vitro* model for ischemia/reperfusion (Herr et al. 1999). Exogeneous ceramide have been shown to reduce the infarct size in focal cerebral ischemia with an upregulation of Bcl-2 and a reduction of TUNEL-positive cells (Chen et al. 2001).

In addition, dopaminergic and other neurons in primary cultures derived from the mesencephalon, a primary region of neuronal degeneration in PD, undergo apoptosis through a ceramide-dependent mechanism that may be identical to the cytokine-stimulated signaling pathway in the immune system. The presence of a ceramide-dependent apoptotic system in mesencephalic dopaminergic neurons suggests that inappropriate activation of such a cell death mechanism may be a factor contributing to PD (Brugg et al. 1996).

3. Kainate-induced excitotoxic neuronal injury

Excitotoxicity refers to a process of neuronal death caused by excessive or prolonged activation of glutamate receptors (GluRs) by the excitatory amino acid neurotransmitter glutamate (Olney et al. 1971). GluRs are categorized into two classes, ionotropic and metabotropic receptors (reviewed in Ozawa et al. 1998). Glutamate activates postsynaptic receptors, including the ionotropic receptors. Upon activation, these receptors open their associated ion channel to allow the influx of Ca^{2+} and Na^{+} ions. Although physiological elevations in intracellular Ca^{2+} are salient to normal cell functioning, the excessive influx of Ca^{2+} together with any Ca^{2+} release from intracellular compartments can overwhelm Ca^{2+}-regulatory mechanisms and lead to cell death (Choi 1987). This phenomenon known as excitotoxicity contributes to neuronal degeneration in many acute CNS disorders, including ischemia, trauma, and epilepsy, and may also play a role in chronic neurodegenerative diseases (reviewed in Arundine and Tymianski 2003).

Kainic acid (KA) is a rigid analog of the excitatory amino acid glutamate that binds to and activates ionotropic glutamate receptor. Kainate-induced epileptic seizures have been widely used as a model for studying human temporal lobe epilepsy (Sloviter and Dempster 1985; Represa et al. 1990; Sutula et al. 1992). A single systemic injection of a convulsive dose of kainate results in both short- and long-term effects on the rat CNS. Within 1 h of its administration to the rats, the neuronal circuitry of the hippocampus is activated and later the animal undergoes robust and recurrent seizures. Within 3-4 days after kainate injection, pyramidal cells in CA1 and CA3 field of the hippocampus begin to

degenerate (Coyle et al. 1983; Sutula et al. 1992; Bing et al. 1996). 1-2 weeks later, spontaneous convulsions can be observed in kainate-treated rats. KA produces selective degeneration of neurons after intraventricular and intracerebral injection, especially in the striatal and hippocampal areas of the brain (Lerma 1997; Ben-Ari and Cossart 2000). Axons and nerve terminals are more resistant to the destructive effects of KA than the cell soma. In developing brains, however, administration of KA fails to produce neurotoxicity (Sperber et al. 1991). Instead, low doses of KA appear to exert trophic effects such as increases in survival and neurite outgrowth in cultured neurons derived from the cerebellum, hippocampus, and spinal cord (Balazs and Hack 1990).

KA has been injected into the ventral globus pallidus of rats to produce neurodegeneration of cholinergic neurons in a pattern similar to nerve cell loss in AD (Johnston et al. 1979). Neurofibrillary tangles and neuritic plaques similar to those found in AD have been shown in cerebral cortical and hippocampal neurons after KA injection in rats (Arendash et al. 1987). In addition, KA injections into the rat striatum produce behavioral, biochemical and morphological effects similar to those described in human afflicted with Huntington's chorea (Coyle and Schwarcz, 1976; McGeer and McGeer 1976).

An increasing number of studies suggest a caused relation between excitotoxicity and free radicals *in vivo* (Bondy and Lebel 1993; Nakao and Brundin 1998). Increased concentration of malonaldehyde and 4-hydroxyalkenals, which was measured as an index of lipid peroxidation, was found in rat cerebral cortex, cerebellum, hippocampus, hypothalamus, and corpus striatum after

administration with KA (Melchiorri et al. 1995; Bruce and Baudry 1995). These results suggest the involvement of oxygen free radicals in the initial phases of KA-induced pathology.

KA can cause excitotoxic neuronal death through interacting with kainic acid-type receptors in neurons, which induces neuronal Ca^{2+} overloading. The alteration in Ca^{2+} homeostasis and its short duration may lead to neuronal degeneration by the activation of PLA_2 and subsequent arachidonic acid cascade. Elevated levels of arachidonic acid and its metabolites produce a variety of detrimental effects on neural membrane structure, activities of membrane enzymes, and neurotransmitter uptake systems (Farooqui and Horrocks 1994; Farooqui et al. 1997). Thus, KA receptor-mediated degradation of neuronal membrane phospholipids, calcium overload, and oxidative stress can disrupt cellular homeostasis and thus threaten cellular membrane integrity and viability and lead to neurodegeneration (Farooqui et al. 2000b).

4. Aims of the present study

In contrast to kainate-induced dysregulated phospholipid metabolism, relatively little is known about altered cholesterol and ceramide metabolisms after kainate injury. In view of importante role of these two membrane lipids in the brain function, the present study aimed to elucidate changed concentrations of cholesterol, 24-hydroxycholesterol, 7-ketocholesterol, and ceramides after kainate injury. The altered expression and activity of a cholesterol metabolic enzyme, cholesterol 24-hydroxylase, and a ceramide synthetic enzyme, SPT,

after kainate injury were also carried out. Finally, the role of apoD in modulation of kainate-induced changed levels of cholesterol, cholesterol oxidative products, and an oxidative stress biomarker, F_2-isoprostanes, and neurodegeneration were elucidated. This study is composed of several parts as follows:

4.1. Dysregulation of cholesterol metabolism after kainate injury

Kainate injection has been shown to result in increased immunoreactivity to cholesterol in the affected CA fields of the hippocampus (Ong et al. 2003). However, it is not known whether this increased cholesterol expression is associated with changes in the expression of the cholesterol metabolic enzymes and with the disturbance of cholesterol turnover in the kainate-induced excitotoxic brain. The effect of an inhibitor of cholesterol biosynthesis, lovastatin, on kainate-induced brain injury is still not clear.

The methods of western blot, immunohistochemistry, immunofluorescence and electron microscopy were carried out to investigate the expression change of cholesterol 24-hydroxylase, and any correlation with cholesterol levels in the rat hippocampus after kainate lesion. The method of GS/MS was carried out to quantify the concentration of cholesterol, 24-hydroxycholesterol and 7-ketocholesterol in kainate or kainate plus lovastatin treated rat hippocampus and hippocampal slices. Cell survival was measured using MAP2 immunostaining and LDH assay.

4. 2. Dysregulation of ceramide metabolism after kainate injury

Recent studies suggest that in addition to the alterations of cholesterol metabolism, an abnormality in ceramide metabolism is involved in neurodegenerative diseases such as AD and stroke. Although previous studies have demonstrated a role for sphingomyelinase activity in ceramide accumulation during neurodegeneration, relatively little is known about possible contributions from ceramide biosynthetic activity.

The methods of western bloting, immunohistochemistry, immunofluorescence, electron microscopy and SPT enzyme activity assay were used to elucidate the altered distribution and activity change of SPT, and any correlation with ceramide levels in the rat hippocampus after kainate lesion. The method of ESI-MS was carried out to quantify ceramide levels in the kainate or kainate plus SPT inhibitor treated hippocampal slices. Cell survival was measured using MAP2 immunostaining and LDH assay.

4. 3. Effect of apolipoprotein D on the neuronal injury after kainate injury

ApoD has the ability to bind several small hydrophobic ligands, including arachidonic acid and cholesterol. A marked increase of apoD expression in the rat hippocampus after kainate-induced neuronal injury has been shown (Ong et al. 1997), and the increase in apoD is paralleled by decreases in phospholipid level and increases in arachidonic acid, ceramide and cholesterol levels in the kainate-injured hippocampus. One possibility is that apoD may be upregulated in injured neurons as part of a cellular defensive mechanism by regulating lipid metabolism.

The method of GC/MS was carried out to quantify F_2-isoprostane, cholesterol, 24-hydroxylcholsterol, and 7-ketocholesterol levels in kainate-treated hippocampal slices. The effect of oxidative stress on cultured fibroblasts from wild type and apoD knockout mice was also studied, as a comparison. Cell survival was measured using MAP2 immunostaining and LDH assay.

CHAPTER II

EXPERIMENTAL STUDIES

I. Lovastatin modulates increased cholesterol and oxysterol levels and has a neuroprotective effect on rat hippocampal neurons after kainate injury

1. Introduction

Oxysterols or cholesterol oxidation products are products of cholesterol metabolism, and play important roles in cholesterol turnover, atherosclerosis and inflammation (Björkhem and Diczfalusy 2002). Because of their ability to pass through cell membranes and the blood-brain barrier at a faster rate than cholesterol itself, they are also important as transport forms of cholesterol. Oxysterols can be formed by direct oxidation of cholesterol, or through the action of oxysterol biosynthetic enzymes (Russell 2000). 7β-Hydroxycholesterol and 7-ketocholesterol are formed by the direct oxidation of cholesterol (Miguet-Alfonsi et al. 2002). In contrast, 24-hydroxycholesterol, 25-hydroxycholesterol and 27-hydroxycholesterol are produced by enzymatic action. Increased levels of 7β-hydroxycholesterol and 7-ketocholesterol are present in atherosclerotic plaques (Brown et al. 1997). These two oxysterols are also increased in patients with aceruloplasminemia (Miyajima et al. 2001).

The enzyme cholesterol 24-hydroxylase synthesizes 24-hydroxycholesterol, and to a lesser extent, 25-hydroxycholesterol. This enzyme is expressed mainly in the brain, and is normally present in neurons (Lund et al. 1999). The conversion of CNS cholesterol to 24-hydroxycholesterol, which readily crosses the blood brain barrier, is a major pathway for brain cholesterol efflux and maintenance of CNS cholesterol homeostasis (Björkhem et al. 1998; 1999; Lund et al. 2003). Increased expression of cholesterol 24-hydroxylase has been reported in the brain in Alzheimer's disease (Bogdanovic et al. 2001; Brown et al. 2004). Oxysterols including 7-ketocholesterol (Lizard et al. 2000; Ong et al.

2003) and 24-hydroxycholesterol (Kolsch et al. 1999; 2001) are toxic to cells in culture.

Intracerebroventricular injection of kainate, a model of excitotoxic injury, causes acute neuronal death of the affected CA subfields in the hippocampus, and proliferation and hypertrophy of glial cells in the glial scar (Farooqui et al. 2001). Our previous study has shown that there is significant *de novo* synthesis of cholesterol in the degenerating hippocampus after neuronal injury (Ong et al. 2003), and that the cholesterol is directly oxidized to oxysterols at relatively short time intervals (3 days) after kainate injury. The present study was carried out to determine whether there could be changes in oxysterol biosynthetic enzyme expression and oxysterol formation at longer time intervals after kainate injections. HMG-CoA is the rate-limiting enzyme for cholesterol synthesis in liver and other tissues (Brown and Goldstein 1980). We also examined whether treatment by a brain permeable 3-hydroxy 3-methylglutaryl coenzyme A (HMG-CoA) reductase inhibitor, lovastatin, could affect brain cholesterol and oxysterol levels and neuronal survival after kainate injury.

2. Materials and Methods

2. 1. Animals and intracerebroventricular kainate injection

Wistar rats weighing approximately 200 g were anesthetized with an intraperitoneal injection of 1.2 ml of 7% chloral hydrate, and the cranial vault exposed. Kainate (1 µl of a 1 mg/ml solution) was injected into the right lateral ventricle (coordinates: 1.0 mm caudal to bregma, 1.5 mm lateral to the midline,

4.5 mm from the surface of the cortex) using a microliter syringe. The needle was withdrawn 10 min later, and the scalp sutured. Experimental control rats were injected with 1 μl of saline instead of kainate. All procedures involving animals were in accordance with guidelines of the Guide of National Research Council of Singapore for the care and use of laboratory animals, and approved by the Institutional Animal Care and Use Committee.

2. 2. Western blots

This was carried out to demonstrate specificity of the cholesterol 24-hydroxylase antibody. Two kainate-injected rats and two saline-injected rats were killed 2 weeks after injection. The rats were deeply anesthetized with an intraperitoneal injection of 7% chloral hydrate, and killed by decapitation. The right hippocampi from both animals in each treatment group were pooled, and homogenized in 10 volumes of ice-cold buffer containing 0.32 M sucrose, 4 mM Tris-Cl, pH 7.4, 1 mM EDTA, and 0.25 mM dithiothreitol (DTT). After centrifugation at 1000 xg for 15 min, the supernatant was collected, and protein concentrations in the preparation measured using the BioRad protein assay kit. Total proteins (50 μg) were resolved in 10% SDS-polyacrylamide gels under reducing conditions and electrotransferred to a polyvinylidene difluoride (PVDF) membrane (Amersham Pharmacia Biotech, Little Chalfont, UK). Nonspecific binding sites on the PVDF membrane were blocked by incubation with 5% non-fat milk for 1 h. The PVDF membrane was then incubated overnight with a rabbit polyclonal antibody to cholesterol 24-hydroxylase (diluted to 2 μg/ml in Tris

buffered saline [TBS]). The antibody to cholesterol 24-hydroxylase was raised in the rabbit against amino acids 254-270 of the mouse cholesterol 24-hydroxylase, and has been shown to detect a single band at ~56 kDa in brain (Lund et al. 1999). After washing with 0.1% Tween-20 in TBS, the membrane was incubated with horseradish peroxidase-conjugated goat anti-rabbit immunoglobulin IgG (Amersham) for 2 h at room temperature. The protein was visualized with an enhanced chemiluminescence kit (Pierce, Rockford, IL, USA) according to the manufacturer's instructions.

2. 3. Immunohistochemical analyses

2. 3. 1. Immunoperoxidase labeling

Four kainate-injected rats at each post-injection time interval were killed at 1 day, 3 days, 1 week, 2 weeks and 4 weeks after injection. Four saline-injected rats at 2 weeks after injection were used as experimental controls. The rats were deeply anesthetized by intraperitoneal injection of 1.5 ml of 7% chloral hydrate and perfused through the left cardiac ventricle with a solution of 4% paraformaldehyde in 0.1 M phosphate buffer (pH 7.4). The brains were removed, and a block consisting of the posterior two thirds of the forebrain, including the hippocampi, dissected out. The blocks were sectioned coronally at 100 μm using a vibrating microtome. The sections were divided into four sets, for cresyl fast violet (Nissl), and immunohistochemical staining as follows: sections were washed for 3 h in phosphate buffered saline (PBS) to remove traces of fixative. They were then incubated overnight with a mouse monoclonal antibody to

cholesterol (MAb 2C5-6, 1:50 dilution), or a rabbit polyclonal antibody to cholesterol 24-hydroxylase (diluted to 10 μg/ml in PBS). MAb 2C5-6 has previously been characterized and shown to be specific for cholesterol (Swartz et al. 1998). The sections were washed in three changes of PBS, and incubated for 1 h at room temperature in a 1:200 dilution of biotinylated horse anti-mouse IgG, or goat anti-rabbit IgG (Vector, Burlingame, CA, USA). The sections were then reacted for 1 h at room temperature with an avidin-biotinylated horseradish peroxidase complex, and the reaction visualized by treatment for 5 min in 0.05% 3,3-diaminobenzidine tetrahydrochloride (DAB) solution in Tris buffer containing 0.05% hydrogen peroxide. The color reaction was stopped with several washes of Tris buffer, followed by PBS. Some sections were mounted on glass slides and lightly counterstained with methyl green before cover slipping. The remaining sections were processed for electron microscopy. Control sections were incubated with cholesterol-absorbed antibody (prepared by incubating 5 μg/ml of cholesterol with 1:50 dilution of cholesterol antibody overnight), pre-immune rabbit serum, or PBS, instead of primary antibodies. They showed absence of staining.

2. 3. 2. Quantitation of labeled cells *in vivo*

The number of cholesterol positive neurons or cholesterol 24-hydroxylase positive glial cells in lesioned areas of dosal CA1 subregion of the right hippocampus of each rat was counted manually using a light microscope. The counts were conducted in a "blind" manner on coded slides at 200 x

magnification with the help of a grid. A total area of 200 x 300 μm from each section, and four sections from each of the four rats in each category were analyzed. The pyramidal neurons in CA fileds are dispersed and can be separated for counting with the help of microscope. The mean number of stained cells/ mm^2 was then calculated for each group of rats at a specific time interval after kainate injection (n = 4 per group). The 'unlesioned' control group consisted of four rats at 2 weeks after saline injection.

2. 3. 3. Electron microscopy

Electron microscopy was carried out by subdissecting some of immunostained sections into smaller portions that included the lesioned CA1 field. These were osmicated, dehydrated in an ascending series of ethanol and acetone, and embedded in Araldite. Thin sections were obtained from the first 5 μm of the sections, mounted on copper grids coated with Formvar, and stained with lead citrate. They were viewed using a Jeol 1010EX electron microscope.

2. 3. 4. Double immunofluorescence labeling

Four kainate-injected rats and four saline-injected rats were killed at 2 week post-injection. The rats were deeply anesthetized by intraperitoneal injection of 1.5 ml of 7% chloral hydrate, and transcardially perfused with normal saline, followed by a fixative, consisting of 4% paraformaldehyde in 0.1 M phosphate buffer (pH 7.4). The brains were dissected out and blocks containing the hippocampus sectioned coronally at 30 μm thickness using a freezing

microtome. They were washed for 3 h in phosphate buffered saline containing 0.1% Triton-X 100 (PBS-Tx) to remove traces of fixative, and immersed for 1 h in a solution of 5% normal goat serum (Vector) in PBS-Tx to block non-specific binding of antibodies. The sections were then incubated overnight with a rabbit polyclonal antibody to cholesterol 24-hydroxylase (diluted to 10 µg/ml in PBS), and a mouse monoclonal antibody to GFAP (a marker for astrocytes, diluted to 1 µg/ml in PBS, Chemicon, Temecula, CA, USA). This was followed by three washes of PBS and incubation for 1 h at room temperature in 1:200 dilution of fluorescein isothiocyanate (FITC)-conjugated goat anti-mouse IgG, and Cy3-conjugated goat anti-rabbit IgG (both from Chemicon). The sections were mounted and examined using an Olympus FluoView FV500 confocal microscopy. Control sections incubated with PBS instead of primary antibodies. They showed absence of staining.

2. 4. Hippocampal slice cultures

Hippocampal slice cultures were prepared as previously described (Stoppini et al. 1991) with minor modifications (Lu et al. 2001). In brief, 10 day old Wistar rat pups were anesthetized with intraperitoneal injections of 3.5% chloral hydrate, decapitated, and the brain removed. The hippocampi were dissected out, and sectioned transversely at 350 µm thickness using a tissue chopper. The slices were transferred to 30 mm Millicell CM culture plate inserts with 0.4 µm polytetrafluoroethylene membranes (Millipore, Bedford, MA, USA), and placed in 6-well culture plates containing culture medium (50% minimum essential medium

[Gibco], 25% horse serum [Sigma, St Louis, MO, USA], 25% Hanks balanced salt solution [Gibco], supplemented with D-glucose [6.5 mg/ml, Sigma], glutamine [2 mM, Gibco], penicillin G [1 unit/ml, Gibco] and streptomycin sulfate [1 µg / ml, Gibco], pH 7.15). The slices were maintained at 37°C, 100% humidity, 95% air and 5% CO_2. The medium was changed to fresh medium every 3 days in culture. The effects of kainate and other agents were tested in cultures after 14 days *in vitro*.

2. 5. Gas chromatographic/mass spectrometric (GC/MS) analysis

2. 5. 1. Kainate and lovastatin treatment

Initial experiments were performed to elucidate the time course of cholesterol and oxysterol formation after kainate injection. Four kainate-injected rats were killed at 3 days, 1 week, 2 weeks and 4 weeks after injection. The animals were anaesthetized by intraperitoneal injections of chloral hydrate and decapitated. The lesioned right hippocampi were quickly removed, and snap frozen in liquid nitrogen, and kept in an -80°C freezer till analysis. Four 2 week post-saline-injected rats were used as experimental controls.

Subsequent experiments were carried out to investigate possible effects of lovastatin on cholesterol and oxysterol levels after kainate treatment. For *in vivo* analyses, eleven kainate-injected rats were injected intracerebroventricularly with kainate and intraperitoneally with lovastatin (4 mg/kg) 3 h after the kainate injection, followed by daily injections of the same dose of lovastatin till the time of sacrifice at 1 week (6 rats) or 2 weeks (5 rats) after kainate injection. The rats

showed status epilepticus that peaked at 90 to 180 mins after kainate injection (Lothman and Collins 1981), and this had abated by the time of the first injection of lovastatin (3 hours after kainate injection). The lovastatin solution was prepared by dissolving pure lovastatin (kind gift of Ranbaxy Malaysia Sdn Bhd) in 20% ethanol and diluted to the final concentration with saline (pH 7.4). Fresh solutions were used daily. Another nine kainate-injected rats were intraperitoneally injected with 20% ethanol in saline for 1 week (4 rats) or 2 weeks (5 rats), and were used as controls. The right hippocampi of the above rats were removed for analysis.

In vitro analysis of the effect of lovastatin was also carried out. Kainate (100 μM final concentration) was applied to slice cultures for 3 h in serum-free medium. The medium was removed, and the slices treated with fresh serum-free medium containing lovastatin or vehicle for 24 h. The above concentration of kainate has been shown to be toxic to neurons in hippocampal slice cultures (Lu et al. 2001). Lovastatin was prepared as a 25 mM stock solution in 100% ethanol and stored at 4°C. This was diluted to a 2.5 mM solution in sterile water and further diluted in serum-free medium to a final concentration of 1 μM. The vehicle consisted of similarly diluted ethanol. Material from twelve to sixteen slices in each treatment group was collected for a single experiment. The mean and standard deviation from three separate experiments were then calculated.

All reagents for GC/MS analysis were of analytical grade. Standards for cholesterol, 7-ketocholesterol, 25-hydroxycholesterol, cholesterol 5 alpha, 6 alpha-epoxide, cholesterol 5 beta, 6beta-epoxide, 5α-cholestane and ergosterol

were purchased from Sigma and of at least 95% purity. 24S-hydroxycholesterol (non-deuterated) was purchased from Medical Isotopes (Pelham, AL, USA). 5α-cholestane and ergosterol were used as internal standards. Standard solutions of cholesterol, oxysterols, 5α-cholestane and ergosterol were diluted in ethanol.

2. 5. 2. Lipid extraction

Extraction of lipids was carried out using Folch's method (Folch et al. 1957) with slight modification. Hippocampal specimens were homogenized at 4°C with 1.5 ml PBS (pH 7.4) and 6 ml Folch organic solvent mixture (chloroform/methanol 2:1, containing 0.05% butylated hydroxytoluene [BHT]). The cultured hippocampal slices were homogenized at 4°C with 0.5 ml PBS (pH 7.4) and 2 ml Folch organic solvent mixture. The homogenates were sealed under N_2 and centrifuged at 1000 x g for 10 min at 4 °C. The upper phase was discarded and the lower organic phase carefully transferred to a glass vial and evaporated under a stream of N_2.

2. 5. 3. Lipid hydrolysis

2 ml of 0.5 M KOH (in 50% methanol) was added with 400 ng ergosterol and 10 μg 5α-cholestane, and the vial sealed under N_2. The lipid extract was hydrolyzed at 23°C for 2 h in the dark.

2. 5. 4. Cholesterol and oxysterol extraction

2.7 ml formic acid (40 mM), 0.2 ml HCl (5 M) and 0.5 ml methanol were added in the above dydrolysed lipid extract and thoroughly mixed before loading onto a 3 ml, 60 mg Oasis Mixed Anion Exchange (MAX) solid phase extraction column (Waters, Milford, MA, USA) previously conditioned with 2 ml methanol and 2 ml formic acid (20 mM). The column was then washed with 2 ml 2% ammonium hydroxide followed by 2 ml methanol/formic acid (40/60). Cholesterol and oxysterols were eluted with 2 ml hexane followed by 2 ml ethyl acetate/hexane (30/70), and collected together into a glass tube containing 50 mg Isolute HM-N (International Sorbent Technologies) to remove traces of water. 50 µl of the extract was aliquoted into a separate glass vial and evaporated under N_2 for cholesterol analysis, and the remaining organic solvent was evaporated under N_2 for oxysterols analysis. Aliquots for cholesterol analysis were derivatized with 25 µl acetonitrile and 25 µl N,O-bis(trimethylsilyl)trifluoroacetamide (BSTFA) + 1% trimethylchlorosilane (TMCS) for 1 h at room temperature and injected directly onto GC/MS. Samples for oxysterol analysis were derivatized with 50 µl acetonitrile and 50 µl BSTFA + 1% TMCS for 1 h at room temperature, evaporated to dryness under N_2 and reconstituted in 30 µl undecane before injection into the GC/MS.

2. 5. 5. GC/MS measurement

Cholesterol and oxysterols were both analyzed with a Hewlett-Packard 5973 mass selective detector interfaced with a Hewlett-Packard 5890II gas chromatograph and equipped with an automatic sampler and a computer

workstation. Separations were carried out on a fused silica capillary column (12 m x 0.2 mm i.d.) coated with cross-linked 5% phenylmethylsiloxane (film thickness 0.33 μm) (Ultra2, Agilent). The carrier gas was helium with a flow rate of 1 ml/min (average velocity = 55 cm/sec). Selected-ion monitoring was performed using the EI mode at 70 eV with the ion source maintained at 230°C and the quadrapole at 150°C. One target ion and two qualifier ions selected from each compound mass spectrum were monitored to optimize sensitivity and specificity. Quantitation of modified bases was achieved by relating the peak area of the analyte with its corresponding internal standard.

2. 5. 6. Cholesterol analysis

Derivatized samples (1 μl) were injected with a 25:1 split into the GC injection port (280°C). Column temperature was increased from 240°C to 300°C at 25°C/min after 1 min at 240°C, and then held at 300°C for 4 min. Cholesterol was monitored using m/z 329 as target ion and m/z 458, 453 as qualifier ions and 5α-cholestane was monitored as internal standard (target ion = m/z 357, qualifier ions = m/z 372, 232).

2. 5. 7. Oxysterol analysis

Derivatized samples (1 μl) were injected with a 5:1 split into the GC injection port (280°C). The column temperature was increased from 175°C to 280°C at 30°C/min after 1 min at 175°C, then increased to 291°C at 2°C /min. Finally, the oven temperature was increased to 306°C at 30°C /min and held for

1.5 min. Ergosterol was monitored as internal standard for the quantification of oxysterols. Target ions for 24-hydroxycholesterol and 7-ketocholesterol were m/z 413 and m/z 472 respectively. Quantification of cholesterol and oxysterols was achieved by relating the peak area of the compound with the internal standard peak area and by applying the following formula: ng/mg hippocampus = (A/AIS) x [IS] x (1/k) ÷ hippocampus weight, where A = peak area of product, AIS = peak area of the internal standard, [IS] = concentration of the internal standard (400 ng ergosterol or 10 μg 5α-cholestane), k = relative molar response factor for each product calculated from the gradient of the calibration curve for each product. Data were expressed as mean ± standard deviation. Calibration curves were constructed from 5 different concentrations in triplicate of cholesterol (5 to 2500 μg) as well as oxysterols (5-2500 ng), and showed good linearity ($r^2 > 0.95$).

2. 6. *In vivo* effect of lovastatin on neuronal survival after kainate injury

A further ten male Wistar rats (each weighing approximately 200 g) were injected with kainate as described above. The injected rats were randomly divided into two groups (5 rats each). The first group received an intracerebroventricular injection of kainate as described previously, followed 3 h later by an intraperitoneal injection of lovastatin (4 mg/kg dissolved in vehicle consisting of 20% ethanol diluted in saline), following by daily injections of the same dose of lovastatin till the time of sacrifice at 2 weeks after kainate injection. The second group of rats was used as controls. These received intracerebroventricular injection of kainate followed by intraperitoneal injections of

vehicle, following the same schedule as the lovastatin-treated rats. The rats were killed at 2 week post-kainate injection by transcardial perfusion. Blocks containing the hippocampus were sectioned as described above. The sections were stained using the Nissl technique, or immunostained for microtubule associated protein 2 (MAP2, Sigma, diluted 1:500) to demonstrate viable neurons. The slides were coded and quantitation was carried out in a “blinded” manner. Due to the patchy nature of the cell loss even within a CA fields (i.e CA1 and CA3), and the enormous total number of cells in entire hippocampus, direct counting of cells was not carried out. Instead the portion of surviving neurons in CA fields was estimated by taking digital images of the entire right hippocampus from 6 Nissl or MAP2 stained sections from each rat, and a discontinous line traced along the row of hippocampal pyramidal neuronal cell bodies from hippocampal fields CA1 to CA3. This was followed by a second trace, along the viable pyramidal neurons in the Nissl stained sections, or pyramidal neurons that showed immunolabeling in their cell bodies and dendrites in the MAP2 labeled sections. The ratio of the second to the first trace was calculated, to indicate the percentage of uninjured neurons in the CA fields.

2. 7. *In vitro* effect of lovastatin on neuronal survival after kainate injury

Kainate (100 μM) was applied to slice cultures for 3 h in the serum-free media before treatment of lovastatin (1 μM) or vehicle 24 h in fresh serum-free media. Slices (6 slices per group) were fixed by immersion in 4% paraformaldehyde in 0.1 M phosphate buffer (pH 7.4), after treatment. The

polytetrafluoroethylene membranes were cut from the culture plate inserts, washed, and immunostained with the attached slices for MAP2. The number of labeled neurons was counted as described in Chapter II, I. 2. 3. 2 (page 44).

Cellular injury in the hippocampal slices was also estimated by quantitation of lactate dehydrogenase (LDH) released from the slices into the culture media. LDH present in the culture supernatant (due to plasma membrane damage) participates in a coupled reaction which converts a yellow tetrazolium salt into a red, formazan-class dye which is measured by absorbance at 492 nm (Decker and Lohmann-Matthes 1988). The culture media were collected after various treatments, and analysed using a LDH cytotoxicity detection kit (Roche, Mannheim, Germany) as follows: neuronal death = [(A-Min)/(Max- Min)]x100, in which A is LDH activity measured in media of test condition, Max is maximum LDH release after 3 h treatment with Triton X-100, defined as 100% of cell death, Min is the LDH activity in media of untreated slices. Media from three culture dishes in each treatment group was collected for a single experiment. The mean and standard deviation from three separate experiments were then calculated.

2. 8. *In vitro* effect of oxysterols on neuronal survival

The toxicity of 24-hydroxycholesterol (15 μM and 50 μM of final concentration) on cultured hippocampall slices was determined by MAP2 staining and LDH release as described above. Oxysterols were dissolved in 100% ethanol at a concentration of 5 mM, and stored at -20°C before use. They were added to slice cultures for 24 h in serum-free medium. Control slices were

treated with vehicle (ethanol). The latter had no effect on cell viability at the concentration used (Wang et al. 2002).

2. 9. Statistical analysis

Experimental data were subjected to statistical analysis using Student's t-test or 1-way ANOVA with Bonferroni's multiple comparison post-hoc test (SPSS for Windows software). $P < 0.05$ was considered significant.

3. Results

3. 1. Western blot analysis (Fig. 1. 1)

The antibody to cholesterol 24-hydroxylase detected a single band at ~56 kDa in both the saline and kainate-injected rat hippocampus (Fig. 1. 1). This is consistent with the expected molecular weight of the enzyme, and similar to results obtained from the mouse brain (Lund et al. 1999; 2003).

3. 2. Immunohistochemical analyses of cholesterol 24-hydroxylase after kainate lesions (Fig. 1. 2 and 1. 3; Table 1. 1)

3. 2. 1. Light microscopy (Fig. 1. 2 and Table 1. 1)

Saline-injected rats

The saline-injected hippocampus showed light labeling for cholesterol (Fig. 1. 2A). The low level of staining may be due to the fact most of the cholesterol in the brain is associated with cellular membranes and hidden within the phospholipid bilayer of the membranes (Ong et al. 2003). Light labeling for

cholesterol 24-hydroxylase (Fig. 1. 2B) was also observed. Labeling was observed in the cell bodies and dendrites of pyramidal neurons and punctate profiles in the neuropil.

Kainate-injected rats

Three days after kainate injection

Loss of neurons was observed in fields CA1 and CA3 of the hippocampus in Nissl stained sections (data not shown). The loss was more extensive on the side of the kainate injection than on the contralateral side. An increase in cholesterol immunoreactivity compared to saline-injected rats was observed in the affected CA fields (Fig. 1. 2C). The increased cholesterol staining was observed in the cell bodies and apical dendrites of pyramidal neurons and diffusely throughout the neuropil of the affected areas. In contrast to the increased immunoreactivity to cholesterol, decreased immunoreactivity to cholesterol 24-hydroxylase (Fig. 1. 2D) was observed in neurons of the affected CA field at this time.

One to two weeks after kainate injection

Loss of neurons, and large numbers of glial cells were observed in fields CA1 and CA3 of the hippocampus as judged by Nissl staining. A further increase in cholesterol immunoreactivity compared to 3 day post-kainate-injected hippocampus was observed in the affected CA fields (Fig. 1. 2E). The number of cholesterol positive neurons was significantly greater in the 1 week (919 ± 104

cells / mm^2) and 2 week (1018 ± 145 cells / mm^2) post-kainate-injected rats, compared to saline-injected rats (0 ± 0 cells / mm^2) (Table 1. 1). The increased cholesterol staining was observed in the cell bodies and apical dendrites of pyramidal neurons of the affected areas (Fig. 1. 2E).

An increased immunoreactivity to cholesterol 24-hydroxylase (Fig. 1. 2F) was observed in glial cells in the affected CA fields at this time. The number of cholesterol 24-hydroxylase positive glial cells was significantly greater in the 1 week (1312 ± 195 cells / mm^2) and 2 week (1815 ± 225 cells / mm^2) post-kainate-injected rats, compared to saline-injected rats (0 ± 0 cells / mm^2) (Table 1. 1). The labeled cells had large diameter processes that tapered gradually from the cell bodies. They were shown to be astrocytes by electron microscopy and double immunofluorescence labeling with GFAP (see below).

No increase in cholesterol 24-hydroxylase immunoreactivity in glial cells was observed in areas of the hippocampus, or other parts of the brain that were unaffected by the kainate injections (data not shown).

Four weeks after kainate injection

Little immunoreactivity to cholesterol was observed in the degenerating CA field at this time (Fig. 1. 2G), and the number of cholesterol positive neurons was significantly less than at earlier post-injection time intervals (Table 1. 1). The number of cholesterol 24-hydroxylase immunoreactive cells was similarly fewer, compared to that at 1 week or 2 week post-kainate injection (Fig. 1. 2H; Table 1. 1).

3. 2. 2. Electron microscopy (Fig. 1. 3A, B)

Dense staining for cholesterol 24-hydroxylase was observed in glial cells, in the 2 week post-kainate-injected rats. The glial cells had large cell bodies with irregular cell outlines. The nucleus contained evenly dispersed fine heterochromatin clumps, and absence of dense marginated heterochromatin on the inner aspect of the nuclear envelope. The cytoplasm contained dense bundles of glial filaments. They thus had features of astrocytes (Fig. 1. 3A, B).

3. 2. 3. Double immunofluorescence labeling of cholesterol 24-hydroxylase and GFAP (Fig. 1. 3C, D)

Dense staining for cholesterol 24-hydroxylase in glial cells in the 2 week post-kainate-injected rats. The glial cells had large cell bodies with irregular cell outlines and were double immunolabeled for GFAP, confirming their identity as astrocytes (Fig. 1. 3C, D). The cholesterol 24-hydroxylase and GFAP stainings merged and showed that cholesterol 24-hydroxylase was only present in astrocyes at this time.

3. 3. GC/MS analysis of cholesterol and oxysterols in the kainate-injected rat hippocampus (Table 1. 2)

Kainate injection resulted in significantly greater levels of cholesterol at 1 week (63.0 ± 10.2 μg/mg), 2 weeks (98.6 ± 16.7 μg /mg) and 4 weeks (67.0 ± 4.2

μg /mg) after injection, compared to the saline-injected rats (23.0 ± 15.8 μg/mg) (Table 1. 2).

Significantly greater levels of 24-hydroxycholesterol were also observed at 1 week (26.2 ± 6.3 ng/mg) and 2 weeks (30.1 ± 4.9 ng/mg) after kainate injection, compared to the saline-injected rats (7.2 ± 5.4 ng/mg) (Table 1. 2). The level of 24-hydroxycholesterol returned to baseline level, and was not significantly greater than that of the saline-injected rats, at 4 weeks after kainate injection (Table 1. 2).

The level of 7-ketocholesterol was also significantly greater at 2 weeks (4.2 ± 0.9 ng/mg) after kainate injection, compared to saline injection (1.4 ± 0.4 ng/mg) (Table 1. 2). Very low or undetectable levels of cholesterol epoxides, and 25-hydroxycholesterol were found in the hippocampi of the kainate or saline-injected rats.

3. 4. Effect of lovastatin on cholesterol and oxysterol concentrations after kainate injury (Table 1. 3 and 1. 4)

3. 4. 1. *In vivo* analyses (Table 1. 3)

Systemic administration of lovastatin resulted in significantly lower cholesterol and oxysterol levels in the hippocampus after kainate injection. The level of cholesterol in the 1 week post-kainate plus lovastatin injected rats was 41.6 ± 16.0 μg/mg (Table 1. 3). This was significantly less than that of the kainate plus vehicle injected rats (67.6 ± 15.6 μg/mg, Table 1. 3), and approximately 65%

of the increase in cholesterol level after kainate treatment was blocked by lovastatin.

Lovastatin injection also resulted in significantly lower levels of 24-hydroxycholesterol, in the kainate plus lovastatin injected rats (7.2 ± 2.9 and 11.6 ± 3.0 ng/mg at 1 week and 2 weeks postinjection respectively) compared to the kainate plus vehicle injected rats (23.1 ± 10.6 and 27.2 ± 7.8 ng/mg) (Table 1. 3). This effect was even more pronounced than that of cholesterol, and approximately 85% of the increase in 24-hydroxycholesterol after kainate treatment was blocked by lovastatin.

The level of 7-ketocholesterol in the kainate plus lovastatin injected rats (2.0 ± 0.9 ng/mg) was comparable to that of the kainate plus vehicle injected rats (2.9 ± 1.1 ng/mg) at 1 week after kainate injection, but was significantly lower compared to the kainate plus vehicle injected rats at 2 weeks after kainate injection (1.4 ± 0.2 ng/mg compared to 3.8 ± 0.8 ng/mg) (Table 1. 3).

3. 4. 2. *In vitro* analyses (Table 1. 4)

The changes in cholesterol and oxysterol levels after kainate / kainate plus lovatstatin treatment *in vivo* were also observed *in vitro*, although the absolute levels of cholesterol and oxysterols per weight of “slice tissue” was much lower than the brain. This could be due to increased extracellular space in the slices. Kainate treatment of hippocampal slice cultures also resulted in significantly greater levels of cholesterol, 24-hydroxycholesterol and 7-ketocholesterol, compared to the untreated slices (Table 1. 4). The levels of cholesterol and

oxysterols in the kainate plus lovastatin treated slices were significantly lower compared to the kainate plus vehicle treated slices (Table 1. 4).

3. 5. Effect of lovastatin on neuronal survival after kainate injury (Fig. 1. 4 and 1. 5)

3. 5. 1. *In vivo* analyses (Fig. 1. 4)

Systemic administration of lovastatin partially protected hippocampal neurons after kainate injection as shown by representative Nissl stained sections (Fig. 1. 4A). Nissl stained sections showed 48.9 ± 10.6% cell survival in the kainate plus lovastatin injected rats. This was significantly more than the 17.0 ± 8.7% uninjured neurons in the kainate plus vehicle injected rats (Fig. 1. 4B). MAP2 immunostained sections similarly showed greater proportion of uninjured neurons (47.3 ± 5.7 %) in the kainate plus lovastatin injected rats, compared to the kainate plus vehicle injected rats (19.2 ± 9.6%, Fig. 1. 4B).

3. 5. 2. *In vitro* analyses (Fig. 1. 5)

Lovastatin also partially protected hippocampal neurons from kainate injury in slice cultures. Significantly lower MAP2 positive neuronal cells in fields CA1 and CA3 of the hippocampus were detected after kainate treatment, compared to the untreated slices (Fig. 1. 5A, B). Slices that had been treated with the kainate plus lovastatin showed significantly lower neuronal loss, compared to those treated with the kainate plus vehicle (Fig. 1. 5A, B). The protective effect of lovastatin was confirmed by detection of lower LDH activity in

the culture media of kainate plus lovastatin treated slices (50.9 ± 10.2% of total LDH release), compared to kainate plus vehicle treated slices (75.2 ± 8.3% of total LDH release) (Fig. 1. 5C).

3. 6. Effect of 24-hydroxycholesterol on neuronal injury (Fig. 1. 6)

In vitro analyses (Fig. 1. 6)

Treatment of the lower concentration of 24-hydroxycholesterol (15 μM) had no toxic effect on cultured hippocampal slices as shown by MAP2 stained sections (Fig. 1. 6A). In contrast, the higher concentration of 24-hydroxycholesterol (50 μM) showed significantly fewer number of MAP2 positive neuronal cells in both CA1 and CA3 of the cultured hippocampus, compared to the untreated slices (Fig. 1. 6A, B).

24-Hydroxycholesterol induced neuronal injury was confirmed by the detection of increased LDH release in the culture media of the 24-hydroxycholesterol (50 μM) treated slices, compared to the vehicle treated slices (Fig. 1. 6C). Treatment with 7-ketocholesterol (50 μM) also resulted in toxicity (Fig. 1. 6C).

4. Discussion

Increased cholesterol immunoreactivity was detected in the degenerating CA fields of the hippocampus after kainate lesions, using a specific antibody to cholesterol. The cholesterol labeling was observed in the cell bodies and dendrites of pyramidal neurons, which are known to degenerate after kainate

injury (Sandhya et al. 1998). An increased immunolabeling of the oxysterol biosynthetic enzyme, cholesterol 24-hydroxylase was also observed in glial cells, in the affected areas. Electron microscopy confirmed that the glial cells had dense bundles of glial filaments, whilst double immunofluorescence labeling showed that cholesterol 24-hydroxylase positive glial cells were double labeled with GFAP, confirming that they were astrocytes.

The increase in cholesterol levels after kainate injury was confirmed by GC/MS analysis. A significant elevation in cholesterol levels was detected at 1 week, 2 weeks, and 4 weeks after kainate injection, compared to saline-injected controls. Similar increases in cholesterol were detected in hippocampal slice cultures after kainate treatment. The technique of GC/MS measures the absolute amount of cholesterol in tissue samples, regardless of whether it is present within cell membranes, or free in the cytosol. Since little cholesterol is thought to enter the brain from the bloodstream (Dietschy and Turley 2004), the increase in brain cholesterol that is detected by this method therefore indicates *de novo* cholesterol synthesis. Increases in 24-hydroxycholesterol and 7-ketocholesterol levels were also detected by GC/MS after kainate injury, *in vivo* and *in vitro*. The *in vitro* results suggest that the increased cholesterol and oxysterols in brain tissue after kainate injury may be a consequence of increased cholesterol synthesis and cholesterol 24-hydroxylase expression in the degenerating brain tissue, and not only or primarily uptake from the bloodstream. This notion is supported by a previous study which found that most of the 24-hydroxycholesterol in the serum is derived from the brain (Björkhem et al. 1998).

The present study adds to our previous study, which showed that there is increased cholesterol and oxysterol levels in the hippocampus at short time intervals (3 days) after kainate injury (Ong et al. 2003). In this study, we showed that there were further significant increases in cholesterol, 24-hydroxycholesterol and 7-ketocholesterol levels in the degenerating hippocampus, at later time points, i.e. two weeks after the initial excitotoxic insult. The increases in cholesterol and oxysterols followed a similar pattern, increasing up to two weeks after kainate injection, followed by a decrease to near pre-lesion levels at four week post-injection. Other oxysterols such as cholesterol 5 alpha, 6 alpha-epoxide, cholesterol 5 beta, 6 beta-epoxide, and 25-hydroxycholesterol were also analyzed in our samples, but these were not detected.

Neurotoxic effects of cholesterol metabolites have been reported recently (Nelson and Alkon 2005). 24-hydroxycholesterol and 7-ketocholesterol are toxic to cultured cerebellar granule neurons SH-SY5Y human neuroblastoma cells (Chang and Liu 1998; Kolsch et al. 2001). 24-hydroxycholesterol and 7-ketocholesterol produce neuronal death (apoptosis) by caspase-3 activation, DNA fragmentation, and decreasing mitochondrial membrane potential (Kolsch et al. 1999; Lizard et al. 2005). Our recent studies also showed that 7-ketocholesterol, cholesterol 5 alpha, 6 alpha-epoxide and cholesterol 5 beta, 6 beta-epoxide were neurotoxic to pyramidal neurons in slice preparations of the rat hippocampus (Ong et al. 2003). The oxysterols, together with other factors such as iron-induced free radical damage (Wang et al. 2002), might contribute to increasing neuronal death in the hippocampus with time after kainate injury

(Sandhya et al. 1998). The toxicity of 24-hydroxycholesterol has been reported to be equal to that of 7-ketocholesterol in SH-SY5Y cells (Kolsch et al. 1999).

Slice cultures were treated with low (15 μM) and high (50 μM) concentrations of 24-hydroxycholesterol, to determine its possible neurotoxicity on hippocampal neurons. These concentrations were chosen based on 24-hydroxycholesterol levels detected *in vivo* (~ 7.2 ng/mg tissue in the saline-injected hippocampus and ~ 26.2 ng/mg tissue in the 1 week post-kainate-injected hippocampus), and assuming a specific gravity of 1.05 g/cm^3 (Morano and Seibyl 2003). The results showed that the lower concentration of 24-hydroxycholesterol (15 μM or ~7.2 ng/mg tissue) was not toxic to hippocampal neurons, whereas the higher concentration (50 μM or ~26.2 ng/mg tissue) was neurotoxic. These results suggest that the level of 24-hydroxycholesterol encountered *in vivo* after kainate injury was sufficient to cause neuronal damage.

The effect of lovastatin on brain oxysterol levels and neuronal survival after kainate injury was also investigated. Rats that had been injected with kainate plus lovastatin showed lower levels of cholesterol, 24-hydroxycholesterol, and 7-ketocholesterol at 1 and 2 weeks after injection, compared to rats injected with kainate and vehicle. Interestingly, the level of 24-hydroxycholesterol was ~ 7.2 ng/mg tissue (non-toxic range) after lovastatin treatment. This could be related to an observed protective effect of lovastatin on hippocampal neurons after kainate treatment. Nissl-stained, or MAP2 immunostained sections showed significantly lower neuronal death in the hippocampus, in kainate plus lovastatin

injected rats, compared to kainate plus vehicle injected rats. Lovastatin was also found to show neuroprotective effect on kainate-treated hippocampal slices.

Although high concentrations (10–25 μM) of lovastatin can suppress cell proliferation and induce apoptosis in various cell lines (Choi and Jung 1999; Crick et al. 1998; Garcia-Roman et al. 2001), low concentrations (4 μM) of lovastatin did not affect cell viability of cultured hippocampal neurons (Chou et al. 2003; Fassbender et al. 2001). The concentration of lovastatin (1 μM) used in the present study is therefore unlikely to cause cellular injury. The findings of neuroprotective effect of lovastatin in slice cultures support the notion that inhibition of excess cholesterol synthesis could have a neuroprotective effect, apart from its effects on the microvasculature (see below). Together, the above findings suggest that increased brain cholesterol synthesis and oxysterol formation play a role in propagation of neuronal death after kainate injury.

The findings of the present paper may have implications in neuropathology. The use of statins has been reported to reduce the risk of AD (Jick et al. 2000; Wolozin et al. 2000), and also improve the outcome after stroke (Jacobs 2004; Vaughan 2003). Statins have also been shown to protect cortical neurons from excitotoxicity in cell culture (Zacco et al. 2003).There are several ways in which statins could exert their beneficial effects. One possibility is that statins might upregulate brain endothelial nitric oxide synthase, thus increasing blood flow, inhibiting platelet aggregation, and improving neurologic outcome (Amin-Hanjani et al. 2001; Vaughan et al. 2001). A second possibility is that statins might have anti-inflammatory actions including reducing interleukin-1 and

tumor necrosis factor production, thus inhibiting the consequences of neuronal damage (Balduini et al. 2003). A third possibility is that statins may enhance brain plasticity by increasing vascular endothelial growth factor, angiogenesis, endogenous cell proliferation and neurogenesis, thus improving functional outcome after neuronal injury (Chen et al. 2003). A fourth possibility is that neuroprotective effects of statins may be related to preservation of copper/zinc superoxide dismutase activity (Kumagai et al. 2004). A fifth possibility, in view of the present study, is that the neuroprotective effect of statins may be related to decreased cholesterol and oxysterol synthesis in the brain areas undergoing neurodegeneration / neuroinflammation. It is to be noted, however, that severe depletion of cholesterol in the brain (> 23% by use of experimental compounds, compared to lovastatin, < 10%) could result in seizures (Serbanescu et al. 2004). Further studies are necessary to elucidate changes in brain oxysterols, and possible protective effect of statins on other forms of neuronal injury.

II. Expression, activity, and role of serine palmitoyltransferase in the rat hippocampus after kainate injury

1. Introduction

Ceramides or N-acylsphingosines are components of distinct domains or rafts, which serve the spatial organization of signaling molecules in the cell membrane. They can be generated by hydrolysis of sphingomyelin through the action of sphingomyelinases in cellular membranes (reviewed in Marchesini and Hannun 2004). Surface acid sphingomyelinase is activated by receptors or stress stimuli and generates ceramide that fuse small rafts to form large ceramide-enriched membrane platforms. The latter cluster receptor molecules and recruit intracellular signaling molecules to aggregated receptors (reviewed in Gulbins and Li 2006). Neutral, membrane-bound Mg^{2+}-independent sphingomyelinase activity is increased in response to TNFα, heat stress, ischemia/reperfusion, arachidonic acid, and glutathione depletion (Liu et al. 1998; reviewed in Levade and Jaffrezou 1999).

Besides sphingomyelin breakdown, ceramides could be generated by *de novo* synthesis. The first reaction in the biosynthetic pathway consists of condensation of serine and palmitoyl CoA, a reaction catalyzed by serine palmitoyltransferase (SPT). This enzyme consists of heterodimers of 53-kDa regulatory SPT1 and catalytic 63-kDa SPT2 subunits bound to the endoplasmic reticulum (Hanada et al. 1997; Hanada 2003). The resulting keto-sphinganine is reduced and acylated to dihydroceramide, and desaturated to ceramide (reviewed in Perry 2002). Ceramides could also be formed from sphingosine through the action of (dihydro)ceramide synthase (sphingosine N-acyltransferase). Ceramide biosynthesis is activated by free palmitoyl CoA, TNFα,

and chemotherapeutic agents, and could lead to apoptosis (Paumen et al. 1997; Xu et al. 1998).

Increased ceramide levels have been detected in the brains of patients with Alzheimer's disease (Han et al. 2002; 2005; Cutler et al. 2004b; Satoi et al. 2005) and HIV dementia (Haughey et al. 2004). Elevated levels of ceramide have also been detected in the brain after cerebral ischemia (Herr et al. 1999; Nakane et al. 2000; Takahashi et al. 2004; Ohtani et al. 2004) and status epilepticus (Mikati et al. 2003). Although previous studies have demonstrated a role for sphingomyelinase activity in ceramide accumulation during neurodegeneration (Yu et al. 2000; Alessenko et al. 2004), relatively little is known about possible contributions from ceramide biosynthetic activity. It has been suggested that sphingolipid biosynthesis is a necessary but potentially dangerous pathway that could lead to cell death (Merrill 2002).

Our previous study has shown significant increases in 16:0, 18:0, 20:0, 22:0 and 24:1 ceramide species and decreases in sphingomyelin species in the rat hippocampus after intracerebroventricular injection of the excitotoxin, kainate (Guan et al. 2006). The purpose of the present study is to elucidate the expression and activity of SPT in the rat hippocampus after kainate injury. Possible contributions of this enzyme to ceramide accumulation and neuronal injury after kainate treatment were also elucidated using hippocampal slice cultures.

2. Materials and Methods

2. 1. Animals and intracerebroventricular kainate injection

This was carried out as described in Chapter II, I. 2. 1 (Page 41).

2. 2. SPT expression by Western blot analyses

This was carried out as described in Chapter II, I. 2. 2 (Page 42). The PVDF membrane was then incubated overnight in primary antibody, a rabbit polyclonal antibody to SPT (Cayman 10005260, MI, USA, diluted 1 μg/ml in Tris buffered saline [TBS]). The affinity purified antibody to SPT was raised against amino acids 548-562 of the human SPT catalytic subunit, SPT2. Immunoreactivity was visualized using a chemiluminescent substrate (Supersignal West Pico, Pierce, Rockford, IL, USA). Equivalent protein loading was confirmed by re-probing of membrane with antibody to β-actin (Sigma, St Louis, MO, USA). Films were scanned and the densities of the bands measured using the Quantity One software (BioRad, CA). The densities of the SPT bands were normalized against those of β-actin and the ratios calculated. Possible significant differences in the mean ratios between the kainate and saline treated animals were analyzed using 1 way ANOVA with Bonferroni's multiple comparison post-hoc test. $P < 0.05$ was considered significant.

2. 3. SPT activity assay

Kainate-injected rats were sacrificed at 3 days and 2 weeks post-injection (8 rats at each time point. Controls consisted of saline-injected rats of 2 weeks post-injection, 6 rats). The animals were deeply anesthetized with an

intraperitoneal injection of Nembutal and decapitated. The right hippocampus was then rapidly removed. Material from two hippocampi were pooled as a single sample for analysis. SPT activity was assayed in microsomal fractions of the hippocampi as previously described (Merrill et al. 1985). The reaction mixture consisted of 100 mM Hepes (pH 8.3, Sigma), 5 mM DTT, 2.5 mM EDTA, and 50 μM pyridoxal phosphate (Sigma). Microsomal proteins (100-200 μg), 150 μM palmitoyl-CoA (Sigma) and 1 mM L-[^{3}H] serine (PerkinElmer, Waltham, Ma, USA) were added to the reaction mixture and incubated at 37 °C for 10 min. The reaction was terminated by addition of 0.2 ml of 0.5 M NH_4OH on ice. This was followed by addition of 1.5 ml of chloroform/methanol (1:2, v/v), 2 ml of 0.5 M NH_4OH, and 50 μg of sphinganine (Sigma) as a carrier. The aqueous phase was discarded, and the organic phase rinsed twice with 2 ml of water. A sample (0.8 ml) was then obtained and dried. Radioactivity was quantified using scintillation counting (Beckman, Fullerton, CA, USA). To correct for radioactivity that may not have been due to SPT activity, control assays were performed with each sample in the absence of palmitoyl-CoA. SPT activity was expressed as product formed/min·mg protein. Possible significant differences in mean SPT activity of samples from kainate or saline treated rats were analyzed using 1 way ANOVA with Bonferroni's multiple comparison post-hoc test. $P < 0.05$ was considered significant.

2. 4. SPT immunohistochemistry

2. 4. 1. Immunoperoxidase labeling

This was carried out as described in Chapter II, I. 2. 3. 1 (Page 43). The sections were then incubated overnight with primary antibody, a rabbit polyclonal a rabbit polyclonal antibody to SPT (Cayman, diluted to 1 µg/ml in PBS). Control sections were incubated with pre-immune rabbit serum or SPT immunizing peptide-absorbed antibody (Cayman) instead of primary antibody. The latter were prepared by incubating 20 µg/ml of SPT immunizing peptide with 1:1000 dilution of SPT antibody overnight, followed by centrifugation, and collection of the supernatant for immunostaining. They showed absence of labeling.

Quantitation of SPT labeled cells was carried out as described in Chapter II, I. 2. 3. 2 (Page 44).

2. 4. 2. Double immunofluorescence labeling

This was carried out as described in Chapter II, I. 2. 3. 4 (Page 45). The sections were then incubated overnight with polyclonal antibodies to SPT (diluted to 1 µg/ml in PBS) and mouse monoclonal antibody to GFAP (Chemicon, Temecula, CA, USA, diluted 1:1000). The sections were then washed three times in PBS, and incubated for 1 h at room temperature in 1:200 dilution of fluorescein isothiocyanate (FITC)-conjugated goat anti-mouse IgG, and Cy3-conjugated goat anti-rabbit IgG (Chemicon). They were mounted and examined using an Olympus FluoView FV500 confocal microscopy. Control sections incubated with SPT immunizing peptide-absorbed antibody or pre-immune rabbit serum instead of primary antibody. They showed absence of labeling.

2. 4. 3. Electron microscopy

This was carried out as described in Chapter II, I. 2. 3. 3 (Page 45).

2. 5. Hippocampal slice cultures

This was carried out as described in Chapter II, I. 2. 4 (Page 46).

2. 6. Electrospray ionization mass spectrometry (ESI-MS)

Hippocampal slices were treated with 100 μM kainate for 3 hours, followed by treatment with SPT inhibitors, ISP-1 (myriocin) (Sigma, M1177, 100 nM) or L-cycloserine (Sigma, 30018, 10 μM); a ceramide synthase inhibitor, fumonisin B1 (Sigma, F1147, 10 μM); or a neutral sphingomyelinase inhibitor, GW4869 (Sigma, D1692 10 μM) for 24 h. Controls consisted of untreated slices. The concentrations of ISP-1 (Furuya et al. 1998; Cutler et al. 2004b), fumonisin B1 (Merrill et al. 1993) and GW4869 (Luberto et al. 2002) have previously been shown to be effective in inhibiting the respective enzymes *in vitro*.

Each sample consisted of material pooled from 8-12 slices. Lipids were extracted using the protocol of Bligh and Dyer (1959). Briefly, 400 μl of chloroform-methanol (1:2, v/v) were added to 10 mg hippocampal slice homogenate and 1 μg of internal standards, C19-CER and C12-SPM were added. After 10 min incubation on ice, 300 μl of chloroform and 200 μl of 1 M hydrochloric acid (HCl) were added to the mixture and the lipids were isolated from the organic phase following centrifugation. The sample was vacuum dried

(Thermo Savant SpeedVac, Thermo, Waltham, MA, USA), resuspended in 1 ml of chloroform-methanol (1:1, v/v) and used for analysis.

Quantification of individual molecular species was performed using multiple reaction monitoring (MRM) with an Applied Biosystems 4000 Q-Trap mass spectrometer (Applied Biosystems, Foster City, CA). Typically 10 µl of samples were injected for analysis. The inlet system consisted of an autosampler and a pump and chloroform-methanol (1:1, v/v) at a flow rate of 200 µl/min was used as the mobile phase. In these experiments, the first quadrupole, Q1, was set to pass the precursor ion of interest to the collision cell, Q2, where it underwent collision induced dissociation. The third quadruple, Q3, was set to pass the structure specific product ion characteristic of the precursor lipid of interest. Each individual ion dissociation pathway was optimized with regard to collision energy to minimize variations in relative ion abundance due to differences in rates of dissociation. Ceramide or sphingomyelin levels were calculated relative to relevant internal standards. The mean of 4 samples from each treatment group was calculated, and possible significant differences between the means analyzed using 1 way ANOVA with Bonferroni's multiple comparison post-hoc test. $P < 0.05$ was considered significant.

2. 7. Quantification of cellular injury by microtubule associated protein (MAP2) immunolabeling

Hippocampal slices were treated with 100 µM kainate for 3 hours, followed by treatment with ISP-1 (1 nM, 10 nM and 100 nM) or LCS (0.1, 1, 10, and 100

μM). Controls consisted of untreated slices. The above concentration of kainate has previously been shown to be toxic to neurons in hippocampal slices (Lu et al. 2001). The slices were fixed at 24 h after treatment by immersion in 4% paraformaldehyde in 0.1 M phosphate buffer (pH 7.4). Polytetrafluoroethylene membranes were cut from the culture plate inserts, washed, and immunostained with the attached slices using an antibody to MAP2 (Sigma, diluted 1:500) to demonstrate viable neurons. The number of MAP2 positive cells in representative regions of CA fields of the hippocampal slices was then counted as described in Chapter II, I. 2. 3. 2 (Page 44). The mean of 6-8 slices in each treatment group was calculated, and possible significant differences in the means analyzed using 1 way ANOVA with Bonferroni's multiple comparison post-hoc test. $P < 0.05$ was considered significant.

2. 8. Quantitation of cellular injury by lactate dehydrogenase (LDH) assay

Hippocampal slice cultures were treated with 100 μM kainate for 3 hours, followed by treatment with ISP-1 (100 nM), LCS (10 μM), fumonisin B1 (10 μM), or GW4869 (10 μM) for 24 h. Controls consisted of untreated slices. Media from three culture wells (4 slices in each well) was pooled as a single sample, and analyzed using a LDH cytotoxicity detection kit (Roche, Mannheim, Germany) as follows: neuronal death = [(A-Min)/(Max- Min)]x100, in which A is LDH activity measured in media of test condition, Max is maximum LDH release after 3 h treatment with Triton X-100, defined as 100% of cell death, Min is the minimum LDH activity in media of untreated slices. The mean of four samples in each

treatment group was calculated, and possible significant differences between the means analyzed using 1 way ANOVA with Bonferroni's multiple comparison post-hoc test. $P < 0.05$ was considered significant.

3. Results

3. 1. SPT expression by Western blot analyses (Fig. 2. 1A, B)

The affinity purified polyclonal antibody to SPT detected a single band at ~65 kDa in saline- and kainate-injected rat hippocampus, consistent with the molecular weight of the SPT2 subunit (Batheja et al. 2003; Hanada 2003) (Fig 2. 1A). The antibody to β-actin reacted against a band at ~42 kDa. SPT protein level was similar between kainate- and saline-injected rats at 1 or 3 day post-injection, but was significantly greater in kainate injected rats at 1 and 2 weeks post-injection (Fig. 2. 1A, B).

3. 2. SPT activity assay (Fig. 2. 1C).

SPT activity was 28.4 ± 1.9 pmol/min·mg in the saline-injected rat hippocampus (Fig. 2. 1C). This is consistent with the results of a previous study (30.1 ± 4.2 pmol/min·mg in the normal rat brain) (Merrill et al. 1985). SPT activity was significantly increased at 2 weeks post-injection in kainate-injected rats compared to saline injected controls (Fig. 2. 1C).

3. 3. SPT immunohistochemistry (Fig. 2. 2 and 2. 3; Table 2. 1)

3. 3. 1. Immunoperoxidase labeling (Fig. 2. 2 and Table 2. 1)

Control rats

Light labeing for SPT (Fig. 2. 2A) was observed in pyramidal neurons in the CA fields of the hippocampus.

Three day post-kainate injection

Loss of neurons was observed in fields CA1 and CA3 of the hippocampus in Nissl stained sections (data not shown). The damage was more extensive on the side of the kainate injection, but was also observed on the contralateral side, possibly due to diffusion of the toxin via the ventricular system. Also, unilateral excitotoxicity can drive the commissural projections of CA3, which can cause a contralateral excitotoxicity and cell death (Yasuda et al. 2001). The lesioned areas showed loss of SPT immunolabeling in neurons, but occasional labeling in glial cells (Fig. 2. 2B).

One week post-kainate injection

Loss of neurons, and large numbers of glial cells were observed in fields CA1 and CA3 of the hippocampus in Nissl stained sections (data not shown). Increased labeling of glial cells was observed at this time (Fig. 2. 2C; Table 2. 1). The latter were double labeled with GFAP, a marker for astrocytes (see below).

Two week post-kainate injection

A further increase in number of SPT positive glial cells was observed at this time (Fig. 2. 2D, E; Table 2. 1).

Four week post-kainate injection

A decline in SPT (Fig. 2. 2F) immunoreactivity was observed, and the number of SPT immunolabeled glial cells was fewer than that at 2 week post-kainate injection (Table 2. 1).

3. 3. 2. Double immunofluorescence labeling (Fig. 2. 3A, B)

Immunolabeling for SPT was observed in glial cells in the kainate-lesioned hippocampus. The latter were double immunolabeled for GFAP, a marker for astrocytes (Fig. 2. 3 A, B).

3. 3. 3. Electron microscopy (Fig. 2. 3 C, D)

Dense immunoreactivity to SPT was observed in reactive glial cells at 2 weeks after kainate lesions. The nucleus contained fine heterochromatin clumps and the cytoplasm contained dense bundles of glial filaments characteristic of astrocytes (Fig. 2. 3C, D). Immunoreactivity was also present in end feet around blood vessels (Fig. 2. 3C, D).

3. 4. Role of SPT in kainate injury (Fig. 2. 4- Fig. 2. 6)

3. 4. 1. Effect on ceramide and sphingomyelin concentrations (Fig. 2. 4)

A significant increase in 16:0, 18:0 and 20:0 ceramide species was detected after kainate treatment (Fig. 2. 4A). Slices treated with kainate plus ISP-1, LCS, or fumonisin B1 showed significantly lower levels of several ceramide

species, compared to slices treated with kainate alone. LCS attenuated the kainate-induced increases in 16:0 and 20:0 ceramide, whereas ISP-1 and fumonisin B1 attenuated increases in 16:0, 18:0 and 20:0 ceramide. Slices treated with kainate plus GW4869 showed non-significant decrease in ceramide compared to slices treated with kainate alone (Fig. 2. 4A).

A trend to a decrease but non-significant was observed in several sphingomyelin species after kainate treatment. No change in sphingomyelin species was detected after treatment of slices with kainate plus inhibitors (Fig. 2. 4B). Possible significant differences were analyzed using 1 way ANOVA with Bonferroni's multiple comparison post-hoc test. $P < 0.05$ was considered significant.

3. 4. 2. Effect on MAP2 immunolabeling (Fig. 2. 5)

Kainate treatment resulted in a significant decrease in MAP2 immunoreactivity in the CA fields of hippocampal slices, compared to controls. Treatment of slices with 100 nM ISP-1 or 10 and 100 μM LCS significantly attenuated the kainate-induced decrease in MAP2 staining (Fig. 2. 5).

3. 4. 3. Effect on lactate dehydrogenase (LDH) release (Fig. 2. 6).

Kainate treatment resulted in a significant increase in LDH activity in the culture media compared to controls (Fig. 2. 6). Significantly lower LDH activity was detected in the culture media after treatment with kainate plus ISP1, LCS, or

fumonisin B1, compared to treatment with kainate alone. No significant difference was detected after treatment with kainate plus GW4869 (Fig. 2. 6).

4. Discussion

The present study aimed to determine the expression, activity, and possible role of the first enzyme in the ceramide biosynthetic pathway, SPT, after kainate-induced neuronal injury. Western blot analyses and enzyme activity assay were carried out to elucidate SPT expression and activity after intracerebroventricular kainate injections. SPT enzyme protein levels of the hippocampus remained at near baseline levels at 1-3 days after kainate injections, but increased significantly at 1 week and 2 weeks after kainate injection. The increase in enzyme protein was paralleled by significantly increased hippocampal SPT enzyme activity at two weeks post-kainate injection, compared to saline injected controls.

Immunohistochemical analyses showed baseline expression of SPT in neurons. This finding is consistent with a previous study which showed neuronal expression of the enzyme in the brain (Batheja et al. 2003). Kainate treatment resulted in decreased labeling in neurons but increased labeling in glial cells, in the affected CA fields. The number of SPT positive glial cells peaked at 2 weeks after kainate injection. The glial cells were double labeled for GFAP, confirming that they were astrocytes. Non-specific binding by the antibody is unlikely, since sections incubated with antigen-absorbed antibody showed absence of labeling.

In vitro studies were carried out using hippocampal slice cultures to

elucidate ceramide biosynthesis after kainate lesions. Kainate treatment resulted in significant increases in 16:0, 18:0 and 20:0 ceramide species. The greatest increase was in C18:0 ceramide. These results are similar to that observed after intracerebroventricular kainate injections (Guan et al. 2006). Slices which had been treated with kainate plus SPT inhibitors ISP-1 or LCS, or the ceramide synthase inhibitor fumonisin B1, showed significantly lower levels of 16:0, 18:0 and 20:0 ceramide species, compared to those treated with kainate alone. Treatment with a neutral sphingomyelinase inhibitor GW4869 resulted in no significant difference. A trend to a decrease, but non-significant, was detected in sphingomyelin after kainate treatment. Together, these findings indicate a role for ceramide biosynthesis contributing to the ceramide increase after kainate injury although additional effects of sphingomyelinases cannot be excluded.

A possible effect of ceramide biosynthesis in kainate injury was then investigated. Neuronal injury was determined by quantitation of MAP2 immunostaining of viable neurons in CA fields of hippocampal slices, and assay of LDH released into the culture media from damaged neurons. Addition of kainate to slices resulted in neuronal injury, as demonstrated by *decrease* in MAP2 immunolabeling of slices, but *increase* in LDH released into the culture media. Treatment of slices with kainate plus ISP-1 or LCS resulted in significantly reduced neuronal injury, compared to treatment with kainate alone. Treatment with GW4869 showed no significant protective effect. These results indicate that SPT might contribute to neuronal injury after kainate treatment. These findings are consistent with previous studies which showed that ISP-1 prevented A beta

induced death of hippocampal neurons (Cutler et al. 2004b). ISP-1 also attenuated ethanol-induced cell death in SK-N-SH neuroblastoma cells (Saito et al. 2005). ISP-1 or LCS could act by reducing ceramide biosynthesis in neurons or astrocytes even though decreased neuronal expression of SPT was observed after injury. Our data also showed significant kainate-induced cell death that was not inhibited by SPT inhibitors. This might be attributed to excitotoxicity / calcium mediated neuronal injury, which is well-known to play an important role in kainate injury (Mattson et al. 1991).

Ceramide causes apoptotic and non-apoptotic cell death in cultured neurons depending on model system and experimental conditions (Brugg et al. 1996; Sortino et al. 1999; Movsesyan et al. 2002; Kim et al. 2005). The C16:0 ceramide has been reported to be more potent than ceramides of other chain lengths in inducing apoptosis (Osawa et al. 2005). The mechanism of ceramide action may include: (a) Ceramide-mediated clustering of membrane receptors, thus enabling membrane domains to be involved in induction of apoptosis by death receptors (Dobrowsky and Carter 1998; reviewed in Gulbins and Li 2006), (b) formation of ceramide-mediated large protein permeable channels on the outer membrane of mitochondria (Siskind 2005). This could facilitate the release of proapoptotic proteins including cytochrome c from mitochondria to the cytoplasm, and trigger the induction of mitochondrial-dependent intrinsic caspase pathway (Stoica et al. 2005). (c) Besides apoptosis, ceramides could produce non-apoptotic, caspase-independent cell death through activation of cytosolic phospholipase $A_2\alpha$ ($cPLA_2\alpha$) in glial cells (Kim et al. 2005). Ceramide-1-

phosphate could facilitate translocation and activation of $cPLA_2\alpha$ directly and by a PKC-dependent pathway (Nakamura et al. 2006). This could lead to increased generation of arachidonic acid from membrane phospholipids, and formation of toxic lipid peroxidation products such as 4-hydroxynonenal (Farooqui et al. 2004).

Further studies are necessary to elucidate effects of inhibition of SPT after kainate injury *in vivo*, and possible roles of various sphingomyelinases in kainate injury.

III. Effect of apolipoprotein D on neuronal survival, cholesterol and lipid oxidation product formation after kainate-induced neuronal injury

1. Introduction

Apolipoprotein D (apoD) is a 169-amino acid glycoprotein that was originally identified as a component of high-density plasma lipoproteins (McConathy and Alaupovic 1973). ApoD is not a typical apolipoprotein, but belongs to the lipocalin superfamily of transporter proteins that carry various small hydrophobic ligands (Flower 1996). ApoD is widely expressed in both neural and non-neural tissues (Boyles et al.1990a; Provost et al. 1990; Seguin et al.1994). It is present in neurolemma cells and endoneurial fibroblasts in peripheral nerves (Boyles et al. 1990b), and oligodendrocytes, astrocytes, and perivascular cells in the brain (Boyles et al. 1990a; Smith et al. 1990; Patel et al. 1995; Navarro et al. 1998).

A 40-fold accumulation of apoD has been detected in the extracellular space of regenerating crushed rat nerve (Spreyer et al. 1990). An even more marked increase in apoD has also been reported in regenerating peripheral nerves of rabbits, and monkeys (Boyles et al. 1990a). Elevated apoD levels was present after experimental brain injury (Ong et al. 1997; Montpied et al. 1999, Franz et al. 1999; Terrisse et al. 1999), and in neurodegenerative conditions such as Alzheimer's disease (Terrisse et al. 1998; Thomas et al. 2003), Niemann–Pick type C disease (Suresh et al. 1998) and prion disease (Dandoy-Dron et al. 1998).

ApoD has the ability to bind several small hydrophobic ligands, including arachidonic acid, cholesterol, progesterone, porphyrins and heme-related molecules (Lea 1988; Peitsch and Boguski 1990; Boyles et al. 1990b; Morais-

Cabral et al. 1995; Patel et al. 1997). Although the exact physiological function for apoD in the brain is not known, the diversity of ligands transported by apoD suggests that it may have wide-ranging physiological cellular functions.

The excitotoxin, kainate, is commonly used to induce neuronal injury in studies of diseases of the CNS. KA treatment results in neuronal death in rat brain (Pohle and Rauca 1994; Lan et al. 2000; Boldyrev et al. 1999). We have previously shown a marked increase of apoD expression in the rat hippocampus after neuronal injury induced by kainate (Ong et al. 1997). The increase in apoD is paralleled by decreases in phospholipid levels and increases in arachidonic acid and cholesterol levels in the degenerating hippocampus (Farooqui et al. 2001, Guan et al. 2006; He et al. 2006). One possibility is that apoD may be upregulated in injured neurons as part of a cellular defense mechanism to bind and perhaps limit the increase in free arachidonic acid or cholesterol. The present study was therefore carried out to examine potential neuroprotective effects of apoD by regulating lipid abnormalities, in hippocampal slice cultures. The effect of oxidative stress on cultured fibroblasts from wild type and apoD knockout mice was also studied as a comparison.

2. Materials and methods

2. 1. hippocampal slice cultures

This was carried out as described in Chapter II, I. 2. 4 (page 46). After initial kainate treatment, cultures were incubated with 1) different concentrations of apoD, diluted in fresh serum-free medium 2) 10 μg/ml of apoD and 1:100

dilution of rabbit antibody to apoD, and 3) 10 µg/ml beta-lactoglobulin (BLG, Sigma). Beta-lactoglobulin is a lipocalin with limited affinity to cholesterol and arachidonic acid. Purified apoD protein from human breast cystic fluid was prepared by centrifugation at 35,000 g for 2 h, followed by dialysis of the aqueous phase against K_2HPO_4 10 mM pH 7.4, and hydroxyapatite in same buffer. ApoD elutes in the flow through and is concentrated on DEAE-agarose and eluted with 400 mM NaCl. Stock apoD and BLG (1 mg/ml) were dissolved in serum-free medium and sterilized through 0.22 µm filter for sterilization. Controls consisted of untreated slices.

2. 2. Quantitation of cellular injury by MAP2 immunolabeling

This was carried out as described in Chapter II, II. 2. 7 (page 75).

2. 3. Quantitation of cellular injury by LDH assay

This was carried out as described in Chapter II, II. 2. 8 (page 76).

2. 4. GC/MS analysis

2. 4. 1. Chemicals

High purity (> 99%) F_2-isoprostanes (F_2-isoPs), 8-iso-$PGF_{2\alpha}$ ($iPF_{2\alpha}$-III), and deuterium-labeled heavy isotopes 8-iso-$PGF_{2\alpha}$-d_4 (iPF2α-III-d4) and $iPF_{2\alpha}$-VI-d_4 were purchased from Cayman Chemical (Ann Arbor, MI, USA). Standards for cholesterol, 7-ketocholesterol, 5α-cholestane and ergosterol were purchased from Sigma (St Louis, MO, USA) and of at least 95% purity. 24S-

hydroxycholesterol (non-deuterated) was purchased from Medical Isotopes (Pelham, AL, USA). 5α-cholestane and ergosterol were used as internal standards. Standard solutions of cholesterol, oxysterols, 5α-cholestane and ergosterol were diluted in ethanol. Formic acid (Lancaster, England), ammonium hydroxide, potassium hydroxide, butylated hydroxytoluene (BHT), hydrochloric acid (Merck, Darmstadt, Germany), and hexane (Tedia, Fairfield, OH, USA) were of analytical grade. Methanol (EM Science, Darmstadt, Germany) and ethyl acetate (Fisher Scientific, UK) were of HPLC grade. N,O-bis(trimethylsilyl)trifluoroacetamide +1% trimethylchlorosilane (BSTFA+TMCS) silylating agent was obtained from Pierce Chemicals (Rockford, IL, USA). Pentafluorbenzylbromide (PFBBr) and N,N-diisopropylethylamine (DIPEA) were purchased from Sigma Chemicals. Oasis Mixed Anion Exchange (MAX) cartridges were from Waters Corp (Milford, MA, USA).

2. 4. 2. Lipid extraction

This was carried out as described in Chapter II, I. 2. 5. 2 (Page 49)

2. 4. 3. Lipid hydrolysis

2 ml of 0.5 M KOH (in 50% methanol) was added with 400 ng ergosterol and 10 µg 5α-cholestane, an internal standard for cholesterol and oxysterol analysis, and 20 µl mixed heavy isotopes (0.5 ng 8-iso-$PGF_{2\alpha}$-d_4 and 0.5 ng $iPF_{2\alpha}$), an internal standard for F_2-isoprostanes analysis, and the vial sealed under N_2. The lipid extract was hydrolyzed at 23°C for 2 h in the dark.

2. 4. 4. Mixed anion exchange solid phase extraction

2.7 ml formic acid (40 mM), 0.2 ml HCl (5 M) and 1 ml methanol were added and thoroughly mixed before loaded onto a 3 ml, 60 mg Oasis Mixed Anion Exchange (MAX) solid phase extraction column previously conditioned with 2 ml methanol and 2 ml formic acid (20 mM). The column was then washed with 2 ml 2% (v/v) ammonium hydroxide followed by 2 ml 40% methanol/formic acid. Cholesterol and oxysterols were eluted with 2 ml hexane followed by 2 ml ethyl acetate/hexane (30/70) and collected together into a glass tube, while isoprostanes are eluted with 1.6 ml ethyl acetate.

2. 4. 5. Derivatization

The eluted solvent was evaporated under N_2. Samples for cholesterol analysis were derivatized with 25 µl acetonitrile and 25 µl BSTFA with 1% TMCS for 30 min at room temperature and injected directly onto GC/MS. Samples for oxysterol analyses were derivatized with 50 µl acetonitrile and 50 µl BSTFA + 1% TMCS for 30 min at room temperature, evaporated to dryness under N_2 and reconstituted in 30 µl undecane before injection into the GC/MS. Samples for F_2-isoprostanes were firstly derivatized with 15 µl DIPEA (10% v/v acetonitrile) and 30 µl PFBBr (10% v/v acetonitrile) for 30 min then secondly derivatized with 20 µl acetonitrile and BSTFA with 40 µl 1% TMCS for 30 min at 40 ^{0}C for silylation of the F_2-isoPs. Samples were evaporated to dryness under N_2 and reconstituted in

30 µl undecane before injection onto GC/MS. GC/MS running will be described as below.

2. 4. 6. GC/MS analysis of cholesterol and oxysterols

This was carried out as described in Chapter II, I. 2. 5. 5- 2. 5. 7 (Page 50).

2. 4. 7. GC/MS analysis of F_2-isoprostanes

The derivatized samples were analyzed by a Hewlett-Packard 5973 mass selective detector interfaced with a Hewlett-Packard 6890 gas chromatograph, equipped with an automatic sampler and a computer workstation. The injection port and GC/MS interface were kept at 280 and 290 °C, respectively. The mass spectrometer was used in the negative chemical ionization (NCI) mode with the ion source and quadrapole at 150 and 106 °C, respectively, and the methane flow rate at 2 ml/min. Separations were carried out on a fused silica capillary column (30m x 0.2 mm i.d.) coated with cross-linked 5% phenylmethylsiloxane (film thickness 0.33 µm) (Agilent). Helium was the carrier gas with a flow rate of 1 ml/min. Derivatized samples (1 µl) were injected splitless into the GC injection port. The column temperature was maintained at 170 °C for 2 min, and then increased to 275 °C at 15 °C /min, then held at 275 °C for 11 min. Finally temperature was raised to 295 °C at 25 °C /min and held for 3 min. Emission energy was 250 µA. Selected ion monitoring was performed to monitor the carboxylate ion (M-181: loss of pentafluorobenzyl, $CH_2C_6F_5$) at ions m=z 569 for

8-iso-$PGF_{2\alpha}$ and at m=z 573 for deuterium-labeled (8-iso-$PGF_{2\alpha}$-d_4 and $iPF2_{\alpha}$-VI-d_4) internal standards. Quantitation was achieved by relating the peak area of the total F_2-isoPs with the sum of the 2 different F_2-isoPs' internal standard peaks. Concentration values were expressed as total F_2-isoPs per gram tissues and expressed as mean $\pm$ standard deviation.

2. 5. Statistical analysis

The results were subjected to statistical analyses, using 1 way ANOVA with Bonferroni's multiple comparison post-hoc test and Student's t-Tests. $P < 0.05$ was considered significant.

3. Results

3. 1. Effect of apoD on kainate-induced injury (Fig. 3. 1- Fig. 3. 3)

Treatment of hippocampal slice cultures with kainate (100 μM) for 3h caused neuronal injury in the hippocampal field CA1 and CA3. This was shown by the light microscopic observation of fewer MAP2 immunostained pyramidal neurons in hippocampal CA fields of kainate-treated slices compared to that in the untreated control slices (Fig. 3. 1 and 3. 2A). In addition, kainate-induced neuronal death was confirmed by increase in LDH activity in the culture media of kainate-treated slices compared to untreated control slices (Fig. 3. 2B).

ApoD treatment resulted in a dose-dependent neuroprotective effect on the kainate-injured hippocampal slices. There were a greater number of MAP2 immunostained pyramidal neurons in hippocampal CA fields of kainate and 10

μg/ml apoD, or kainate and 20 μg/ml apoD treated slices compared to the kainate-treated slices (Fig 3. 1). 10 μg/m ApoD protected about 53%, and 20 μg/ml apoD protected about 37% kainate-injured neurons in the CA fields. The neuroprotective effect was not detected in the kainate plus 1 μg/ml apoD or kainate plus 5 μg/ml apoD treated slices (Fig. 3. 1). Further examination of MAP2 immunostained pyramidal neurons in hippocampal subfields showed that post-treatment with 10 μg/ml apoD produced protection in CA1 and CA3 (Fig. 3. 2 A). The effect of apoD on neuronal survival was further studied LDH assay. Post-treatment of 10 μg/ml apoD significantly reduced LDH released from cultures after kainate treatment, confirming a neuroprotective effect of apoD (Fig 3. 2B).

In contrast to apoD, addition of the lipocalin, beta lactoglobulin (BLG), did not result in neuroprotection in the kainate-treated slices. Addition of apoD plus apoD antibody to slices also resulted in reduced neuroprotective effect compared to treatment with apoD alone (Fig. 3. 3)

3. 2. Effect of apoD on F_2-isoprostanes, cholesterol, and oxysterol levels in cultured hippocampal slices (Fig. 3. 4)

An increased level of the arachidonic peroxidation products, F_2-isoPs were detected in the kainate-treated slices, compared to untreated controls. The elevation in F_2-isoP level was modulated by treatment of slices with 10 μg/ml apoD (Fig. 3. 4A). Kainate treatment also resulted in significantly increased cholesterol, 7-ketocholesterol, and 24-hydroxycholesterol levels in slices, and these increases were similarly attenuated by apoD (Fig. 3. 4B, C, D).

3. 3. Effect of apoD on F_2-isoprostane and oxysterol levels in cultured fibroblasts after hydrogen peroxide treatment (Fig. 3. 5)

Similar levels of F_2-isoPs were detected in untreated fibroblasts from wild type or apoD knockout mice. After treatment with hydrogen peroxide for 4 and 8 h however, significantly greater increases in F_2-isoP levels were detected in fibroblasts from apoD knockout mice, compared to those from the wild type mice (Fig. 3. 5 A).

The levels of 7-ketocholesterol levels were also similar, between untreated fibroblasts from wild type- and apoD knockout mice, but significantly greater in the fibroblrasts from the apoD knockout mice, after treatment with hydrogen peroxide (Fig 3. 5C). No significant differences in cholesterol or 24-hydroxycholsterol levels were detected between wild type and apoD knockout fibroblasts, either in the untreated state or after hydrogen peroxide treatment (Fig 3. 5B, D).

4. Discussion

ApoD is a member of the lipocalin family of transport proteins, with ability to sequester small hydrophobic ligands such as arachidonic acid and cholesterol. The latter may be related to physiological function of the lipocalin. The present study was carried out to elucidate potential effects of exogenous apoD on neuronal survival and lipid oxidation products in hippocampal slices cultures, after kainate treatment. Slice cultures preserve several characteristics of the

intrahippocampal circuitry observed *in vivo*. Addition of kainate to hippocampal has also been shown to result in cell death, similar to the effect of kainate in intact animals (Lu et al. 2001). The results showed that apoD treatment dose-dependently resulted in protection of neurons against kainate-induced neuronal injury, as determined by MAP2 immunohistochemistry and assay of LDH released into the culture media. The neuroprotective effect of apoD was partially blocked by antibody to apoD. Neuroprotective effect was also not observed after application of another lipocalin, beta lactoglobulin, suggesting that the effect was perhaps specific to apoD.

There is increasing evidence that early alteration of lipid metabolism during injury may play a critical role in neuronal death (Relton et al. 1993; Geddes et al. 1997; Keller et al. 1997; Cutler et al. 2004b). Kainate treatment results in a rapid breakdown of phospholipids and accumulation of arachidonic acid (Farooqui et al. 2001). The increase in arachidonic acid is accompanied by increases in the level of its toxic lipid peroxidation product, 4-hydroxynonenal, suggesting that this could play a major role in neuronal death after kainate excitotoxicity (Ong et al. 1999; Lu et al. 2001). The present results showed that addition of apoD significantly modulated the levels of lipid peroxidation product F2-isoPs in hippocampal slice cultures after kainate treatment. The latter are stable decomposition products of arachidonic acid peroxidation, and one of the most reliable biomakers of oxidative stress (Roberts and Morrow 2000; Basu 2004). The results suggest that the neuroprotective effect of apoD may be due to its ability to bind arachidonic acid, thus resulting in reduction of its lipid

peroxidation products. Although F_2-isoPs were measured in this study due to their stability, it is possible that other more reactive and toxic lipid peroxidation products such as 4-hydroxynonenal (4-HNE) might also be reduced by apoD.

Another way in which apoD might exert its neuroprotective effect could be through binding to cholesterol. Our recent studies showed that there is an increased cholesterol synthesis in the hippocampus after kainate treatment (Ong et al. 2003; He et al. 2006). Since apoD is known to bind cholesterol (Patel et al. 1995; Suresh et al. 1998), one possibility is that apoD may sequester excess cholesterol in the degenerating hippocampus after kainate treatment, and prevent the formation of its oxidation products. This may have a neuroprotective function, since excess cholesterol oxidation products such as 7-ketocholesterol or 24-hydroxycholesterol are known to be toxic to neurons (Kolsch et al. 2001, Chang et al. 1998; He et al. 2006). The present study support this hypothesis, by showing that apoD treatment significantly modulates kainate-induced increases in 7-ketocholesterol and 24-hydroxycholesterol levels in hippocampal slices. Increased sequestration of cholesterol by apoD could reduce the content of both 7-ketocholesterol which is formed by direct oxidation of cholesterol (Miguet-Alfonsi et al. 2002), and 24-hydroxycholesterol, produced by the brain specific enzyme, cholesterol 24-hydroxylase (Russell 2000).

Together, the ability of apoD to prevent the formation of kainate-induced F_2-isoPs and oxysterols suggests that this lipocalin may be an important antioxidant protein in the brain. This was directly studied by comparing cell survival and lipid oxidation in fibroblasts from wild-type mice and apoD knockout

mice. Fibroblasts from apoD knockout mice showed reduced cell survival after hydrogen peroxide treatment. Similarly F_2-isoP, cholesterol, 7–ketocholesterol and 24-hydroxycholesterol levels were detected in untreated fibroblasts from both wild type and apoD knockout mice. In contrast, treatment with hydrogen peroxide treatment for 4h and 8h resulted in significantly greater F_2-isoP and 7-ketocholesterol levels in fibroblasts from apoD knockout mice, compared to those from the wild type mice. No significant difference in cholesterol and 24-hydroxycholsterol levels were detected between wild type and apoD knockout fibroblasts, consistent with the reported neuron-specific localization of cholesterol 24-hydroxylase (Russell 2000).

Besides kainate lesions, an increase in apoD levels has also been detected in the brain in neurodegenerative conditions such as Alzheimer's disease (Terrisse et al. 1998; Thomas et al. 2003), Niemann–Pick type C disease (Suresh et al. 1998) and prion disease (Dandoy-Dron et al. 1998). It is possible, in view of the present findings, that apo D might play a similar role in sequestering arachidonic acid and cholesterol, in the brain tissue in these conditions. Further studies are necessary to study signaling mechanisms that regulate apoD expression in the brain.

CHAPTER III

CONCLUSION

The brain is the organ with the second highest concentration of lipids, exceeded only by adipose tissue. There is increasing evidence that early alteration of lipid metabolism during injury may play a critical role on neuronal death in neurodegenerative diseases. Kainate intracerebroventricular injection in rat brain and kainate-treated hippocampal slice cultures are widely used as *in vivo* and *in vitro* models of neurodegeneration. Using these models, kainate treatment results in breakdown of phospholipids and accumulation of arachidonic acid. The increase in arachidonic acid is accompanied by increases in the level of the toxic lipid peroxidation product, 4-hydroxynonenal, suggesting that altered phospholipid metabolism and lipid peroxidation could play a major role in neuronal death after kainate excitotoxicity.

Beside phospholipids, alterations in other major membrane lipids such as cholesterol and ceramide have been implicated in many neurological diseases such as AD, PD or stroke. However, the role of misregulation of cholesterol and ceramide metabolism in neurodegeneration is poorly understood. The present study was carried out to elucidate the dysregulation of cholesterol and ceramide metabolism after kainate injury. The role of apoD in modulation of kainate-induced changed levels of lipid oxidative products and neurodegeneration was also elucidated.

Increased immunolabeling to cholesterol and the oxysterol biosynthetic enzyme, cholesterol 24-hydroxylase, was observed in the rat hippocampus after kainate lesions. This was accompanied by increased levels of cholesterol, 24-hydroxycholesterol (product of cholesterol 24-hydroxylase enzymatic activity) and

7-ketocholesterol in homogenates of the degenerating hippocampus, as detected by gas chromatography / mass spectrometry (GC/MS) *in vivo* and *in vitro*.

The *in vitro* results suggest that the increased cholesterol and oxysterols in brain tissue after kainate injury may be a consequence of increased cholesterol synthesis and cholesterol 24-hydroxylase expression in the degenerating brain tissue, and not only or primarily uptake from the bloodstream. In order to determine the possible neurotoxicity of oxysterol on hippocampal neurons, the hippocampal slices were treated with different concentrations of 24-hydroxycholesterol. The results showed that the lower concentration of 24-hydroxycholesterol (15 μM or ~7.2 ng/mg in normal tissue) was not toxic to hippocampal neurons, whereas the higher concentration (50 μM or ~26.2 ng/mg in kainate-treated tissue) was neurotoxic. These suggest that the level of 24-hydroxycholesterol encountered *in vivo* after kainate injury was sufficient to cause neuronal damage. Hippocampi from rats or organotypic slices that had been treated with kainate plus lovastatin showed significantly lower levels of cholesterol, 24-hydroxycholesterol, and 7-ketocholesterol, compared to those that had been treated with kainate only.

Lovastatin also modulated hippocampal neuronal loss after kainate treatment, *in vivo* and *in vitro*. Together, the above findings suggest alterations in cholesterol metabolism after neuronal injury may be induced by kainate. Increased brain cholesterol synthesis and oxysterol formation play a role in propagation of neuronal death after kainate injury, and brain permeable statins such as lovastatin could have a neuroprotective effect by limiting the oxysterol

levels in brain areas undergoing neurodegeneration.

An increased ceramide level has also been shown in the kainate-injured brain by lipidomic analysis. Ceramide accumulation derives from a biosynthsis or from breakdown of sphingomyelin. In this study, increased expression of SPT, the first enzyme in the ceramide biosynthetic pathway was shown in reactive astrocytes of the hippocampus after kainate injections. The increase in enzyme expression was paralleled by increased SPT enzyme activity in the hippocampus at two weeks post-kainate injection. *In vitro* ESI/MS studies showed that treatment of hippocampal slice cultures with the SPT inhibitors ISP-1 and L-cycloserine modulated increases in 16:0, 18:0 and 20:0 ceramide species. A possible effect of ceramide biosynthesis in kainate injury was also investigated. Neuronal injury was determined by quantitation of MAP2 immunostaining of viable neurons in CA fields of hippocampal slices, and by assay of LDH released into the culture. Treatment of hippocampal slices with SPT inhibitors partially reduced kainate-induced cell death. The above findings indicate changes in another major membrane lipid, ceramide, after kainate-induced neuronal injury. They also suggest that increased SPT activity and resulting accumulation of ceramide might contribute to neuronal injury after kainate excitotoxicity.

These finding suggest that the decreased phospholipids, increased lipid peroxidation, arachidonic acid, ceramide biosynthesis and cholesterol synthesis are involved in the neuronal injury induced by kainate. Prevention of these lipid changes may confer neuroprotection. Inhibition of abnormal kainate-induced accumulation of cholesterol and ceramide by lovastatin and SPT inhibitors, was

shown to prevent neural injury. The effect of a lipocalin, apoD, on the neuronal injury after kainate treatment was also investigated since it can carry various small hydrophobic ligands such as arachidonic acid and cholesterol. A previous study showed a marked increase of apoD expression in the rat hippocampus induced by kainate (Ong et al. 1997). The present study was carried out to examine potential effects of apoD on neuronal survival after kainate injury. Addition of purified human apoD to kainate-treated hippocampal slice cultures resulted in reduction in neuronal death, and modulation of kainate-induced increases in arachidonic oxidation product (F_2-isoprostanes), cholesterol, 24-hydroxycholesterol and 7-ketocholesterol. The results showed that the neuroprotective effect of apoD may be due to its ability to bind arachidonic acid, thus resulting in reduction of lipid peroxidation products, and its ability to prevent the formation of neurotoxic cholesterol oxidation products by regulating cholesterol metabolism. Fibroblasts from apoD knockout mice showed increased F_2-isoprostane and 7-ketocholesterol levels after hydrogen peroxide-induced oxidative stress, suggesting that this lipocalin may be an important antioxidant in the brain. No significant difference in 24-hydroxycholsterol level was detected between wild type and apoD knockout fibroblasts, which is consistent with the reported neuron-specific localization of cholesterol 24-hydroxylase.

Phospholipids, cholesterol and sphingolipids in the brain are indispensable. Interactions among their mediators are not only necessary for normal function and survival of neurons but also for their death. Kainate can cause excitotoxic neuronal death through interacting with kainic acid-type receptors in neurons,

which induces neuronal Ca^{2+} overloading. The alteration in Ca^{2+} homeostasis and its short duration may lead to the degradation of phospholipids by the activation of PLA_2 and subsequent arachidonic acid cascade. Arachidonic acid sets a stage to genarate oxidative stress. Oxidative stress and kainate-induced abnormally accumulated ceramide may be important factors that promote the increased cholesterol levels in kainate-treated tissue. Studies of non-neuronal and neuronal cells have shown that oxidative stress and ceramide production can induce the accumulation of cholesterol in cells by activating sterol regulatory element binding protein (SREBP), a family of transcription factors regulating synthesis of cholesterol (Zager and Kalhorn 2000, Culter et al. 2004). Depleted hippocampal neurons of ceramide with ISP-1 showed inhibition effect on the cholesterol level (Culter et al. 2004). Oxidative stress, which alters membrane lipid metabolism, may result in increased amounts of ceramides and cholesterols. The derangements of sphingolipid and cholesterol metabolism, in combination with AA-induced oxidative stress may cause synaptic dysfunction and neuronal degeneration.

Taken together, these findings indicate that deleterious changes in lipid homeostasis and signaling may be a key factor in the onset and progression of pathologies of the nervous system. Beside the dysregulation of membrane phospholipids, the misregulation of the other two major membrane lipids, cholesterol and ceramide, was also found in kainate-lesioned hippocampus. Similar to the degraded phospholipids, abnormally accumulated cholesterol and ceramide after kainate injury may contribute to neuronal cell. The results are

useful for understanding the mechanism of dysregulation of lipids involved in the pathology of neurodegeneration (Fig. 4). Prevention of dysregulated lipid metabolism may confer neuroprotection and provide clues to the development of pharmaceutical strategies to treat neurodegenerative disorders.

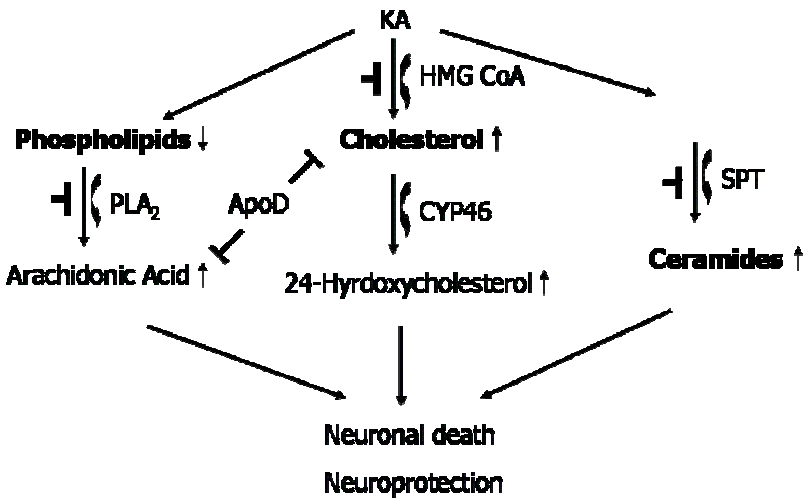

Figure 4. Lipid alterations after KA injury

CHAPTER IV

REFERENCES

Adibhatla RM, Hatcher JF, Dempsey RJ (2006) Lipids and lipidomics in brain injury and diseases. AAPS J 8:E314-21

Alberts et al (1994) Molecular Biology of the Cell, Third edition, Garland Publishing, NY

Alessenko AV, Bugrova AE, Dudnik LB (2004) Connection of lipid peroxide oxidation with the sphingomyelin pathway in the development of Alzheimer's disease. Biochem Soc Trans 32:144–146

Amin-Hanjani S, Stagliano NE, Yamada M (2001) Mevastatin, an HMG-CoA reductase inhibitor, reduces stroke damage and upregulates endothelial nitric oxide synthase in mice. Stroke 32:980-986

Andersson M, Elmberger PG, Edlund C, Kristensson K, Dallner G (1990) Rates of cholesterol, ubiquinone, dolichol and dolichyl-P biosynthesis in rat brain slices. FEBS Lett 269:15-18

Arendash GW, Millard WJ, Dunn AJ, Meyer EM (1987) Long-term neuropathological and neurochemical effects of nucleus basalis lesions in the rat. Science 238:952-956

Arundine M, Tymianski M (2003) Molecular mechanisms of calcium-dependent neurodegeneration in excitotoxicity. Cell Calcium 34:325-337

Balazs R, Hack N (1990) Trophic effects of excitatory amino acids in the developing nervous system. Adv Exp Med Biol 268:221-228

Balbin M, Freije JM, Fueyo A, Sanchez LM, Lopez-Otin C (1990) Apolipoprotein D is the major protein component in cyst fluid from women with human breast gross cystic disease. Biochem J 271:803-807

Balduini W, Mazzoni E, Carloni S (2003) Prophylactic but not delayed administration of simvastatin protects against long-lasting cognitive and morphological consequences of neonatal hypoxic-ischemic brain injury, reduces interleukin-1β and tumor necrosis factor-α mRNA induction, and does not affect endothelial nitric oxide synthase expression. Stroke 34:2007-2012

Basu S (2004) Isoprostanes: novel bioactive products of lipid peroxidation. Free Radic Re 38:105–122

Batheja AD, Uhlinger DJ, Carton JM, Ho G, D'Andrea MR (2003) Characterization of serine palmitoyltransferase in normal human tissues. J Histochem Cytochem 51:687-696

Ben-Ari Y, Cossart R (2000) Kainate, a double agent that generates seizures: two decades of progress. Trends Neurosci 23:580-587

Bevers EM, Comfurius P, Dekkers DW, Harmsma M and Zwaal RF (1998) Transmembrane phospholipid distribution in blood cells: controlmechanisms and pathophysiological significance. Biol Chem 379:973–986

Bieberich E, Mackinnon S, Silva J, Yu RK (2001) Regulation of apoptosis during neuronal differentiation by ceramide and b-series complex gangliosides. J Biol Chem 276:44396-44404

Bing G, McMillian M, Kim H, Pennypacker K, Feng Z, Qi Q, Kong LY, Iadarola M, Hong JS (1996) Long-term expression of the 35,000 mol. Wt fos-related antigen in rat brain after kainic acid treatment. Neuroscience 73:1159-1174

Bionda C, Portoukalian J, Schmitt D, Rodriguez-Lafrasse C, Ardail D (2004) Subcellular compartmentalization of ceramide metabolism: MAM (mitochondria-associated membrane) and/or mitochondria? Biochem J 382:527-533

Björkhem I (2006) Crossing the barrier: oxysterols as cholesterol transporters and metabolic modulators in the brain. J Intern Med 260:493-508

Björkhem I, Lütjohann D, Breuer O, Sakinis A, Wennmalm A (1997) Importance of a novel oxidative mechanism for elimination of brain cholesterol: Turnover of cholesterol and 24(S)-hydroxycholesterol in rat brain as measured with $18O_2$ techniques in vivo and in vitro. J Biol Chem 272: 30178–30184

Björkhem I, Lütjohann D, Diczfalusy U, Stahle L, Ahlborg G, Wahren J (1998) Cholesterol homeostasis in human brain: turnover of 24S-hydroxycholesterol and evidence for a cerebral origin of most of this oxysterol in the circulation. J Lipid Res 39:1594–1600

Björkhem I, Diczfalusy U, Lütjohann D (1999) Removal of cholesterol from extrahepatic sources by oxidative mechanisms. Curr Opin Lipidol 10:161-165

Björkhem I, Diczfalusy U (2002) Oxysterols: friends, foes, or just fellow passengers? Arterioscler Thromb Vasc Biol 22:734-42

Björkhem I, Meaney S (2004) Brain cholesterol: long secret life behind a barrier. Arterioscler Thromb Vasc Biol 24:806–815

Bligh EG, Dyer WJ (1959) A rapid method of total lipid extraction and purification. Can J Biochem Physiol 37:911-917

Bock J, Szabo I, Gamper N, Adams C, Gulbins E (2003) Ceramide inhibits the potassium channel Kv1.3 by the formation of membrane platforms. Biochem Biophys Res Commun 305:890-897

Bogdanovic N, Bretillon L, Lund EG (2001) On the turnover of brain cholesterol in patients with Alzheimer's disease. Abnormal induction of the cholesterol-catabolic enzyme CYP46 in glial cells. Neurosci Lett 314:45-48

Boldyrev A, Song R, Lawrence D, Carpenter DO (1999) Carnosine protects against excitotoxic cell death independently of effects on reactive oxygen species. Neuroscience 94:571-517

Bollinger CR, Teichgraber V, Gulbins E (2005) Ceramide-enriched membrane domains. Biochim Biophys Acta 1746:284-294

Bondy SC, LeBel CP (1993) The relationship between excitotoxicity and oxidative stress in the central nervous system. Free Radic Biol Med 14:633-642

Bourre JM, Clement M, Gerard D, Legrand R, Chaudiere J (1990) Precursors for cholesterol synthesis (7-dehydrocholesterol,7-dehydrodesmosterol, and desmosterol): cholesterol/7-dehydrocholesterol ratio as an index of development and aging in PNS but not in CNS. J Neurochem 54:1196-1199

Boyles JK, Notterpek LM, Wardell MR, Rall SC Jr (1990a) Identification, characterization, and tissue distribution of apolipoprotein D in the rat. J Lipid Res 31:2243-2256

Boyles JK, Notterpek LM, Anderson LJ (1990b) Accumulation of apolipoproteins in the regenerating and remyelinating mammalian peripheral nerve. Identification of apolipoprotein D, apolipoprotein A-IV, apolipoprotein E, and apolipoprotein A-I. J Biol Chem 265:17805-17815

Bretillon L, Siden A, Wahlund LO, Lütjohann D, Minthon L, Crisby M (2000) Plasma levels of 24S-hydroxycholesterol in patients with neurological diseases. Neurosci Lett 293:87–90

Brown AJ, Leong SL, Dean RT, Jessup W (1997) 7-Hydroperoxycholesterol and its products in oxidized low density lipoprotein and human atherosclerotic plaque. J Lipid Res 38:1730-1745

Brown J 3rd, Theisler C, Silberman S (2004) Differential expression of cholesterol hydroxylases in Alzheimer's disease. J Biol Chem 279:34674-34812

Brown MS, Goldstein JL (1980) Multivalent feedback regulation of HMG CoA reductase, a control mechanism coordinating isoprenoid synthesis and cell

growth. J Lipid Res 21:505-517

Bruce AJ, Baudry M (1995) Oxygen free radicals in rat limbic structures after kainate-induced seizures. Free Radic Biol Med 18:993-1002

Brugg B, Michel PP, Agid Y, Ruberg M (1996) Ceramide induces apoptosis in cultured mesencephalic neurons. J Neurochem 66:733–739

Buhaescu I, Izzedine H (2007) Mevalonate pathway: a review of clinical and therapeutical implications.Clin Biochem 40:575-584

Camandola S, Poli G, Mattson MP (2000) The lipid peroxidation product 4-hydroxy-2,3-nonenal increases AP-1-binding activity through caspase activation in neurons. J Neurochem 74:159–168

Cameron PL, Ruffin JW, Bollag R, Rasmussen H, Cameron RS (1997) Identification of caveolin and caveolin-related proteins in the brain. J Neurosci 17:9520-9535

Capell A, Beher D, Prokop S, Steiner H, Kaether C, Shearman MS, Haass C (2005) γ-Secretase complex assembly within the early secretory pathway. J Biol Chem 280:6471-6478

Garcia-Roman N, Alvarez AM, Toro MJ, Montes A, Lorenzo MJ (2001) Lovastatin induces apoptosis of spontaneously immortalized rat brain neuroblasts: involvement of nonsterol isoprenoid biosynthesis inhibition. Mol Cell Neurosci 17:329-341

Carrer DC, Maggio B (1999) Phase behavior and molecular interactions in mixtures of ceramide with dipalmitoylphosphatidylcholine. J Lipid Res 40:1978-1989

Castro GR, Fielding CJ (1985) Effects of postprandial lipemia on plasma cholesterol metabolism. J Clin Invest 75:874-882

Cavender CP, Turley SD, Dietschy JM (1995) Sterol metabolism in fetal, newborn, and suckled lambs and their response to cholesterol after weaning. Am J Physiol 269:E331-340

Centeno F, Mora A, Fuentes JM, Soler G, Claro E (1998) Partial lithiumassociated protection against apoptosis induced by C2-ceramide in cerebellar granule neurons. NeuroReport 9:4199–4203

Chang JY, Liu LZ (1998) Neurotoxicity of cholesterol oxides on cultured cerebellar granule cells. Neurochem Int 32:317-323

Chen J, Zhang ZG, Li Y (2003) Statins induce angiogenesis, neurogenesis, and synaptogenesis after stroke. Ann Neurol 53:743-751

Chen Y, Ginis I, Hallenbeck JM (2001) The protective effect of ceramide in immature rat brain hypoxia-ischemia involves up-regulation of bcl-2 and reduction of TUNEL-positive cells. J Cereb Blood Flow Metab 21:34–40

Choi DW (1987) Ionic dependence of glutamate neurotoxicity. J Neurosci 7:369–379

Choi JW, Jung SE (1999) Lovastatin-induced proliferation inhibition and apoptosis in C6 glial cells. J Pharmacol Exp Ther 289:572-579

Chou YC, Lin SB, Tsai LH, Tsai HI, Lin CM (2003) Cholesterol deficiency increases the vulnerability of hippocampal glia in primary culture to glutamate-induced excitotoxicity. Neurochem Int 43:197-209

Christie RH, Chung H, Rebeck GW, Strickland D, Hyman BT (1996) Expression of the very low-density lipoprotein receptor (VLDL-r), an apolipoprotein-E receptor, in the central nervous system and in Alzheimer's disease. J Neuropathol Exp Neurol5:491-498

Colombaioni L, Garcia-Gil M (2004) Sphingolipid metabolites in neural signalling and function. Brain Res Brain Res Rev 46:328–355

Cook RP (1958) Cholesterol, Chemistry, biochemistry and pathology. New York:Academic Press

Cordy JM, Hussain I, Dingwall C, Hooper NM, Turner AJ (2003) Exclusively targeting beta-secretase to lipid rafts by GPI-anchor addition up-regulates beta-site processing of the amyloid precursor protein. Proc Natl Acad Sci USA 100:11735–11740

Cornea RL, Thomas DD (1994) Effects of membrane thickness on the molecular dynamics and enzymatic activity of reconstituted Ca-ATPase. Biochemistry 33:2912-2920

Coyle JT, Schwarcz R (1976) Lesion of striatal neurones with kainic acid provides a model for Huntington's chorea. Nature 263:244-246

Coyle JT, Ferkany JW, Zaczek R (1983) Kainic acid: insights from a neurotoxin into the pathophysiology of Huntington's disease. Neurobehav Toxicol Teratol 5:617-624

Cremesti AE, Goni FM, Kolesnick R (2002) Role of sphingomyelinase and ceramide in modulating rafts: do biophysical properties determine biologic outcome? FEBS Lett 531:47-53

Cremona O, De Camilli P (2001) Phosphoinositides in membrane traffic at the synapse. J Cell Sci 114:1041–1052

Crick DC, Andres DA, Danesi R, Macchia M, Waechter CJ (1998) Geranylgeraniol overcomes the block of cell proliferation by lovastatin in C6 glioma cells. J Neurochem 70:2397-2405

Cutler RG, Haughey NJ, Tammara A, McArthur JC, Nath A, Reid R, Vargas DL, Pardo CA, Mattson MP (2004a) Dysregulation of sphingolipid and sterol metabolism by ApoE4 in HIV dementia. Neurology 63:626–630

Cutler RG, Kelly J, Storie K, Pedersen WA, Tammara A, Hatanpaa K, Troncoso JC, Mattson MP (2004b) Involvement of oxidative stress-induced abnormalities in ceramide and cholesterol metabolism in brain aging and Alzheimer's disease. Proc Natl Acad Sci U S A 101:2070-2075

Dandoy-Dron F, Guillo F, Benboudjema L, Deslys JP, Lasmezas C, Dormont D, Tovey MG, Dron M (1998) Gene expression in scrapie. Cloning of a new scrapie-responsive gene and the identification of increased levels of seven other mRNA transcripts. J Biol Chem 273:7691-7697

Dawkins JL, Hulme DJ, Brahmbhatt SB, Auer-Grumbach M, Nicholson GA (2001) Mutations in SPTLC1, encoding serine palmitoyltransferase, long chain base subunit-1, cause hereditary sensory neuropathy type I. Nat Genet 27:309-312

de Chaves EP, Bussiere M, MacInnis B, Vance DE, Campenot RB, Vance JE (2000) Ceramide inhibits axonal growth and nerve growth factor uptake without compromising the viability of sympathetic neurons. J Biol Chem 276:36207–36214

Decker T, Lohmann-Matthes ML (1988)A quick and simple method for the quantitation of lactate dehydrogenase release in measurements of cellular cytotoxicity and tumor necrosis factor (TNF) activity. J Immunol Methods 115:61-69

Dietschy JM, Kita T, Suckling KE, Goldstein JL, Brown MS (1983) Cholesterol synthesis in vivo and in vitro in the WHHL rabbit, an animal with defective low density lipoprotein receptors. J Lipid Res 24:469-480

Dietschy JM, Turley SD (2001) Cholesterol metabolism in the brain. Curr Opin Lipidol 12: 105–112

Dietschy JM, Turley SD (2004) Thematic review series: brain Lipids. Cholesterol metabolism in the central nervous system during early development and in the mature animal. J Lipid Res 45:1375-1397

Dobrowsky RT, Carter BD (1998) Coupling of the p75 neurotrophin receptor to sphingolipid signaling. Ann N Y Acad Sci 845:32-45

Drayna DT, Fielding C, McLean J, Baer B, Castro G, Chen E, Comstock L, Henzel W, Kohr W, Rhee L (1986) Cloning and expression of human apolipoprotein D cDNA. J Biol Chem 261:16535-16539

Drayna DT, McLean JW, Wion KL, Trent JM, Drabkin HA, Lawn RM (1987) Human apolipoprotein D gene: gene sequence, chromosome localization, and homology to the alpha 2u-globulin superfamily. DNA 6:199-204

Eckert GP, Cairns NJ, Maras A, Gattaz WF, Muller WE (2000) Cholesterol modulates the membrane-disordering effects of beta-amyloid peptides in the hippocampus: specific changes in Alzheimer's disease. Dement Geriatr Cogn Disord 11:181-186

Edgar AD, Strosznajder J, Horrocks LA (1982) Activation of ethanolamine phospholipase A_2 in brain during ischemia. J Neurochem 39:1111–1116

Edsall LC, Cuvillier O, Twitty S, Spiegel S, Milstien S (2001) Sphingosine kinase expression regulates apoptosis and caspase activation in PC12 cells. J Neurochem 76:1573-1584

Ellison DW, Beal MF, Martin JB (1987) Phosphoethanolamine and ethanolamine are decreased in Alzheimer's disease and Huntington's disease. Brain Res 417:389-392

Fahy E, Subramaniam S, Brown HA, Glass CK, Merrill Jr AH,Murphy RC, Raetz CRH, Russell DW, Seyama Y, Shaw W,Shimizu T, Spener F, van Meer G, VanNieuwenhze MS, White SH, Witztum J, Dennis EA (2005) A comprehensive classification system for lipids. J Lipid Res 46: 839–861

Falluel-Morel A, Vaudry D, Aubert N, Galas L, Benard M, Basille M, Fontaine M, Fournier A, Vaudry A, Gonzalez BJ (2005) Pituitary adenylate cyclase-activating polypeptide prevents the effects of ceramides on migration, neurite outgrowth, and cytoskeleton remodeling. Proc Natl Acad Sci USA 102:2637–2642

Fan QW, Yu W, Gong JS, Zou K, Sawamura N, Senda T, Yanagisawa K, Michikawa M (2002) Cholesterol-dependent modulation of dendrite

outgrowth and microtubule stability in cultured neurons. J Neurochem 80:178-190

Farooqui AA and Horrocks LA (1985) Metabolic and functional aspects of neural membrane phospholipids. In: Horrocks LA, Kanfer JN, Porcellati G (Eds) Phospholipids in the Nervous System: Physiological Role. vol. 2. Raven Press New York pp: 341–348

Farooqui AA, Liss L, Horrocks LA (1990) Elevated activities of lipases and lysophospholipases in Alzheimer's disease. Dementia 1:208–214

Farooqui AA, Horrocks LA (1991) Excitatory amino acid receptors, neural membrane phospholipid metabolism and neurological disorders. Brain Res Rev 16:171–191

Farooqui AA, Horrocks LA (1994) Excitotoxicity and neurological disorders: involvement of membrane phospholipids. Int Rev Neurobiol 36:267–323

Farooqui AA, Yang HC, Horrocks LA (1997) Involvement of phospholipase A_2 in neurodegeneration. Neurochem Int 30:517–522

Farooqui AA, Horrocks LA (1998) Plasmalogen-selective phospholipase A_2 and its involvement in Alzheimer's disease. Biochem Soc Trans 26:243–246

Farooqui AA, Horrocks LA, Farooqui T (2000a) Glycerophospholipids in brain: Their metabolism, incorporation into membranes, functions, and involvement in neurological disorders. Chem Phys Lipids 106:1–29

Farooqui AA, Ong WY, Horrocks LA, Farooqui T (2000b) Brain cytosolic phospholipase A_2: Localization, role, and involvement in neurological diseases. Neuroscientist 6:169–180

Farooqui AA, Horrocks LA, Farooqui T (2000c) Deacylation and reacylation of neural membrane glycerophospholipids. J Mol Neurosci 14:123-135

Farooqui AA, Horrocks LA (2001) Plasmalogens, phospholipase A_2, and docosahexaenoic acid turnover in brain tissue. J Mol Neurosci 16:263-272

Farooqui AA, Ong WY, Lu XR, Halliwell B, Horrocks LA (2001) Neurochemical consequences of kainate-induced toxicity in brain: involvement of arachidonic acid release and prevention of toxicity by phospholipase A_2 inhibitors. Brain Res Brain Res Rev 38:61-78

Farooqui AA, Ong WY, Horrocks LA (2004) Biochemical aspects of neurodegeneration in human brain: involvement of neural membrane phospholipids and phospholipase A_2. Neurochem Res 29:1961-1977

Fassbender K, Simons M, Bergmann C, Stroick M, Lütjohann D, Keller P, Runz H, Kuhl S, Bertsch T, von Bergmann K, Hennerici M, Beyreuther K, Hartmann T (2001) Simvastatin strongly reduces levels of Alzheimer's disease β -amyloid peptides Aβ42 and Aβ40 *in vitro* and *in vivo*. Proc Natl Acad Sci USA 98:5856-5861

Flower DR (1996) The lipocalin protein family: structure and function. Biochem J 15:1-14

Folch J, Lees M, Sloane Stanley GH (1957) A simple method for the isolation and purification of total lipides from animal tissues. J Biol Chem 226:497-509

Franz G, Reindl M, Patel SC, Beer I, Unterrischter I, Berger T, Schmutzhard E (1999) Increased expression of apolipoprotein D following experimental traumatic brain injury. J Neurochem 73:615-625

Furukawa K, Mattson MP (1998) The transcription factor NF-κB mediates increases in calcium currents and decreases in NMDA- and AMPA/kainate-induced currents induced by tumor necrosis factor-α in hippocampal neurons. J Neurochem 70:1876–1886

Furuya S, Ono K, Hirabayashi Y (1995) Sphingolipid biosynthesis is necessary for dendrite growth and survival of cerebellar Purkinje cells in culture. J Neurochem 65:1551–1561

Furuya S, Mitoma J, Makino A, Hirabayashi Y (1998) Ceramide and its interconvertible metabolite sphingosine function as indispensable lipid factors involved in survival and dendritic differentiation of cerebellar Purkinje cells. J Neurochem 71:366–377

Garcia-Roman N, Alvarez AM, Toro MJ, Montes A, Lorenzo MJ (2001) Lovastatin induces apoptosis of spontaneously immortalized rat brain neuroblasts: involvement of nonsterol isoprenoid biosynthesis inhibition. Mol Cell Neurosci 17:329-341

Gattaz WF, Brunner L (1996) Phospholipase A_2 and the hypofrontality hypothesis of schizophrenia. Prostaglandins Leukot. Essent Fatty Acids 55:109–113

Geddes JW, Panchalingam K, Keller JN, Pettegrew JW (1997) Elevated phosphocholine and phosphatidylcholine following rat entorhinal cortex lesions. Neurobiol Aging 18: 305–308

Gill JS, Windebank AJ (2000) Ceramide initiates NFkappaB-mediated caspase activation in neuronal apoptosis. Neurobiol DiS 7:448–461

Goodman Y, Mattson MP (1996) Ceramide protects hippocampal neurons against excitotoxic and oxidative insults, and amyloid beta-peptide toxicity. J Neurochem 66:869–872

Gordon EL, Danielsson PE, Nguyen TS, Winn HR (1991) A comparison of primary cultures of rat cerebral microvascular endothelial cells to rat aortic endothelial cells. In Vitro Cell Dev Biol 27A:312-326

Gross RW, Jenkins CM, Yang J, Mancuso DJ, Han X (2005)Functional lipidomics: the roles of specialized lipids and lipid-protein interactions in modulating neuronal function. Prostaglandins Other Lipid Mediat 77:52-64

Guan XL, He X, Ong WY, Yeo WK, Shui GH, Wenk MR (2006) Non-targeted profiling of lipids during kainate-induced neuronal injury. FASEB J 20:1152-1161

Gulbins E, Li PL (2006) Physiological and pathophysiological aspects of ceramide. Am J Physiol Regul Integr Comp Physiol 290:R11-26

Haines TH (2001) Do sterols reduce proton and sodium leaks through lipid bilayers? Prog Lipid Res 40:299–324

Hakomori S (1981) Glycosphingolipids in cellular interaction, differentiation, and oncogenesis. Annu Rev Biochem 50:733-764

Halliwell B (1994) Free radicals and antioxidants: a personal view. Nutr Rev 52:253–265

Han X, Holtzman DM, McKeel Jr. DW, Kelley J, Morris JC (2002) Substantial sulfatide deficiency and ceramide elevation in very early Alzheimer's disease: potential role in disease pathogenesis. J Neurochem 83:809–818

Han X (2005) Lipid alterations in the earliest clinically recognizable stage of Alzheimer's disease: implication of the role of lipids in the pathogenesis of Alzheimer's disease. Curr Alzheimer Res 2:65–77

Hanada K, Hara T, Nishijima M, Kuge O, Dickson RC, Nagiec MM (1997) A mammalian homolog of the yeast LCB1 encodes a component of serine palmitoyltransferase, the enzyme catalyzing the first step in sphingolipid synthesis. J Biol Chem 272:32108-32114

Hanada K (2003) Serine palmitoyltransferase, a key enzyme of sphingolipid metabolism. Biochim Biophys Acta 1632:16-30

Hannun YA, Luberto C, Argraves KM (2001) Enzymes of sphingolipid metabolism: from modular to integrative signaling. Biochemistry 40:4893–4903

Hannun YA, Obeid LM (2002) The Ceramide-centric universe of lipid-mediated cell regulation: stress encounters of the lipid kind. J Biol Chem 277:25847-25850

Harel R, Futerman AH (1993) Inhibition of sphingolipid synthesis affects axonal outgrowth in cultured hippocampal neurons. J Biol Chem 268:14476–14481

Harr SD, Uint L, Hollister R, Hyman BT, Mendez AJ (1996) Brain expression of apolipoproteins E, J, and A-I in Alzheimer's disease. J Neurochem 66:2429-2435

Haughey NJ, Cutler RG, Tamara A, McArthur JC, Vargas DL, Pardo CA, Turchan J, Nath A, Mattson MP (2004) Perturbation of sphingolipid metabolism and ceramide production in HIV-dementia. Ann Neurol 55:257-267

He X, Jenner AM, Ong WY, Farooqui AA, Patel SC (2006) Lovastatin modulates increased cholesterol and oxysterol levels and has a neuroprotective effect on rat hippocampal neurons after kainate injury. J Neuropathol Exp Neurol 5:652-663

Herr I, Martin-Villalba A, Kurz E, Roncaioli P, Schenkel J, Cifone MG, Debatin KM (1999) FK506 prevents stroke-induced generation of ceramide and apoptosis signaling. Brain Res 826:210-219

Heverin M, Bogdanovic N, Lütjohann D, Bayer T, Pikuleva I, Bretillon L, Diczfalusy U, Winblad B, Björkhem I (2004) Changes in the levels of cerebral and extracerebral sterols in the brain of patients with Alzheimer's disease. J Lipid Res 45:186–193

Horrocks LA, VanRollins M, Yates AJ (1981) Lipid changes in the ageing brain. Pages 601–630, in Davison AN and Thompson RHS (eds.). The molecular basis of neuropathology. London: Edward Arnold Ltd.

Igbavboa U, Avdulov NA, Chochina SV, Wood WG (1997) Transbilayer distribution of cholesterol is modified in brain synaptic plasma membranes of knockout mice deficient in the low-density lipoprotein receptor, apolipoprotein E, or both proteins. J Neurochem 69:1661-1667

Ikezu T, Ueda H, Trapp BD, Nishiyama K, Sha JF, Volonte D, Galbiati F, Byrd AL, Bassell G, Serizawa H, Lane WS, Lisanti MP, Okamoto T (1998) Affinity-purification and characterization of caveolins from the brain: differential expression of caveolin-1, -2, and -3 in brain endothelial and astroglial cell types. Brain Res 804:177-192

Incerpi S, Jefferson JR, Wood WG, Ball WJ, Schroeder F (1992) Na pump and plasma membrane structure in L-cell fibroblasts expressing rat liver fatty acid binding protein. Arch Biochem Biophys 298:35-42

Irie F, Hirabayashi Y (1998) Application of exogenous ceramide to cultured rat spinal motoneurons promote survival or death by regulation of apoptosis depending on its concentrations. J Neurosci Res 54:475– 485

Jacobs BS (2004) Can statins treat the stroke they fail to prevent? J Neurol Sci 221:1-2

Jana A, Pahan K (2004) Fibrillar aβ peptides kill human primary neurons via NADPH oxidase-mediated activation of neutral sphingomyelinase. Implications for Alzheimer's disease. J Biol Chem 279:51451–51459

Jick H, Zornberg GL, Jick SS, Seshadri S, Drachman DA (2000) Statins and the risk of dementia. Lancet 356:1627-1631

Johnston MV, McKinney M, Coyle JT (1979) Evidence for a cholinergic projection to neocortex from neurons in basal forebrain. Proc Natl Acad Sci USA 76:5392-5396

Jurevics HA, Morell P (1995) Cholesterol for synthesis of myelin is made locally, not imported into brain. J Neurochem 64:895-901

Jurevics HA, Kidwai FZ, Morell P (1997) Sources of cholesterol during development of the rat fetus and fetal organs. J Lipid Res 38:723-733

Kabara JJ (1973) A critical review of brain cholesterol metabolism. Prog Brain Res 40:363-382

Kanfer JN, Hattori H, Orihel D (1986) Reduced phospholipase D activity in brain tissue samples from Alzheimer’s disease patients. Ann Neurol 20:265–267

Katsuki H, Okuda S (1995) Arachidonic acid as a neurotoxic and neurotrophic substance. Prog Neurobiol 46:607–636

Keller JN, Pang Z, Geddes JW, Begley JG, Germeyer A, Waeg G, Mattson MP (1997) Impairment of glucose and glutamate transport and induction of mitochondrial oxidative stress and dysfunction in synaptosomes by amyloid beta-peptide: role of the lipid peroxidation product 4-Hydroxynonenal. J Neurochem 69:273–284

Kim WH, Choi CH, Kang SK, Kwon CH, Kim YK (2005) Ceramide induces non-apoptotic cell death in human glioma cells. Neurochem Res 30:969-979

Kinney HC, Karthigasan J, Borenshteyn NI, Flax JD, Kirschner DA (1994) Myelination in the developing human brain: biochemical correlates. Neurochem Res 19:983-996

Kolesnick R, Kronke M (1998) Regulation of ceramide production and apoptosis. Annu Rev Physiol 60: 643–665

Kolesnick R, Hannun YA (1999) Ceramide and apoptosis. Trends Biochem Sci 24:224-225

Kolesnick R (2002) The therapeutic potential of modulating the ceramide/sphingomyelin pathway. J Clin Invest 110:3-8

Kolsch H, Lütjohann D, Tulke A, Björkhem I, Rao ML (1999) The neurotoxic effect of 24-hydroxycholesterol on SH-SY5Y human neuroblastoma cells. Brain Res 818:171-175

Kolsch H, Ludwig M, Lütjohann D, Rao ML (2001) Neurotoxicity of 24-hydroxycholesterol, an important cholesterol elimination product of the brain, may be prevented by vitamin E and estradiol-17ß. J Neural Transm 108:475-488

Koper JW, Zeinstra EC, Lopes-Cardozo M, van Golde LM (1984) Acetoacetate and glucose as substrates for lipid synthesis by rat brain oligodendrocytes and astrocytes in serum-free culture. Biochim Biophys Acta 796:20-26

Korkotian E, Schwarz A, Pelled D, Schwarzmann G, Segal M, Futerman AH (1999) Elevation of intracellular glucosylceramide levels result in an increase in endoplasmic reticulum density and in functional calcium stores in cultured neurons. J Biol Chem 274:21673-2167

Kostner GM, Steyer E (1988) Activation of lecithin-cholesterol acyltransferase by apolipoprotein D: comparison of proteolisomes containing apolipoprotein D, A-I or C-I. Biochim Biophys Acta 958:484–491

Kroesen BJ, Pettus B, Luberto C, Busman M, Sietsma H, De Leij L (2001) Induction of apoptosis through B-cell receptor cross-linking occurs via de novo generated C16- ceramide and involves mitochondria. J Biol Chem 276:13606–13614

Krueger KE, Papadopoulos V (1990) Peripheral-type benzodiazepine receptors mediate translocation of cholesterol from outer to inner mitochondrial membranes in adrenocortical cells. J Biol Chem 265:15015-15022

Kubota M, Narita K, Nakagomi T,Tamura A, Shimasaki H, Ueta N, Yoshida S (1996) Sphingomyelin changes in rat cerebral cortex during focal ischemia. Neurol Res 18:337–341

Kumagai R, Oki C, Muramatsu Y, Kurosaki R, Kato H, Araki T (2004) Pitavastatin, a 3-hydroxy-3-methylglutaryl Coenzyme A (HMG-CoA) reductase inhibitor, reduces hippocampal damage after transient cerebral ischemia in gerbils. J Neural Transm 111:1103-1120

Lan J, Henshall DC, Simon RP, Chen J (2000) Formation of the base modification 8-hydroxyl-2'-deoxyguanosine and DNA fragmentation following seizures induced by systemic kainic acid in the rat. J Neurochem 74:302-309

Lea OA (1988) Binding properties of progesterone-binding Cyst protein, PBCP. Steroids 52:337-338

Lee JT, Xu J, Lee JM, Ku G, Han X, Yang DI, Chen S, Hsu CY (2004) Amyloid-β peptide induces oligodendrocyte death by activating the neutral sphingomyelinase-ceramide pathway. J Cell Biol 164:123–131

Lee JY, Leonhardt LG, Obeid LM (1998) Cell-cycle dependent changes in ceramide levels preceding retinoblastoma protein dephosphorylation in G2/M. Biochem J 334:457–461

Lerma J (1997) Kainate reveals its targets. Neuron 19:1155-1158

Levade T, Jaffrezou JP (1999) Signalling sphingomyelinases:which, where, how and why? Biochim Biophys Acta 1438: 1–17

Li CM, Park JH, Simonaro CM, He X, Gordon RE, Friedman AH (2002) Insertional mutagenesis of the mouse acid ceramidase gene leads to early embryonic lethality in homozygotes and progressive lipid storage disease in heterozygotes. Genomics 79:218–224

Liu B, Obeid L M, Hannun YA (1997) Sphingomyelinases in cell regulation. Semin Cell Dev Biol 8: 311–322

Liu B, Andrieu-Abadie N, Levade T, Zhang P, Obeid LM, Hannun YA (1998) Glutathione regulation of neutral sphingomyelinase in tumor necrosis factor-alpha-induced cell death. J Biol Chem 273:11313-11320

Lizard G, Miguet C, Bessede G (2000) Impairment with various antioxidants of the loss of mitochondrial transmembrane potential and of the cytosolic release cytochrome c occurring during 7-ketocholesterol-induced apoptosis. Free Rad Biol Med 28:743-753

Lothman EW, Collins RC (1981) Kainic acid induced limbic seizures: metabolic, behavioral,electroencephalographic and neuropathological correlates. Brain Res 218:299-318

Lu XR, Ong WY, Halliwell B, Horrocks LA, Farooqui AA (2001) Differential effects of calcium-dependent and calcium-independent phospholipase A_2 inhibitors on kainate-induced neuronal injury in rat hippocampal slices. Free Radic Biol Med 30:1263-1273

Luberto C, Hassler DF, Signorelli P, Okamoto Y, Sawai H, Boros E,Hazen-Martin DJ, Obeid LM, Hannun YA, Smith GK (2002) Inhibition of tumor necrosis factor-induced cell death in MCF7 by a novel inhibitor of neutral sphingomyelinase. J Biol Chem 277:41128-41139

Lund EG, Guileyardo JM, Russell DW (1999) cDNA cloning of cholesterol 24-hydroxylase, a mediator of cholesterol homeostasis in the brain. Proc Natl Acad Sci USA 96:7238–7243

Lund EG, Xie C, Kotti T, Turley SD, Dietschy JM, Russell DW (2003) Knockout of the cholesterol 24-hydroxylase gene in mice reveals a brain-specific mechanism of cholesterol turnover. J Biol Chem 278:22980-22998

Lütjohann D, Breuer O, Ahlborg G, Nennesmo I, Sidén A, Diczfalusy U and Björkhem I (1996) Cholesterol homeostasis in human brain: Evidence for an age-dependent flux of 24S-hydroxycholesterol from the brain into the circulation. Proc Natl Acad Sci USA 93: 9799–9804

Lütjohann D, Papassotiropoulos A, Bjorkhem I, Locatelli S, Bagli M Oehring RD, Schlegel U, Jessen F, Rao ML, von Bergmann K, Heun R (2000) Plasma 24S-hydroxycholesterol (cerebrosterol) is increased in Alzheimer and vascular demented patients. J Lipid Res 41:195–198

Mandon EC, Ehses I, Rother J, van Echten G, Sandhoff K (1992) Subcellular localization and membrane topology of serine palmitoyltransferase, 3-dehydrosphinganine reductase, and sphinganine N-acyltransferase in mouse liver. J Biol Chem 267:11144-11148

Marchesini N, Hannun YA (2004) Acid and neutral sphingomyelinases: roles and mechanisms of regulation. Biochem Cell Biol 82:27-44

Mason RP, Shoemaker WJ, Shajenko L, Chambers TE, Herbette LG (1992) Evidence for changes in the Alzheimer's disease brain cortical membrane structure mediated by cholesterol. Neurobiol Aging 13:413-419

Mathias S, Pena LA, Kolesnick RN (1998) Signal transduction of stress via ceramide. Biochem J 335:465–480

Mattson MP, Rychlik B, You JS, Sisken JE (1991) Sensitivity of cultured human embryonic cerebral cortical neurons to excitatory amino acid-induced calcium influx and neurotoxicity. Brain Res 542:97-106

McConathy WJ, Alaupovic P (1973) Isolation and partial characterization of apolipoprotein D: a new protein moiety of the human plasma lipoprotein system. FEBS Lett 37:178-182

McGeer EG, McGeer PL (1976) Duplication of biochemical changes of Huntington's chorea by intrastriatal injections of glutamic and kainic acids. Nature 263:517-519

Melchiorri D, Reiter RJ, Sewerynek E, Chen LD, Nistico G (1995) Melatonin reduces kainate-induced lipid peroxidation in homogenates of different brain regions. FASEB J 9:1205-1210

Merrill AH Jr., Nixon DW, Williams RD (1985) Activities of serine palmitoyltransferase (3-ketosphinganine synthase) in microsomes from different rat tissues. J Lipid Res 26:617-622

Merrill AH Jr, Wang E (1986) Biosynthesis of long-chain (sphingoid) bases from serine by LM cells. Evidence for introduction of the 4-trans-double bond after de novo biosynthesis of N-acylsphinganine(s). J Biol Chem 261:3764-3769

Merrill AH Jr, Nixon DW, Williams RD (1989) Activities of serine palmitoyltransferase (3-ketosphinganine synthase) in microsomes from different rat tissues. J Lipid Res 26:617-622

Merrill AH Jr, van Echten G, Wang E, Sandhoff K (1993) Fumonisin B1 inhibits sphingosine (sphinganine) N-acyltransferase and de novo sphingolipid biosynthesis in cultured neurons in situ. J Biol Chem 268:27299-27306

Merrill AH Jr (2002) De novo sphingolipid biosynthesis: A necessary but dangerous pathway. J Biol Chem 277:25843-25846

Michel C, van Echten-Deckert G (1997) Conversion of dihydroceramide to ceramide occurs at the cytosolic face of the endoplasmic reticulum. FEBS Lett 416:153-155

Michelangeli F, East JM, Lee AG (1990) Structural effects on the interaction of sterols with the (Ca^{2+} + Mg^{2+})-ATPase. Biochim Biophys Acta 1025:99-108

Miguet-Alfonsi C, Prunet C, Monier S (2002) Analysis of oxidative processes and of myelin figures formation before and after the loss of mitochondrial transmembrane potential during 7-beta-hydroxycholesterol and 7-

ketocholesterol-induced apoptosis: comparison with various pro-apoptotic chemicals. Biochem Pharmacol 64:527-541

Mikati MA, Abi-Habib RJ, El Sabban ME, Dbaibo GS, Kurdi RM, Kobeissi M, Farhat F, Asaad W (2003) Hippocampal programmed cell death after status epilepticus: evidence for NMDAR-receptor and ceramide-mediated mechanisms. Epilepsia 44:282-291

Mitoma J, Ito M, Furuya S, Hirabayashi Y (1998) Bipotential roles of ceramide in the growth of hippocampal neurons: promotion of cell survival and dendritic outgrowth in dose- and developmental stagedependent manners. J Neurosci Res 51:712–722

Miyajima H, Adachi J, Kohno S, Takahashi Y, Ueno Y, Naito T (2001) Increased oxysterols associated with iron accumulation in the brains and visceral organs of acaeruloplasminaemia patients. QJM 94:417-122

Moncecchi D, Murphy EJ, Prows DR, Schroeder F (1996) Sterol carrier protein-2 expression in mouse L-cell fibroblasts alters cholesterol uptake. Biochim Biophys Acta 1302:110-116

Montes LR, Rutz-Arguello MB, Goni FM, Alonso A (2002) Membrane restructuring via ceramide results in enhanced solute efflux. J Biol Chem 277:11788-11794

Montpied P, de Bock F, Lerner–Natoli M, Bockaert J, Rondouin G (1999) Hippocampal alterations of apolipoprotein E and D mRNA levels in vivo and in vitro following kainate excitotoxicity. Epilepsy Res 35:135-146

Morais-Cabral JH, Atkins GL, Sanchez LM, Lopez-Boado YS, Lopez-Otin C, Sawyer L (1995) Arachidonic acid binds to apolipoprotein D: implications for the protein's function. FEBS Lett 366:53-56

Morano GN, Seibyl JP (2003) Technical overview of brain SPECT imaging: improving acquisition and processing of data. J Nucl Med Techol 31:191-195

Movsesyan VA, Yakovlev AG, Dabaghyan EA, Stoica BA, Faden AI (2002) Ceramide induces neuronal apoptosis through the caspase-9/ caspase-3 pathway. Biochem Biophys Res Commun 299:201–207

Murphy EJ, Schroeder F (1997) Sterol carrier protein-2 mediated cholesterol esterification in transfected L-cell fibroblasts. Biochim Biophys Acta 1345:283-292

Myers-Payne SC, Fontaine RN, Loeffler A, Pu L, Rao AM, Kier AB, Wood WG,Schroeder F (1996a) Effects of chronic ethanol consumption on sterol transfer proteins in mouse brain. J Neurochem 66:313-320

Myers-Payne SC, Hubbell T, Pu L, Schnutgen F, Borchers T, Wood WG, Spener F, Schroeder F (1996b) Isolation and characterization of two fatty acid binding proteins from mouse brain. 66:1648-1656

Nakamura H, Hirabayashi T, Shimizu M, Murayama T (2006) Ceramide-1-phosphate activates cytosolic phospholipase $A_2\alpha$ directly and by PKC pathway. Biochem Pharmacol 71:850-857

Nakane M, Kubota M, Nakagomi T, Tamura A, Hisaki H, Shimasaki H, Ueta N (2000) Lethal forebrain ischemia stimulates sphingomyelin hydrolysis and ceramide generation in the gerbil hippocampus. Neurosci Lett 296:89-92

Nakao N, Brundin P (1998) Neurodegeneration and glutamate induced oxidative stress. Prog Brain Res 116:245-263

Narita Y, Kitazoe Y, Kurihara Y, Okuhara Y, Takamatsu K, Saito N, Doi Y (1997) Increase or decrease of HDL-cholesterol concentrations during pravastatin treatment depending on the pre-treatment HDL cholesterol levels. Eur J Clin Pharmacol 52:461-463

Navarro A, Tolivia J, Astudillo A, del Valle E (1998) Pattern of apolipoprotein D immunoreactivity in human brain. Neurosci Lett 254:17-20

Nelson TJ, Alkon DL (2005) Oxidation of cholesterol by amyloid precursor protein and beta-amyloid peptide. J Biol Chem 280:7377-7787

Ness GC, Miller JP, Moffler MH, Woods LS, Harris HB (1979) Perinatal development of 3-hydroxy-3-methylglutaryl coenzyme A reductase activity in rat lung, liver and brain. Lipids 14:447-450

Nitsch RM, Blusztajn JK, Pittas AG, Slack BE, Growdon JH, Wurtman RJ (1992) Evidence for a membrane defect in Alzheimer disease brain. Proc Nat Acad Sci USA 89:1671–1675

North P, Fleischer S (1983) Alteration of synaptic membrane cholesterol/phospholipid ratio using a lipid transfer protein. Effect on gamma-aminobutyric acid uptake. J Biol Chem 258:1242-1253

Ogretmen B, Pettus BJ, Rossi MJ, Wood R, Usta J, Szulc Z (2002) Biochemical mechanisms of the generation of endogenous long chain ceramide in response to exogenous short chain ceramide in the A549 human lung

adenocarcinoma cell line. Role for endogenous ceramide in mediating the action of exogenous ceramide. J Biol Chem 277:12960–12969

Ohanian J, Ohanian V (2001) Sphingolipids in mammalian cell signaling. Cell Mol Life Sci 58:2053-2068

Ohtani R, Tomimoto H, Kondo T, Wakita H, Akiguchi I, Shibasaki H, Okazaki T (2004) Upregulation of ceramide and its regulating mechanism in a rat model of chronic cerebral ischemia. Brain Res 1023:31-40

Okazaki T, Bell RM, Hannun YA (1989) Sphingomyelin turnover induced by vitamin D3 in HL-60 cells. J Biol Chem 264:19076–19080

Okazaki T, Bielawska A, Bell RM, Hannun YA (1990) Role of ceramide as a lipid mediator of 1a,25-dihydroxyvitamin D3-induced HL-60 cell differentiation. J Biol Chem 265:15823–15831

Olney JW, Ho OL, Rhee V (1971) Cytotoxic effects of acidic and sulphur containing amino acids on the infant mouse central nervous system. Exp Brain Res 14:61-76

Ong WY, He Y, Suresh S, Patel SC (1997) Differential expression of apolipoprotein D and apolipoprotein E in the kainic acid-lesioned rat hippocampus. Neuroscience 79:359-367

Ong WY, Lu XR, Hu CY, Halliwell B (2000) Distribution of hydroxynonenal-modified proteins in the kainate-lesioned rat hippocampus: evidence that hydroxynonenal formation precedes neuronal cell death. Free Radic Biol Med 28:1214-1221

Ong WY, Goh EW, Lu XR, Farooqui AA, Patel SC, Halliwell B (2003) Increase in cholesterol and cholesterol oxidation products, and role of cholesterol oxidation products in kainate-induced neuronal injury. Brain Pathol 13:250-262

Osawa Y, Uchinami H, Bielawski J, Schwabe RF, Hannun YA, Brenner DA (2005) Roles for C16-ceramide and sphingosine 1-phosphate in regulating hepatocyte apoptosis in response to tumor necrosis factor-alpha. J Biol Chem 280:27879-27887

Ozawa S, Kamiya H, Tsuzuki K (1998) Glutamate receptors in the mammalian central nervous system. Prog Neurobiol 54:581-618

Paltauf R (1994) Ether lipids in biomembranes. Chem Phys Lipids 74:101–139

Papassotiropoulos A, Lütjohann D, Bagli M, Locatelli S, Jessen F, Buschfort R (2002) 24S-Hydroxycholesterol in cerebrospinal fluid is elevated in early stages of dementia. J Psychiatr Res 36:27–32

Patel SC, Asotra K, Patel YC, McConathy WJ, Patel RC. Suresh S (1995) Astrocytes synthesize and secrete the lipophilic ligand carried apolipoprotein D. NeuroReport 6:653-657

Patel RC, Lange D, McConathy WJ, Patel YC, Patel SC (1997) Probing the structure of the ligand binding cavity of lipocalins by fluorescence spectroscopy. Protein Eng 10:621-625

Paumen MB, Ishida Y, Muramatsu M, Yamamoto M, Honjo T (1997) Inhibition of carnitine palmitoyltransferase I augments sphingolipid synthesis and palmitate-induced apoptosis. J Biol Chem 272:3324-3329

Peitsch MC, Boguski MS (1990) Is apolipoprotein D a mammalian bilin-binding protein? New Biol 2:197-206

Perry DK, Hannun YA (1998) The role of ceramide in cell signaling. Biochim Biophys Acta 1436:233-243

Perry DK, Carton J, Shah AK, Meredith F, Uhlinger DJ, Hannun YA (2000) Serine palmitoyltransferase regulates de novo ceramide generation during etoposide-induced apoptosis. J Biol Chem 275:9078-9084

Perry DK (2002) Serine palmitoyltransferase: role in apoptotic de novo ceramide synthesis and other stress responses. Biochim Biophys Acta 1585:146-152

Peterson BL, Cummings BS (2006) A review of chromatographic methods for the assessment of phospholipids in biological samples. Biomed Chromatogr 20:227-243

Pettegrew JW (1989) Molecular insights into Alzheimer disease. Ann N Y Acad Sci 568:5–28

Pettegrew JW, Klunk WE, Kanal E, Panchalingam K, McClure RL (1995) Changes in brain membrane phospholipid and high-energy phosphate metabolism precede dementia. Neurobiol Aging 16: 973–975

Pettus BJ, Chalfant CE, Hannun YA (2002) Ceramide in apoptosis: an overview and current perspectives. Biochim Biophys Acta 1585:114-125

Pichler H, Riezman H (2004) Where sterols are required for endocytosis. Biochim Biophys Acta 1666:51-61

Pitas RE, Boyles JK, Lee SH, Hui D, Weisgraber KH (1987) Lipoproteins and their receptors in the central nervous system. Characterization of the lipoproteins in cerebrospinal fluid and identification of apolipoprotein B,E(LDL) receptors in the brain. J Biol Chem 262:14352-14360

Pohle W, Rauca C (1994) Hypoxia protects against the neurotoxicity of kainic acid. Brain Res 644: 297-304

Poirier J, Davignon J, Bouthillier D, Kogan S, Bertrand P, Gauthier S (1993) Apolipoprotein E polymorphism and Alzheimer's disease. Lancet 342:697-699

Posse de Chaves EI (2006) Sphingolipids in apoptosis, survival and regeneration in the nervous system. Biochim Biophys Acta 1758:1995-2015

Prasad MR, Lovell MA, Yatin M, Dhillon H, Markesbery WR (1998) Regional membrane phospholipid alterations in Alzheimer's disease. Neurochem Res 23:81–88

Provost PR, Weech PK, Tremblay NM, Marcel YL, Rassart É (1990) Molecular characterization and differential mRNA distribution of rabbit apolipoprotein D. J Lipid Res 3:2057-2065

Pu L, Foxworth WB, Kier AB, Annan RS, Carr SA, Edmondson R, Russell D, Wood WG, Schroeder F (1998) Isolation and characterization of 26- and 30-kDa rat liver proteins immunoreactive to anti-sterol carrier protein-2 antibodies. Protein Expr Purif 13:337-348

Pu L, Igbavboa U, Wood WG, Roths JB, Kier AB, Spener F, Schroeder F (1999) Expression of fatty acid binding proteins is altered in aged mouse brain. Mol Cell Biochem 198:69-78

Puglielli L, Ellis BC, Saunders AJ, Kovacs DM (2003) Ceramide stabilizes beta-site amyloid precursor protein-cleaving enzyme 1 and promotes amyloid beta-peptide biogenesis. J Biol Chem 278:19777–19783

Rao AM, Hatcher JF, Dempsey RJ (2000) Lipid alterations in transient forebrain ischemia: possible new mechanisms of CDP-choline neuroprotection. J Neurochem 75:2528-2535

Rassart E, Bedirian A, Do Carmo S, Guinard O, Sirois J, Terrisse L, Milne R (1998) Apolipoprotein D. Biochim Biophys Acta 1482:185-198

Relton JK, Strijbos PJ, Cooper AL, Rothwell NJ (1993) Dietary N-3 fatty acids inhibit ischaemic and excitotoxic brain damage in the rat. Brain Res Bull 2:223–226

Represa A, Tremblay E, Ben-Ari Y (1990) Sprouting of mossy fibers in the hippocampus of epileptic human and rat. Adv Exp Med Biol 268:419-424

Riboni L, Prinetti A, Bassi R, Caminiti A, Tettamanti G (1995) A mediator role of ceramide in the regulation of neuroblastoma Neuro2a cell differentiation. J Biol Chem 270:26868–26875

Roberts LJ, Morrow JD (2000) Measurement of F(2)-isoprostanes as an index of oxidative stress in vivo. Free Radic Biol Med 28:505–513

Rordorf G, Uemura Y, Bonventre JV (1991) Characterization of phospholipase A_2 (PLA_2) activity in gerbil brain: Enhanced activities of cytosolic, mitochondrial, and microsomal forms after ischemia and reperfusion. J Neurosci 11:1829–1836

Ross BM, Turenne S, Moszczynska A, Warsh JJ, Kish SJ (1999) Differential alteration of phospholipase A_2 activities in brain of patients with schizophrenia. Brain Res 821:407-413

Ruiz-Arguello MB, Goni FM, Alonso A (1998) Vesicle membrane fusion induced by the concerted activities of sphingomyelinase and phospholipase C. J Biol Chem 273: 22977-22982

Russell DW (2000) Oxysterol biosynthetic enzymes. Biochim Biophys Acta 1529:126-135

Samet D, Barenholz Y (1999) Characterization of acidic and neutral sphingomyelinase activities in crude extracts of HL-60 cells. Chem Phys Lipids 102:65-77

Satoi H, Tomimoto H, Ohtani R, Kitano T, Kondo T, Watanabe M, Oka N, Akiguchi I, Furuya S, Hirabayashi Y, Okazaki T (2005) Astroglial expression of ceramide in Alzheimer's disease brains: a role during neuronal apoptosis. Neuroscience 130:657-666

Saito M, Saito M, Cooper TB, Vadasz C (2005) Ethanol-induced changes in the content of triglycerides, ceramides, and glucosylceramides in cultured neurons. Alcohol Clin Exp Res 29:1374-1383

Sandhya TL, Ong WY, Horrocks LA, Farooqui AA (1998) A light and electron microscopic study of cytoplasmic phospholipase A_2 and cyclooxygenase-2 in the hippocampus after kainate lesions. Brain Res 788: 223– 231

Schiller J, Suss R, Arnhold J, Fuchs B, Lessig J, Muller M, Petkovic M, Spalteholz H, Zschornig O and Arnold K (2004) Matrix-assisted laser

desorption and ionization time-of-flight (MALDITOF) mass spectrometry in lipid and phospholipid research. Prog Lipid Res 43:449–488

Schonknecht P, Lütjohann D, Pantel J, Bardenheuer H, Hartmann T, von Bergmann K (2002) Cerebrospinal fluid 24S-hydroxycholesterol is increased in patients with Alzheimer's disease compared to healthy controls. Neurosci Lett 324:83–85

Schroeder F, Morrison WJ, Gorka C, Wood WG (1988) Transbilayer effects of ethanol on fluidity of brain membrane leaflets.Biochim Biophys Acta 946:85-94

Schroeder F, Jefferson JR, Kier AB, Knittel J, Scallen TJ, Wood WG, Hapala I (1991) Membrane cholesterol dynamics: cholesterol domains and kinetic pools. Proc Soc Exp Biol Med 196:235-252

Schroeder F, Frolov AA, Murphy EJ, Atshaves BP, Jefferson JR, Pu L, Wood WG, Foxworth WB, Kier AB (1996) Recent advances in membrane cholesterol domain dynamics and intracellular cholesterol trafficking. Proc Soc Exp Biol Med 213:150-177

Schuler LA, Toaff ME, Strauss JF 3rd (1981) Regulation of ovarian cholesterol metabolism: control of 3-hydroxy-3-methylglutaryl coenzyme A reductase and acyl coenzyme A:cholesterol acyltransferase. Endocrinology 108:1476-1486

Schwarz A, Futerman AH (1997) Inhibition of sphingolipid synthesis, but not degradation, alters the rate of dendrite growth in cultured hippocampal neurons. Brain Res Dev Brain Res 108:125-130

Seguin D, Desforges M, Rassart É (1994) Molecular characterization and differential mRNA tissue distribution of mouse apolipoprotein D. Mol Brain Res 30:242-250

Serbanescu I, Ryan MA, Shukla R, Cortez MA, Snead OC 3rd (2004) Cunnane SC. Lovastatin exacerbates atypical absence seizures with only minimal effects on brain sterols. J Lipid Res 45:2038-2043

Sharon R, Bar-Joseph I, Frosch MP, Walsh DM, Hamilton JA, Selkoe DJ (2003) The formation of highly soluble oligomers of alpha-synuclein is regulated by fatty acids and enhanced in Parkinson's disease. Neuron 37:583-595

Shimeno H, Soeda S, Sakamoto M, Kouchi T, Kowakame T, Kihara T (1998) Partial purification and characterization of sphingosine N-acyltransferase (ceramide synthase) from bovine liver mitochondrion-rich fraction. Lipids 33:601-605

Simons K, Ikonen E (1997) Functional rafts in cell membranes. Nature 387:569-572

Simons K, Toomre D (2001) Lipid rafts and signal transduction. Nat Rev Mol Cell Biol 2000 1:31-39

Siskind LJ (2005) Mitochondrial ceramide and the induction of apoptosis. J Bioenerg Biomembr 37:143-153

Sloviter RS, Dempster DW (1985) "Epileptic" brain damage is replicated qualitatively in the rat hippocampus by central injection of glutamate or aspartate but not by GABA or acetylcholine. Brain Res Bull 15:39-60

Smart EJ, Ying Y, Donzell WC, Anderson RG (1996) A role for caveolin in transport of cholesterol from endoplasmic reticulum to plasma membrane. J Biol Chem 271:29427-29435

Smith KH, Lawn RM, Wilcox JN (1990) Cellular localization of apolipoprotein D and lecithin: cholesterol acyltransferase mRNA in rhesus monkey tissues by in situ hybridization. J Lipid Res 31:995-1004

Snipes GJ, Suter U (1997) Cholesterol and myelin. Subcell Biochem 28:173-204

Söderberg M, Edlund C, Kristensson K, Dallner, G (1990) Lipid compositions of different regions of the human brain during aging. J Neurochem 54:415–423

Sortino MA, Condorelli F, Vancheri C, Canonico PL (1999) Tumor necrosis factor-alpha induces apoptosis in immortalized hypothalamic neurons: involvement of ceramide-generating pathways. Endocrinology 140:4841-4849

Spady DK, Dietschy JM (1983) Sterol synthesis in vivo in 18 tissues of the squirrel monkey, guinea pig, rabbit, hamster, and rat. J Lipid Res 24:303-315

Sparks DL (1997) Coronary artery disease, hypertension, ApoE, and cholesterol: a link to Alzheimer's disease? Ann N Y Acad Sci 826:128-146

Spence MW, Burgess JK (1978) Acid and neutral sphingomyelinases of rat brain. Activity in developing brain and regional distribution in adult brain. J. Neurochem 30:917–919

Sperber EF, Haas KZ, Stanton PK, Moshe SL (1991) Resistance of the immature hippocampus to seizure-induced synaptic reorganization. Brain Res Dev Brain Res 20:88-93

Spiegel S, Merrill AH Jr (1996) Sphingolipid metabolism and cell growth regulation. FASEB J 10:1388-1397

Spreyer P, Schaal H, Kuhn G, Rothe T, Unterbeck A, Olek K, Müller HW (1990) Regeneration-associated high level expression of apolipoprotein D mRNA in endoneurial fibroblast of peripheral nerve. Eur Mol Biol Org J 9:2479-2484

Stephenson DT, Lemere CA, Selkoe DJ, Clemens JA (1996) Cytosolic phospholipase A_2 ($cPLA_2$) immunoreactivity is elevated in Alzheimer's disease brain. Neurobiol Dis 3:51–63

Stephenson DT, Rash K, Smalstig B, Roberts E, Johnstone E, Sharp J, Panetta J, Little S, Kramer R, Clemens J (1999) Cytosolic phospholipase A_2 is induced in reactive glia following different forms of neurodegeneration. Glia 27:110–128

Stoffel W (1999) Functional analysis of acid and neutral sphingomyelinases *in vitro* and *in vivo*. Chem Phys Lipids 102:107-121

Stoica BA, Movsesyan VA, Knoblach SM, Faden AI (2005) Ceramide induces neuronal apoptosis through mitogen-activated protein kinases and causes release of multiple mitochondrial proteins. Mol Cell Neurosci 29:355-371

Stoppini L, Buchs PA, Muller DA (1991) Simple method for organotypic cultures of nervous tissue. J Neurosci Methods 37:173-182

Strittmatter WJ, Weisgraber KH, Huang DY, Dong LM, Salvesen GS, Pericak-Vance M, Schmechel D, Saunders AM, Goldgaber D, Roses AD (1993) Binding of human apolipoprotein E to synthetic amyloid beta peptide: isoform-specific effects and implications for late-onset Alzheimer disease. Proc Natl Acad Sci USA 90:8098-8102

Strittmatter WJ, Roses AD (1996) Apolipoprotein E and Alzheimer's disease. Annu Rev Neurosci 19:53-77

Sturley SL, Patterson MC, Balch W, Liscum L (2004) The pathophysiology and mechanisms of NP-C disease. Biochim Biophys Acta 1685:83–87

Suresh S, Yan Z, Patel RC, Patel YC, Patel SC (1998) Cellular cholesterol storage in the Niemann–Pick disease type C mouse is associated with increased expression and defective processing of apolipoprotein D. J Neurochem 70:242–251

Sutula T, Cavazos J, Golarai G (1992) Alteration of long-lasting structural and functional effects of kainic acid in the hippocampus by brief treatment with phenobarbital. J Neurosci 12:4173-4187

Swartz GM Jr, Gentry MK, Amende LM, Blanchette-Mackie EJ, Alving CR (1998) Antibodies to cholesterol. Proc Natl Acad Sci 85:1902-1906

Takahashi K, Ginis I, Nishioka R, Klimanis D, Barone FC, White RF, Chen Y, Hallenbeck JM (2004) Glucosylceramide synthase activity and ceramide levels are modulated during cerebral ischemia after ischemic preconditioning. J Cereb Blood Flow Metab 24:623-627

Tamagno E, Robino G, Obbili A, Bardini P, Aragno M, Parola M, Danni O (2003) H_2O_2 and 4-hydroxynonenal mediate amyloid beta-induced neuronal apoptosis by activating JNKs and $p38^{mapk}$. Exp Neurol 180:144-155

Terrisse L, Poirier J, Bertrand P, Merched A, Visvikis S, Siest G, Milne R, Rassart E (1998) Increased levels of apolipoprotein D in cerebrospinal fluid and hippocampus of Alzheimer's patients. J Neurochem 71:643-650

Terrisse L, Séguin D, Bertrand P, Poirier J, Milne R, Rassart É (1999) Modulation of apolipoprotein D and apolipoprotein E expression in rat hippocampus after entorhinal cortex lesion. Mol Brain Res 70:26-35

Thomas EA, Laws SM, Sutcliffe JG, Harper C, Dean B, McClean C, Masters C, Lautenschlager N, Gandy SE, Martins RN (2003) Apolipoprotein D levels are elevated in prefrontal cortex of subjects with Alzheimer's disease: no relation to apolipoprotein E expression or genotype. Biol Psychiatry 54:136-141

Tint GS, Irons M, Elias ER, Batta AK, Frieden R, Chen TS, Salen G (1994) Defective cholesterol biosynthesis associated with the Smith-Lemli-Opitz syndrome. N Engl J Med 330:107-113

Toman RE, Movsesyan V, Murthy SK, Milstien S, Spiegel S, Faden AI (2002) Ceramide-induced cell death in primary neuronal cultures: upregulation of ceramide levels during neuronal apoptosis. J Neurosci Res 68:323–330

Turley SD, Andersen JM, Dietschy JM (1981) Rates of sterol synthesis and uptake in the major organs of the rat in vivo. J Lipid Res 22:551-569

van Amerongen A, Teerlink T, van Heusden GP, Wirtz KW (1985) The non-specific lipid transfer protein (sterol carrier protein 2) from rat and bovine liver. Chem Phys Lipids 38:195-204

Van Heusden GP, Bos K, Wirtz KW (1990) The occurrence of soluble and membrane-bound non-specific lipid transfer protein (sterol carrier protein 2) in rat tissues. Biochim Biophys Acta 1046:315-321

van Meer G (2001) Caveolin, cholesterol, and lipid droplets? J Cell Biol 152: F29–34

van Meer G, Lisman Q (2002) Sphingolipid transport: rafts and translocators. J Biol Chem 277:25855-25858

van Meer G (2005) Cellular lipidomics. EMBO J 24:3159-3165

Vance JE, Pan D, Campenot RB, Bussiere M, Vance DE (1994) Evidence that the major membrane lipids, except cholesterol, are made in axons of cultured rat sympathetic neurons. J Neurochem 62:329-337

Vaena de Avalos S, Jones JA, Hannun YA (2004) Ceramides. In: Nicolaou A, Kokotos G, editors. Bioactive lipids. Bridgwater, England: The Oily Press 135–167

Vance JE, Vance DE (2004) Phospholipid biosynthesis in mammalian cells. Biochem Cell Biol 82: 113–128

Vaudry D, Falluel-Morel A, Basille M, Pamantung TF, Fontaine M, Fournier A, Vaudry H, Gonzalez BJ (2003) Pituitary adenylate cyclase-activating polypeptide prevents C2-ceramide-induced apoptosis of cerebellar granule cells. J Neurosci Res 72:303–316

Vaughan CJ (2003) Prevention of stroke and dementia with statins: Effects beyond lipid lowering. Am J Cardiol 91:23B-29

Voelker DR (2003) New perspectives on the regulation of intermembrane glycerophospholipid traffic. J Lipid Res 44:441–449

Wahrle S, Das P, Nyborg AC, McLendon C, Shoji M, Kawarabayashi T, Younkin LH, Younkin SG, Golde TE (2002) Cholesterol-dependent gamma-secretase activity in buoyant cholesterol-rich membrane microdomains. Neurobiol Dis 9:11–23

Wang E, Norred WP, Bacon CW, Riley RT, Merrill Jr AH (1991) Inhibition of sphingolipid biosynthesis by fumonisins. Implications for diseases associated with fusarium moniliforme. J Biol Chem 266:14486–14490

Wang XS, Ong WY, Connor JR (2002) Increase in ferric and ferrous iron in the rat hippocampus with time after kainate-induced excitotoxic injury. Exp Brain Res 143:137-148

Wenk MR (2005) The emerging field of lipidomics. Nat Rev Drug Discov 4:594-610

Wiesner DA, Dawson G (1996a) Staurosporine induces programmed cell death in embryonic neurons and activation of the ceramide pathway. J Neurochem 66:1418 –1425

Wiesner DA, Dawson G (1996b) Programmed cell death in neurotumor cells involves the generation of ceramide. Glycoconjugate J 13:327–333

Willaime S, Vanhoutte P, Caboche J, Lemaigre-Dubreuil Y, Mariani J, Brugg B (2001) Ceramide-induced apoptosis in cortical neurons is mediated by an increase in p38 phosphorylation and not by the decrease in ERK phosphorylation. Eur J Neurosci 13:2037–2046

Willaime-Morawek S, Brami-Cherrier K, Mariani J, Caboche J, Brugg B (2003) C-Jun N-terminal kinases/c-Jun and p38 pathways cooperate in ceramide-induced neuronal apoptosis. Neuroscience 119:387–397

Wilson JD (1970) The measurement of the exchangeable pools of cholesterol in the baboon. J Clin Invest 49:655-665

Wolf BB, Lopes MB, VandenBerg SR, Gonias SL (1992) Characterization and immunohistochemical localization of alpha 2-macroglobulin receptor (low-density lipoprotein receptor-related protein) in human brain. Am J Pathol 141:37-42

Wolozin B, Kellman W, Ruosseau P, Celesia GG, Siegel G (2000) Decreased prevalence of Alzheimer disease associated with 3-hydroxy-3-methyglutaryl coenzyme A reductase inhibitors. Arch Neurol 57:1439-1443

Wood WG, Cornwell M, Williamson LS (1989a) High performance thin-layer chromatography and densitometry of synaptic plasma membrane lipids. J Lipid Res 30:775-779

Wood WG, Gorka C, Schroeder F (1989b) Acute and chronic effects of ethanol on transbilayer membrane domains. J Neurochem 52:1925-1930

Wood WG, Schroeder F, Hogy L, Rao AM, Nemecz G (1990) Asymmetric distribution of a fluorescent sterol in synaptic plasma membranes: effects of chronic ethanol consumption. Biochim Biophys Acta 1025:243-246

Wood WG, Rao AM, Igbavboa U, Semotuk M (1993) Cholesterol exchange and lateral cholesterol pools in synaptosomal membranes of pair-fed control and chronic ethanol-treated mice. Alcohol Clin Exp Res 2:345-250

Wood WG, Schroeder F, Avdulov NA, Chochina SV, Igbavboa U (1999) Recent advances in brain cholesterol dynamics: transport, domains, and Alzheimer's disease. Lipids 34:225-234

Xu J, Yeh CH, Chen S, He L, Sensi SL, Canzoniero LM, Choi DW, Hsu CY (1998) Involvement of de novo ceramide biosynthesis in tumor necrosis factor-alpha/cycloheximide-induced cerebral endothelial cell death. J Biol Chem 273:16521-16526

Yang DI, Yeh CH, Chen S, Xu J, Hsu CY (2004) Neutral sphingomyelinase activation in endothelial and glial cell death induced by amyloid betapeptide. Neurobiol Dis 17:99–107

Yang SN (2000) Ceramide-induced sustained depression of synaptic currents mediated by ionotropic glutamate receptors in the hippocampus: an essential role of postsynaptic protein phosphatases. Neuroscience 96:253–258

Yasuda H, Fujii M, Fujisawa H, Ito H, Suzuki M (2001) Changes in nitric oxide synthesis and epileptic activity in the contralateral hippocampus of rats following intrahippocampal kainate injection. Epilepsia 42:13-20

Yeagle PL, Young J, Rice D (1988) Effects of cholesterol on (Na^+, K^+)-ATPase ATP hydrolyzing activity in bovine kidney. Biochemistry 27: 6449-6352

Yeagle PL (1992) The Dynamic of Membrane Lipids. In: The Structure of Biological Membranes (Yeagle PL, ed.) CRC Press, Boca Raton, pp.157-174

Yamamoto R, Kallen CB, Babalola GO, Rennert H, Billheimer JT, Strauss JF 3rd (1991) Cloning and expression of a cDNA encoding human sterol carrier protein 2. Proc Natl Acad Sci USA 88:463-467

Yu ZF, Nikolova-Karakashian M, Zhou D, Cheng G, Schuchman EH, Mattson MP (2000) Pivotal role for acidic sphingomyelinase in cerebral ischemia-induced ceramide and cytokine production, and neuronal apoptosis. J Mol Neurosci 15:85–97

Zacco A, Togo J, Spence K, et al (2003) 3-Hydroxy-3-methylglutaryl coenzyme A reductase inhibitors protect cortical neurons from excitotoxicity. J Neurosci 23:11104-11111

Zager RA, Kalhorn TF (2000) Changes in free and esterified cholesterol: hallmarks of acute renal tubular injury and acquired cytoresistance. Am J Pathol 157:1007-1016

Zaleska MM, Wilson DF (1989) Lipid hydroperoxides inhibit reacylation of phospholipids in neuronal membranes.J Neurochem 52:255-260

Zubenko GS, Cohen BM, Boller F, Malinakova I, Keefe N, Chojnacki B (1987) Platelet membrane abnormality in Alzheimer's disease. Ann Neurol 22:237-244

CHAPTER V

TABLES, TABLE CAPTIONS, FIGURES AND FIGURE LEGENDS

Table 1. 1. Number of cholesterol positive pyramidal neurons or cholesterol 24-hydroxylase (CYP46) positive glial cells in field CA1 of saline or kainate-injected rat hippocampus

	S	1D	3D	1W	2W	4W
CHO-Neu	0	313 ± 39	464 ± 63	919 ± 104	1018 ± 145	148 ± 81
CYP46-As	0	157 ± 83	619 ±136	1312 ± 195	1815 ± 225	512 ± 139

1D, 3D, 1 - 4 W refer to 1 day or 3 day, and 1, 2 and 4 week post-kainate injection. CHO, CYP46, Neu, As and S indicate cholesterol staining, cholesterol 24-hydroxylase staining, neurons, astrocytes and saline respectively. The values are mean ± standard deviation of number of cells / mm^2 in field CA1. Four sections were counted in each of the four rats in each category. Results were analyzed by 1-way ANOVA with Bonferroni's multiple comparison post-hoc test, $P < 0.05$ was considered significant. P values < 0.05 are as follows: CHO-Neu: S vs 1D, 3D, 1W, 2W; 1D vs 1W, 2W; 3D vs 1W, 2W, 4W; 1W vs 4W; 2W vs 4W. CYP46-As: S vs 3D, 1W, 2W, 4W; 1D vs 3D, 1W, 2W; 3D vs 1W, 2W; 1W vs 2W, 4W; 2W vs 4W.

Table 1. 2. Concentrations of cholesterol, 24-hydroxycholesterol and 7-ketocholesterol in the right hippocampus of the saline or kainate-injected rats

	S	3D	1W	2W	4W
Chol (μg/mg)	23.0 ± 15.8	37.5 ± 16.8	63.0 ± 10.2	98.6 ± 16.7	67.0 ± 4.2
24-OH-Chol (ng/mg)	7.2 ± 5.4	10.8 ± 3.7	26.2 ± 6.3	30.1 ± 4.9	7.4 ± 2.8
7-keto-Chol (ng/mg)	1.4 ± 0.4	1.4 ± 0.3	2.8 ± 0.7	4.2 ± 0.9	2.6 ± 0.1

3D, 1 - 4 W refer to 3 day, and 1, 2 and 4 week post-kainate injection. Chol, 24-OH-Chol, 7-keto-Chol and S indicate cholesterol, 24-hydroxycholesterol, 7-ketocholesterol and saline respectively. Data was normalized to the tissue weight and expressed as mean ± standard deviation for four rats at each time point. Results were analyzed by 1-way ANOVA with Bonferroni's multiple comparison post-hoc test, $P < 0.05$ was considered significant. P values < 0.05 are as follows: Chol: S vs 1W, 2W, 4W; 3D vs 2W; 1W vs 2W. 24-OH-Chol: S vs 1W, 2W; 3D vs 1W, 2W; 1W vs 4W; 2W vs 4W. 7-keto-Chol: S vs 2W; 3D vs 2W.

Table 1. 3. Effect of intraperitoneal injection of lovastatin on concentrations of cholesterol, 24-hydroxycholesterol and 7-ketocholesterol in the right hippocampi of 1 week and 2 week post-kainate-injected rats

	Time	kainate / saline	kainate / lovastatin
Chol (μg/mg)	1 W	67.6 ± 15.6	41.6 ± 16.0 *
24-OH-Chol (ng/mg)	1 W	23.1 ± 10.6	7.2 ± 2.9 *
24-OH-Chol (ng/mg)	2 W	27.2 ± 7.8	11.6 ± 3.0 *
7-keto-Chol (ng/mg)	1 W	2.9 ± 1.1	2.0 ± 0.9
7-keto-Chol (ng/mg)	2 W	3.8 ± 0.8	1.4 ± 0.2 *

1 W, 2 W, Chol, 24-OH-Chol and 7-keto-Chol indicate 1 week, 2 weeks, cholesterol, 24-hydroxycholesterol and 7-ketocholesterol respectively. Data was normalized to the tissue weight and expressed as mean ± standard deviation. Results were analyzed by Student's t-test, *$P < 0.05$ was considered significant.

Table 1. 4. Effect of lovastatin on concentrations of cholesterol, 24-hydroxycholesterol and 7-ketocholesterol in hippocampal slices

	CONT	KA	KA/LOVA
Chol (µg/mg)	1.56 ± 0.29	2.17 ± 0.11#	1.68± 0.12*
24-OH-Chol (ng/mg)	0.37 ± 0.05	0.61 ± 0.07#	0.43 ± 0.09*
7-keto-Chol (ng/mg)	0.42 ± 0.06	1.27 ± 0.46#	0.45 ± 0.09*

CONT, KA, KA/LOVA, Chol, 24-OH-Chol and 7-keto-Chol indicate untreated cultures, cultures treated with kainate plus vehicle, and cultures treated with kainate plus lovastatin, cholesterol, 24-hydroxycholesterol, and 7-ketocholesterol. Data was normalized to the weight of the slices and expressed as mean ± standard deviation of 3 experiments (12-16 slices were used in each treatment group per experiment). Results were analyzed by 1-way ANOVA with Bonferroni's multiple comparison post-hoc test, $P < 0.05$ was considered significant. # Significant difference compared to CONT group; * Significant difference compared to KA group.

Fig. 1. 1. Immunoblots of cholesterol 24-hydroxylase in the rat hippocampus. The antibody detects a band at ~56kDa in homogenates of both saline (S) and kainate-injected (K) rat hippocampus

Fig. 1. 1.

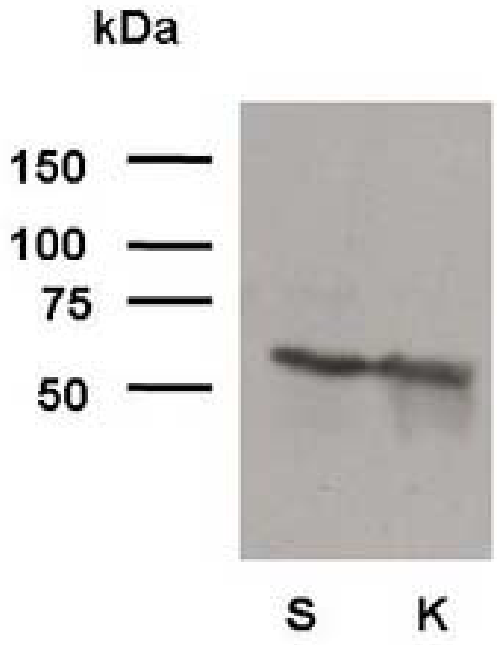

Fig. 1. 2. A,B: light micrographs of sections of hippocampal CA1 field from a saline-injected rat. A: cholesterol immnuostained section, showing little labeling in neurons (asterisk). B: cholesterol 24-hydroxylase immunostained section, showing light labeling of neurons (asterisk). C,D: sections through the affected CA1 field of the right hippocampus, from a rat that had been injected with kainate 3 days earlier. C: cholesterol immunostained section, showing labeled pyramidal cell bodies (arrows) and diffused labeling of the neuropil (asterisk). D: cholesterol 24-hydroxylase immunostained section, showing occasional labeling in glial cells (arrows) but not neurons. E,F: sections through the affected CA1 field of the right hippocampus, from a rat that had been injected with kainate 2 weeks earlier. E: cholesterol immunostained section. Labeling is present in the cell bodies and dendrites of pyramidal neurons (arrows). Inset: control section incubated with antigen (cholesterol)-absorbed antibody, showing absence of staining in pyramidal neurons. F: cholesterol 24-hydroxylase immunostained section, showing labeled glial cells (arrows). G,H: sections through the affected CA1 field of the right hippocampus, from a rat that had been injected with kainate 4 weeks earlier. There is little or no staining for cholesterol (G) or cholesterol 24-hydroxylase (H) in the degenerating CA1 field at this time (asterisks). CTRL: saline-injected rat. 3D, 2W, 4W: 3 days, 2 weeks, and 4 weeks after kainate injection. Scale = 50 μm.

Fig. 1. 2.

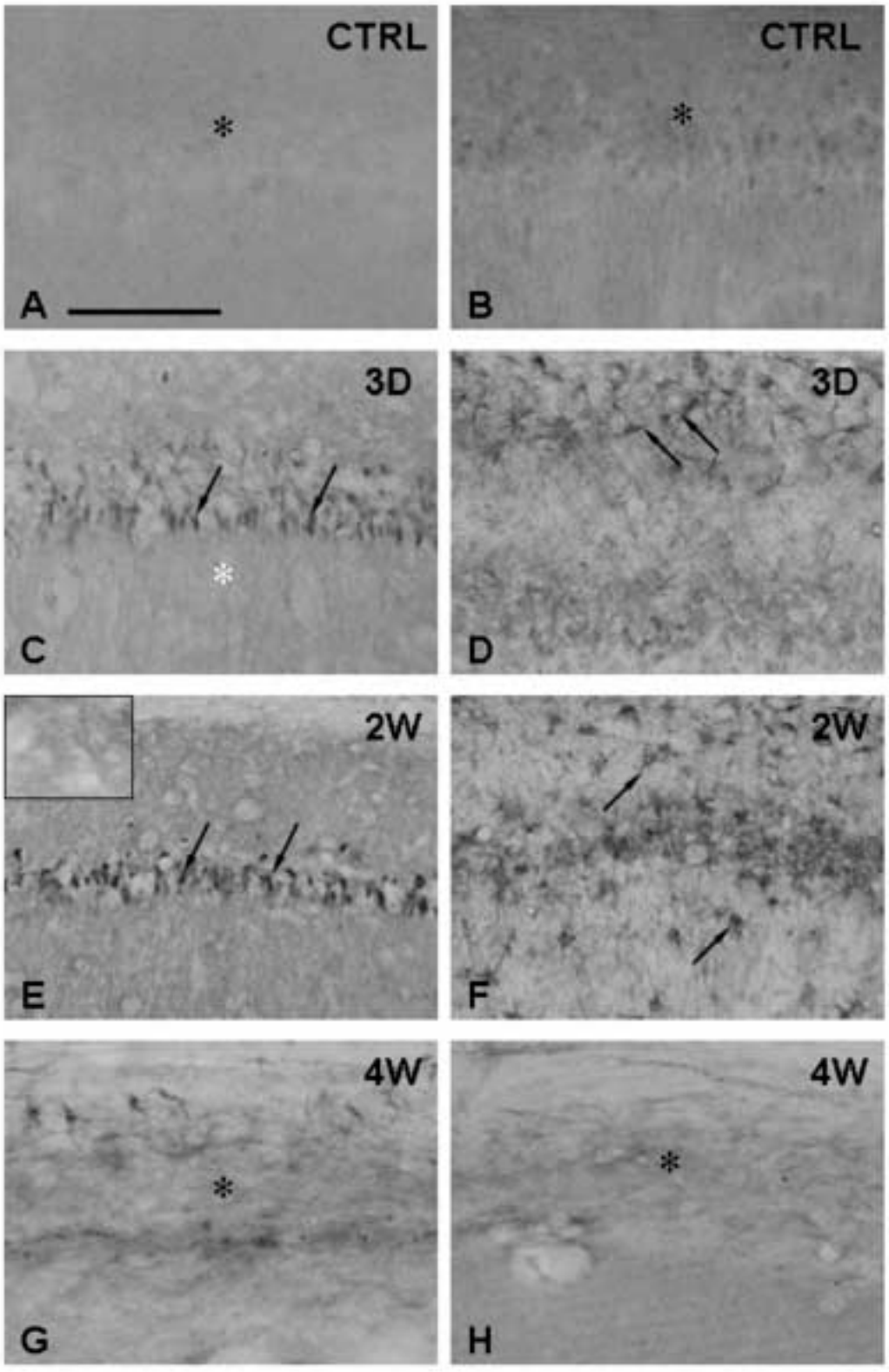
CTRL
A
CTRL
B
3D
C
3D
D
2W
E
2W
F
4W
G
4W
H

Fig. 1. 3. A,B: electron micrographs of cholesterol 24-hydroxylase immunolabeled profiles in the hippocampus of a 2 week post-kainate-injected rat. A: labeled astrocyte (AS), next to an unlabeled microglial cell (M). The nucleus of the astrocyte contains evenly dispersed fine heterochromatic clumps, and are distinguished from the marginated heterochromatin in the microglial cell. F: glial filaments. Arrows indicate reaction product. B: astrocytic end foot (AS), on a blood vessel. F: glial filaments. E: endothelial cell, L: lumen of vessel. Arrows indicate reaction product. C,D: double, cholesterol 24-hydroxylase (C, red channel) and GFAP (D, green channel) immunofluorescence labeled section from field CA1 of a 2 week post-kainate-injected rat. The cells which are positive for cholesterol 24-hydroxylase (arrows in B) are also labeled for GFAP (arrows in C), indicating that they are astrocytes. Scale: A,B = 1 μm, C,D=100 μm.

Fig .1. 3.

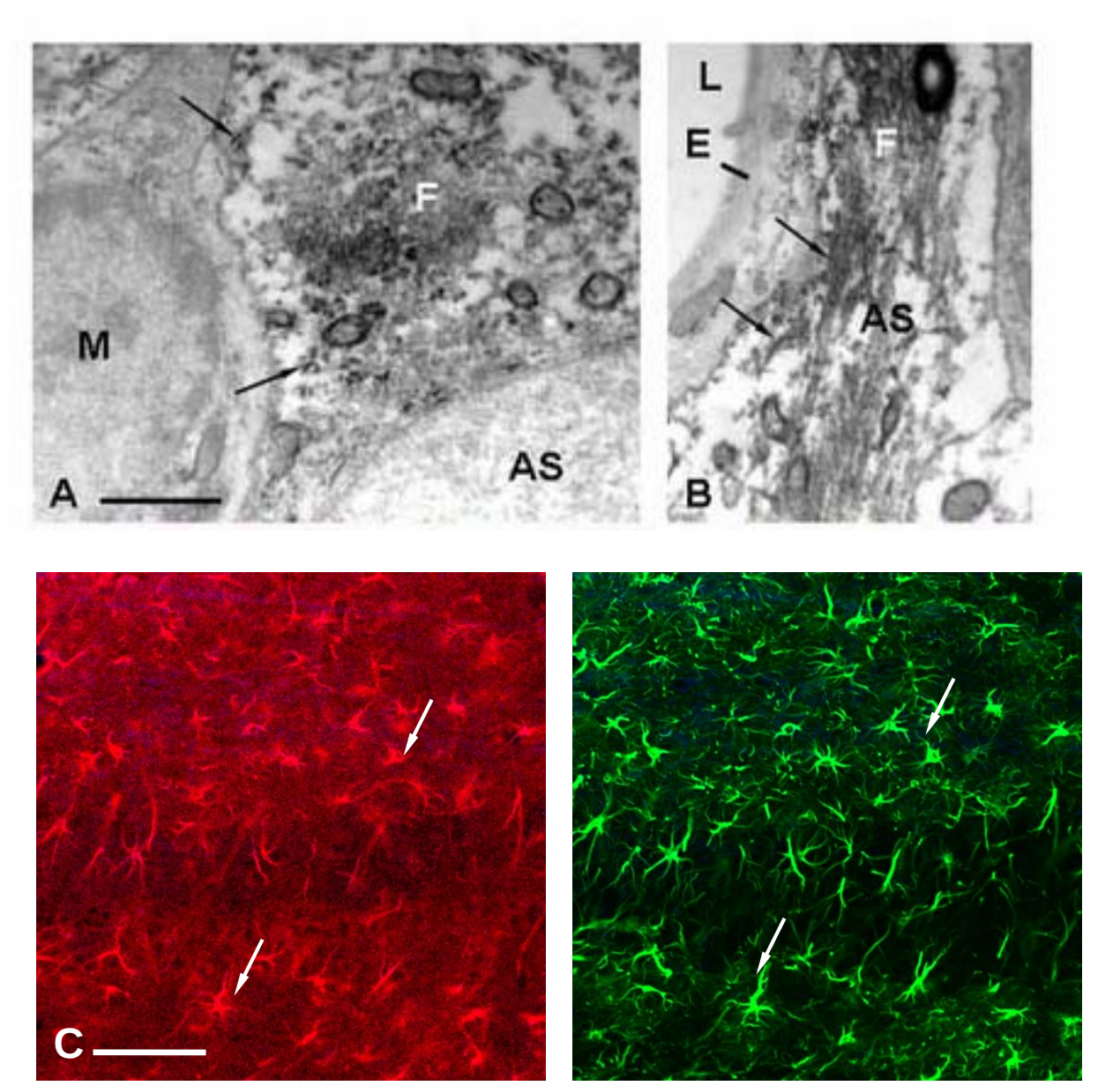

Fig. 1. 4. *In vivo* analyses of the effect of lovastatin on neuronal survival after intracerebroventricular kainate injection. A: Nissl stained sections from the hippocampus from representative animals. CONT, KA and KA/LOVA indicate saline, kainate plus vehicle, and kainate plus lovastatin injected rats. Arrows indicate uninjured neurons in fields CA1 and CA3. Scale = 1 mm. B: percentage of the CA fields that contains uninjured neurons in Nissl or MAP2 stained sections. A significantly greater number of hippocampal neurons is present in the kainate plus lovastatin (KA/LOVA) injected rats, compared to the kainate plus vehicle (KA) injected rats. Data is expressed as mean ± standard deviation. n = 5 in each group. Results were analyzed by Student's t-test, *P < 0.05 was considered significant.

Fig. 1. 4.

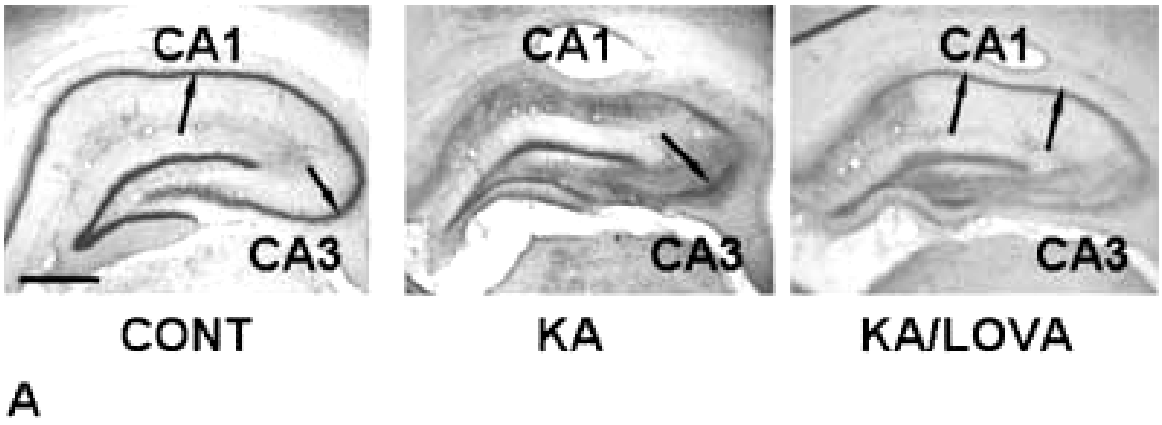
CA1
CA3
CA1
CA3
CA1
CA3
CONT
KA
KA/LOVA
A

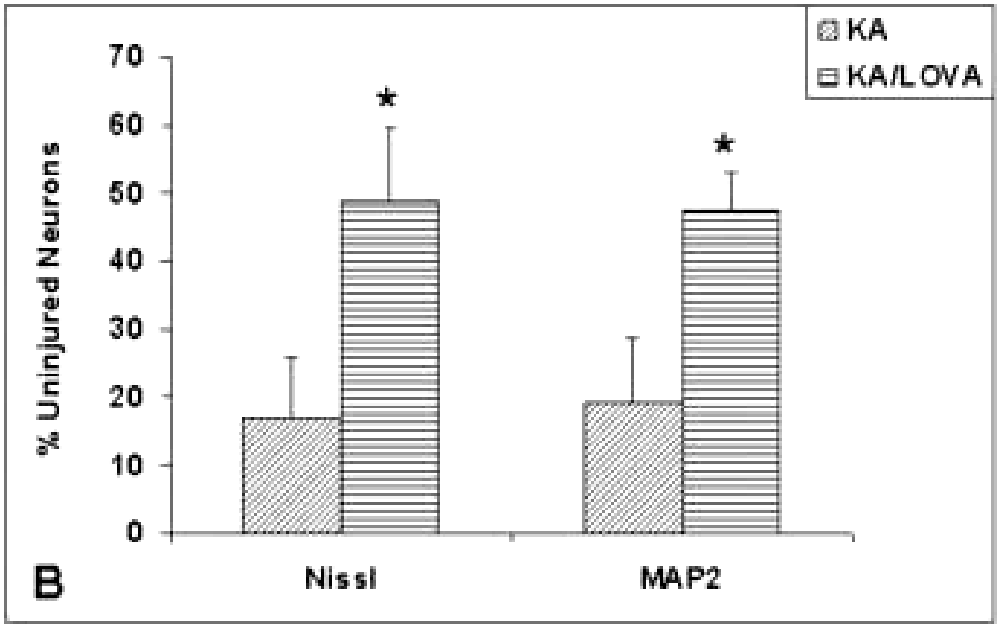
KA
KA/LOVA
% Uninjured Neurons
70
60
50
40
30
20
10
0
*
*
Nissl
MAP2
B

Fig. 1. 5. *In vitro* analyses of the effect of lovastatin on neuronal survival after addition of kainate to hippocampal slices. CONT, KA and KA/LOVA indicate untreated, kainate plus vehicle, and kainate plus lovastatin treated slices. A: MAP2 immunostained sections from representative slices. Arrows indicate uninjured neurons in fields CA1 and CA3. Scale = 300 μm. B: number of MAP2 positive pyramidal neurons in cultured hippocampal slices. Values are mean ± standard deviation of number of cells / mm^2 in fields CA1 or CA3 (n = 6 slices in each group). Results were analyzed by 1-way ANOVA with Bonferroni's multiple comparison post-hoc test, $P < 0.05$ was considered significant. # Significant difference compared to CONT group; * Significant difference compared to KA group. C: effect of lovastatin on LDH activity in hippocampal slice cultures. Data is expressed as percentage of total LDH release (mean ± standard deviation) of 3 experiments. Results were analyzed by Student's t-test, $P < 0.05$ was considered significant. * Significant difference compared to KA group.

Fig. 1. 5.

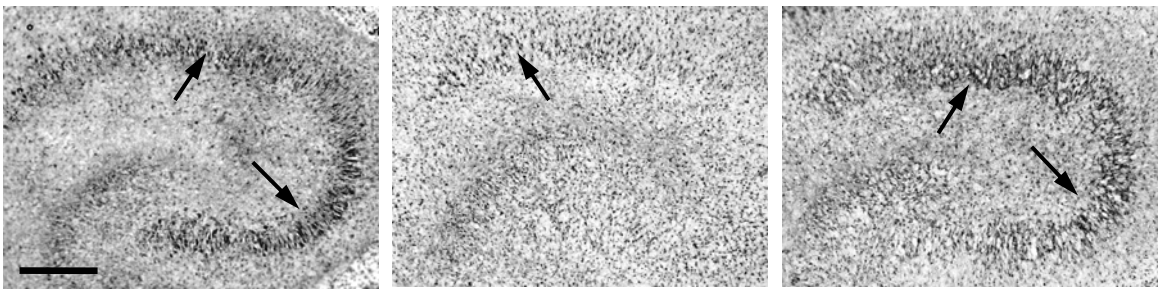

CONT **KA** **KA/LOVA**

A

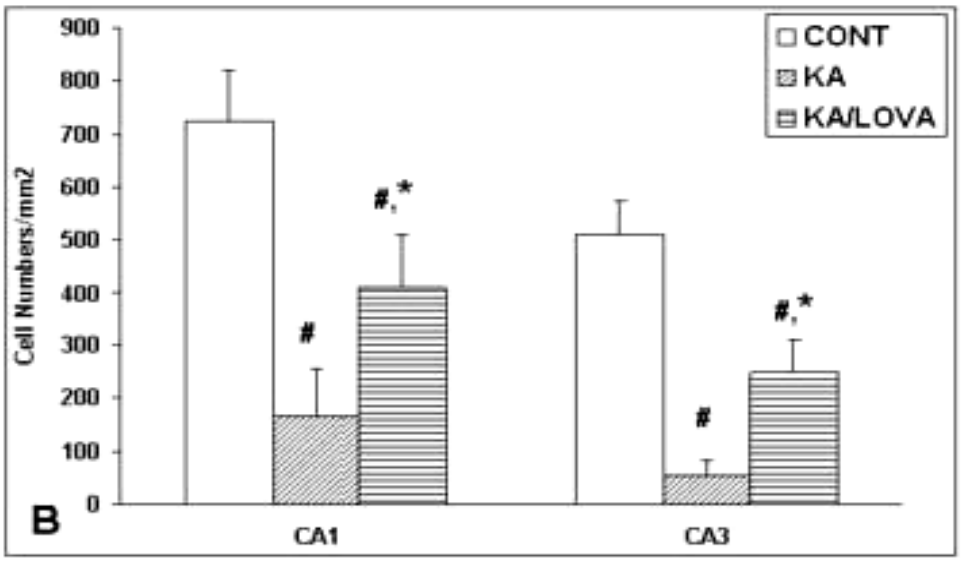

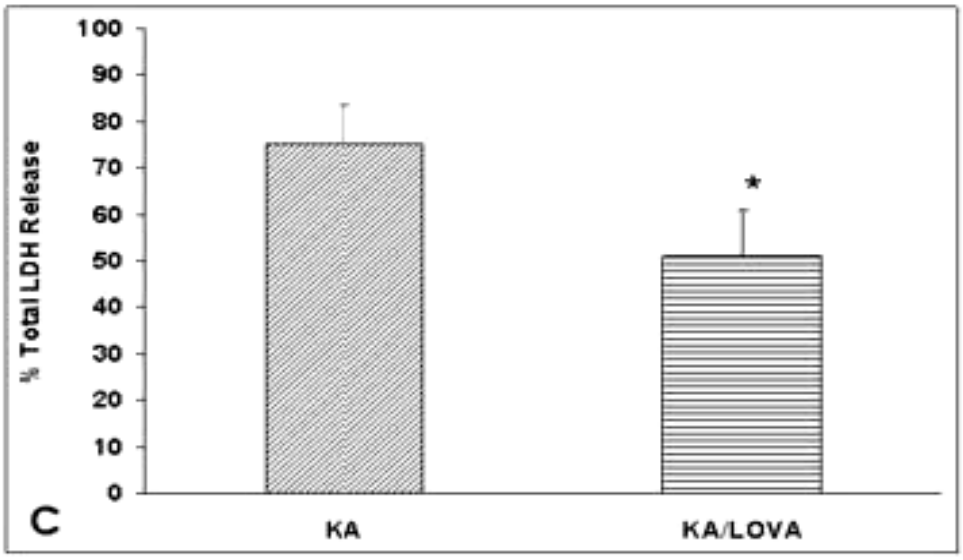

Fig. 1. 6. *In vitro* analyses of neurotoxic effect of 24-hydroxycholesterol on hippocampal slice cultures. CONT, V, 24-OHC(15), 24-OHC(50) and 7-KetoC (50) indicate untreated cultures, cultures treated with vehicle, cultures treated with 15 μM 24-hydroxycholesterol, cultures treated with 50 μM 24-hydroxycholesterol, and cultures treated with 50 μM 7-ketocholesterol. A: MAP2 immunostained sections from representative slices. Arrows indicate uninjured neurons in fields CA1 and CA3. Scale = 250 μm. B: number of MAP2 positive pyramidal neurons in cultured hippocampal slices. Values are mean ± standard deviation of number of cells / mm^2 in fields CA1 or CA3 (n = 6 slices in each group). Results were analyzed by 1-way ANOVA with Bonferroni's multiple comparison post-hoc test, $P < 0.05$ was considered significant. #: significant difference compared to CONT; &: significant difference compared to 24-OHC(15). C: effect of 24-hydroxycholesterol or 7-ketocholesterol on LDH activity in hippocampal slice cultures. Data were expressed as percentage of total LDH release (mean ± standard deviation) of 3 experiments. Results were analyzed by Student's t-test, $P < 0.05$ was considered significant. # Significant difference compared to V.

Fig. 1. 6.

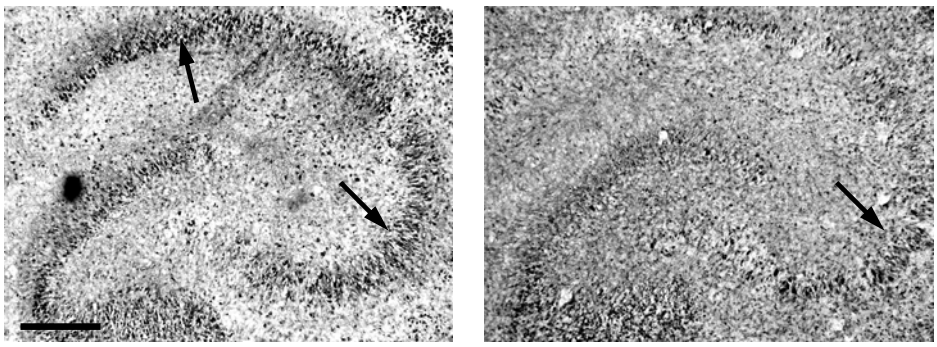

24-OHC (15) 24-OHC (50)

A

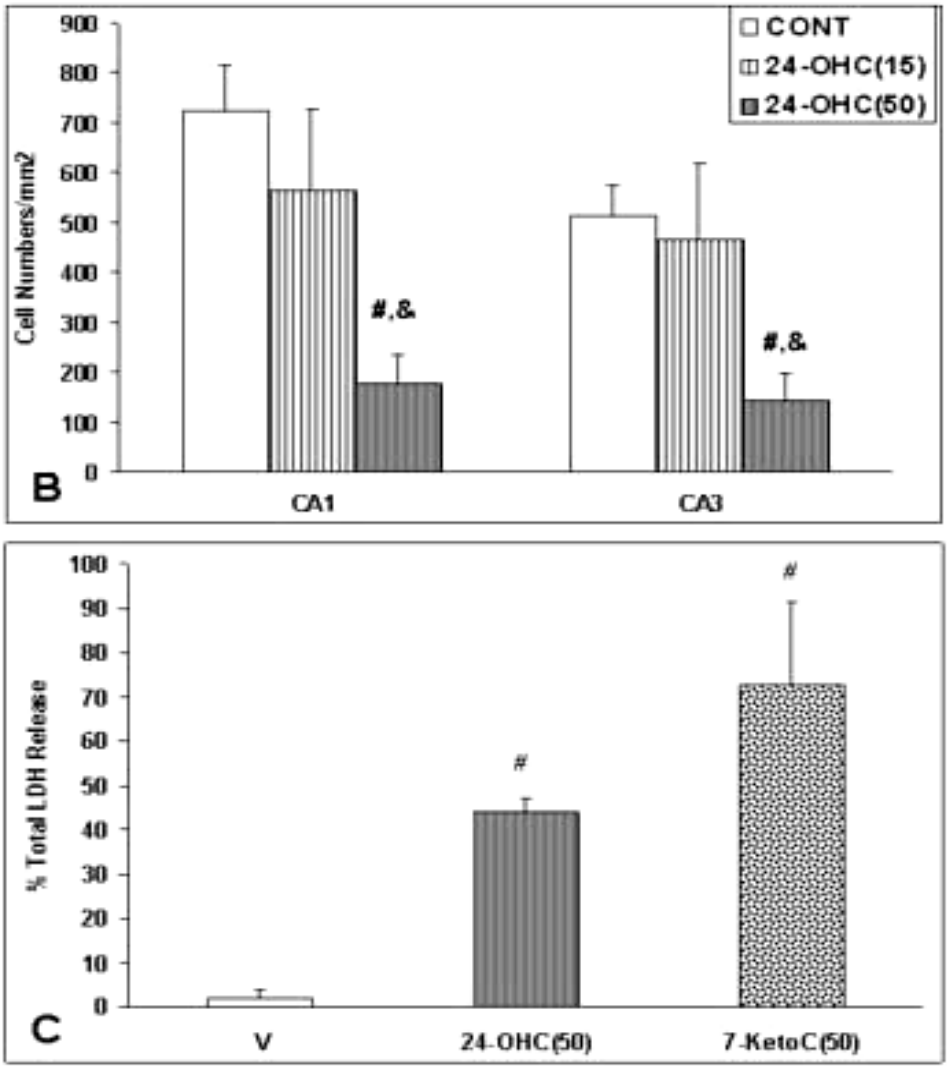

Table 2. 1. Number of SPT-positive neurons and astrocytes in field CA1 of the hippocampus.

	S [a]	1D [b]	3D [c]	1W [d]	2W [e]	4W [f]
Neurons	941 ± 172	128 ± 66	118 ± 50	43 ± 29	0	0
Astrocytes	0	76 ± 45	179 ± 43	433 ± 82	829 ±164	478 ± 126

S, 1D, 3D, 1W, 2W, 4W indicate saline injection (2 week post-injection), 1 day, 3 days, 1 week, 2 week, and 4 week post-kainate-injection. Values indicate mean number of cells / mm^2 ± standard deviation. P values < 0.05 are as follows: Neurons: a vs b, c, d, e, f; b vs d, e, f; c vs d, e, f; d vs e, f. Astrocytes: a vs c, d, e, f; b vs c, d, e, f; c vs d, e, f; d vs e; e vs f.

Fig. 2. 1. SPT enzyme protein level and activity after kainate lesions. A,B: Western blot analyses of saline or kainate-treated hippocampus. The antibody to SPT recognized a single band at 65kDa consistent with the expected molecular weight of the SPT2 catalytic subunit (A). Significantly increased SPT enzyme protein is detected at 1 and 2 weeks after kainate treatment, compared to saline treated controls (B). Values indicate mean relative density of SPT to β-actin ± standard deviation. #: significant difference compared to saline injected controls. &: significant difference compared to 4 weeks post-kainate injection ($P < 0.05$). C: SPT enzymatic activity in microsomal fractions of the hippocampus. The values indicate mean activity ± standard deviation. #: significant difference compared to controls ($P < 0.05$). Abbreviations: S, 1D, 3D, 1W, 2W, 4W indicate saline injection (2 weeks postinjection); and 1 day, 3 days, 1 week, 2 weeks, and 4 weeks post kainate injection.

Fig. 2. 1.

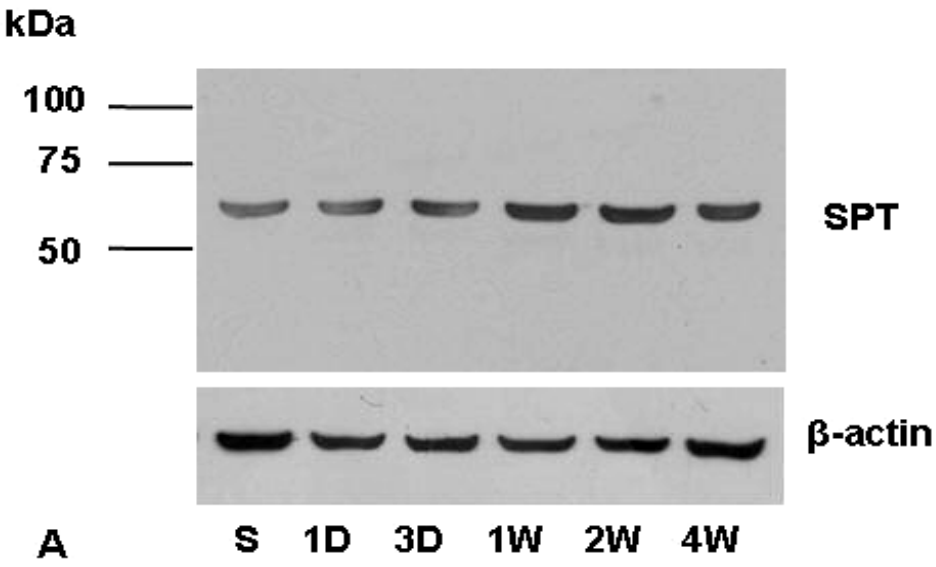
kDa
100
75
50
SPT
β-actin
A
S
1D
3D
1W
2W
4W

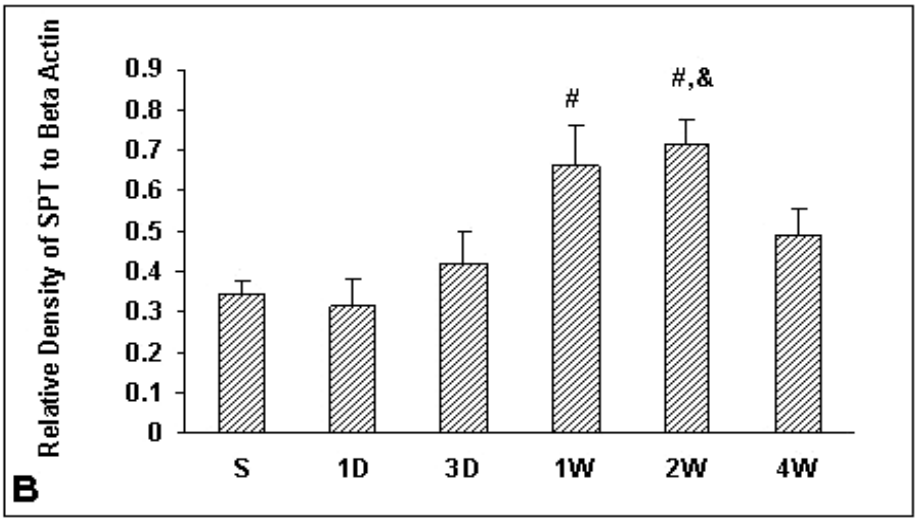
Relative Density of SPT to Beta Actin
0.9
0.8
0.7
0.6
0.5
0.4
0.3
0.2
0.1
0
#
#,&
S
1D
3D
1W
2W
4W
B

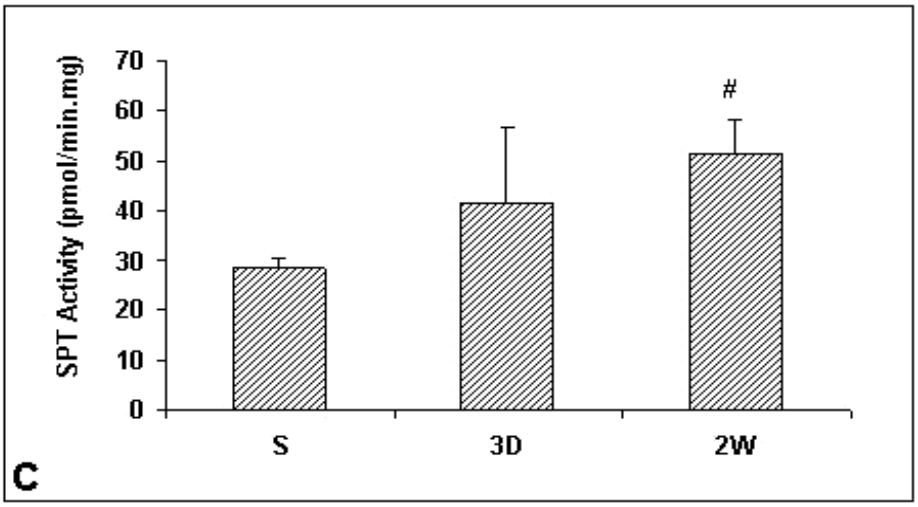
SPT Activity (pmol/min.mg)
70
60
50
40
30
20
10
0
#
S
3D
2W
C

Fig. 2. 2. Light micrographs of field CA1 of the hippocampus. A: SPT immunolabeled section from saline injected rat showing light immunoreactivity in pyramidal neurons (arrowheads). B,C,D: SPT immunolabeled sections from rats that have been injected with kainate 3 days (B), 1 week (C), and 2 weeks (D) earlier. Loss of labeling in neurons, but increased labeling in astrocytes (arrows) is observed in areas affected by kainate. E: adjacent section from the same animal as D incubated with antigen-absorbed antibody, showing absence of labeling (asterisk). F: SPT immunolabeled section from a rat that has been injected with kainate 4 weeks earlier, showing light labeling of glial cells (arrow). Abbreviations: S, 3D, 1W, 2W, 4W indicate saline injection, 3 day, 1 week, 2 week, and 4 week post kainate injection. Scale bar = 50 μm.

Fig. 2. 2.

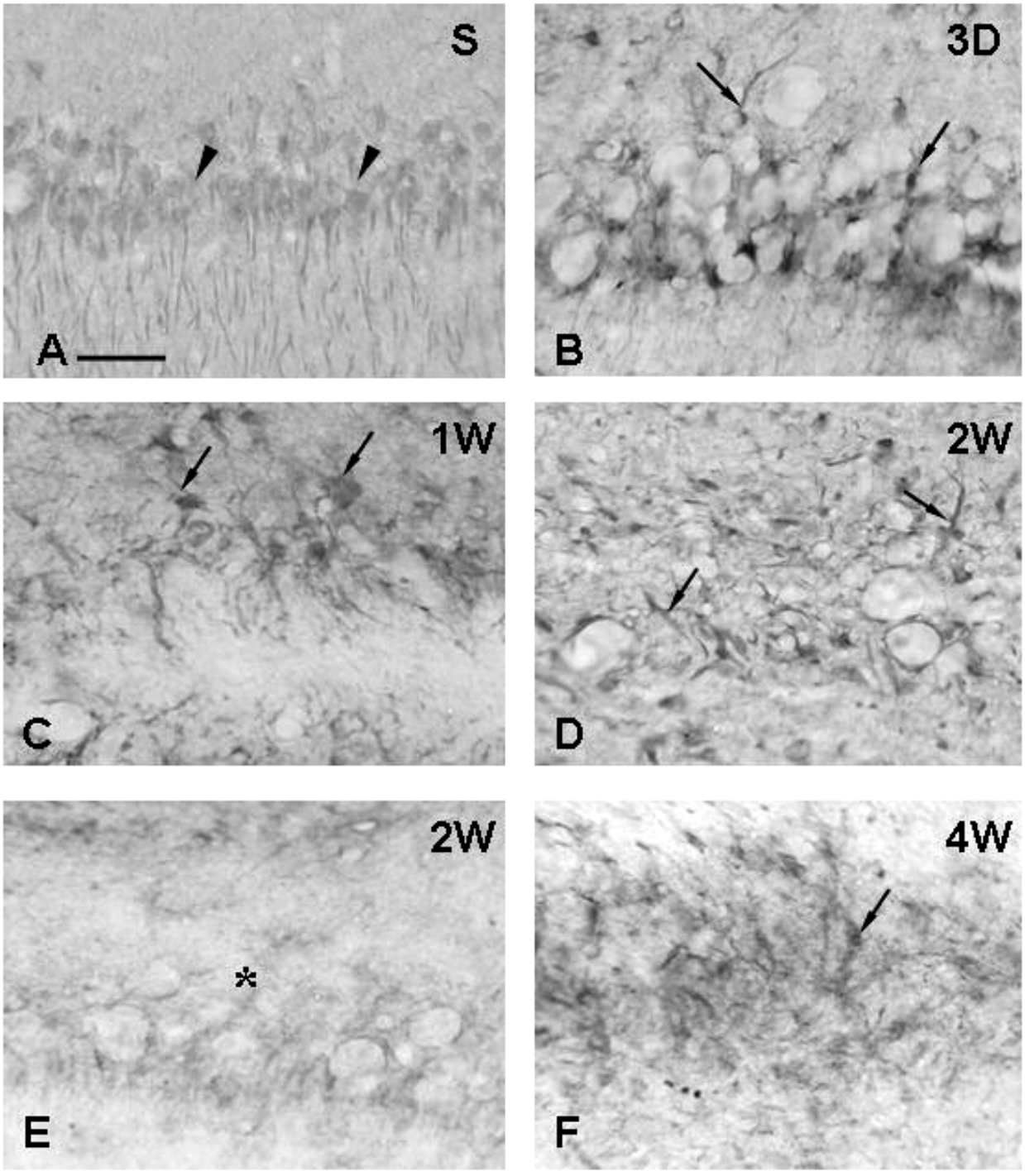

Fig. 2. 3. A,B: SPT (A, red channel) and GFAP (B, green channel) double immunofluorescence labeled section of field CA1, from a rat that had been injected with kainate 2 weeks earlier. Cells which are positive for SPT are also labeled for GFAP (arrows) indicating that they are astrocytes. Scale A,B = 20 μm. C,D: sections immunostained for SPT from a rat that had been injected with kainate 2 weeks earlier, showing an immunoreactive glial cell with morphological features of astrocytes (C) and labeled astrocytic end feet (D) around blood vessel. Label is absent from endothelial cells (E). AS: astrocyte; F: glial filaments; L: lumen of the blood vessel. Arrows indicate immunoreaction products. Scale C,D = 1 μM.

Fig. 2. 3.

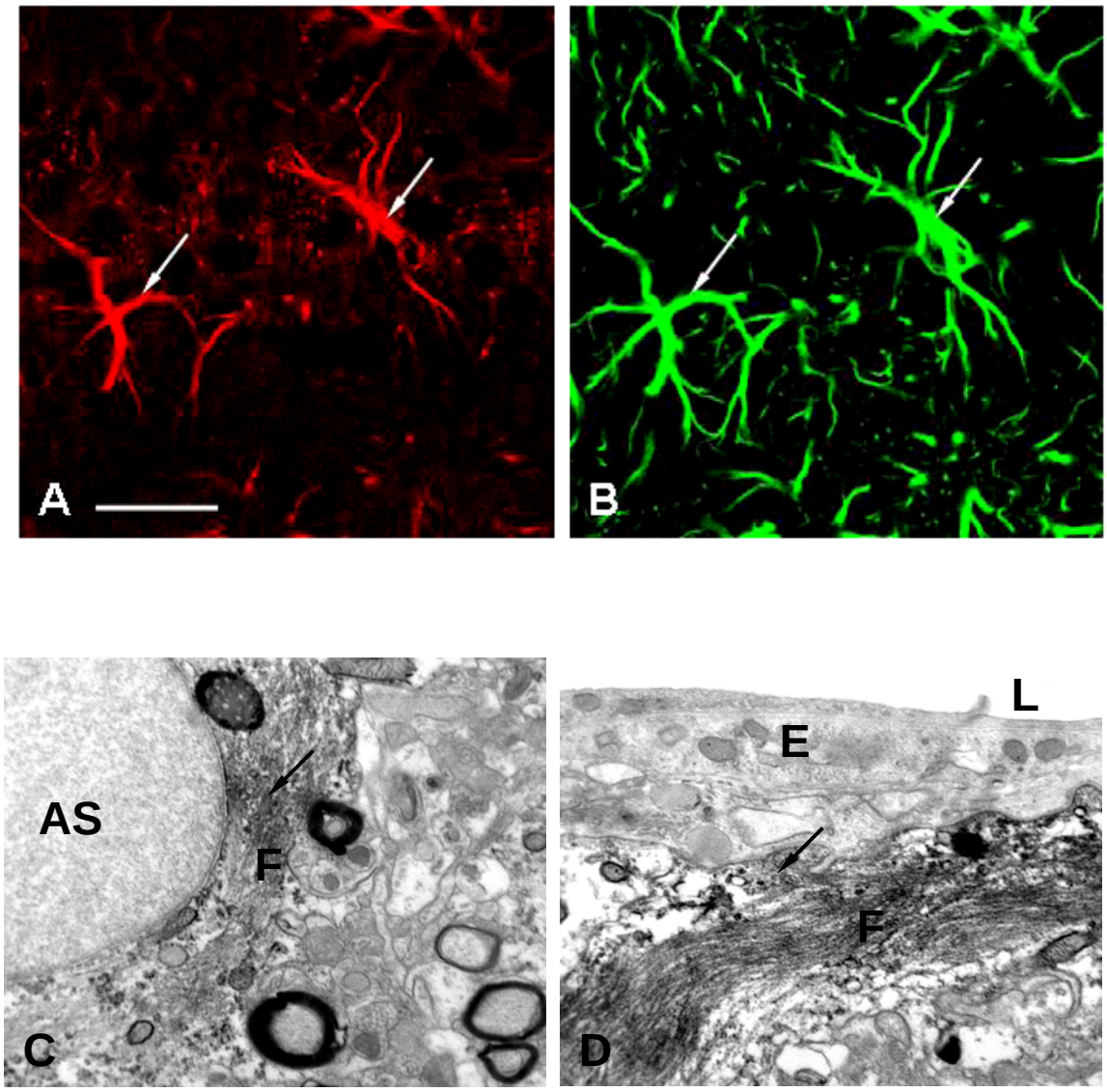

Fig. 2. 4. Mass spectrometric analyses of hippocampal slice cultures. A: changes in ceramide species after kainate treatment, and effects of enzyme inhibitors. Data are calculated as relative abundance of the various molecular species of ceramides (Cer) to internal standard (C19 ceramide) and normalized to protein concentration. Significant increases in 16:0, 18:0, 20:0 ceramide species were detected after kainate injury, and the increase were partially blocked by inhibitors to SPT (ISP-1 or LCS). B: sphingomyelin species after kainate treatment. Data are calculated as relative abundance of the various molecular species of sphingomyelin (SM) to internal standard (C12 sphingomyelin) and normalized to protein concentration. A non-significant trend to a decrease in 18:0 sphingomyelin species was detected after kainate treatment. No significant effect was observed after treatment with any of the enzyme inhibitors. Values indicate mean ± standard error. CONT, KA, KA/ISP-1, KA/LCS, KA/FUM and KA/GW4869 indicate untreated slices, kainate-treated slices, kainate plus ISP-1 treated slices, kainate plus L-cycloserine treated slices, kainate plus fumonisin B1 treated slices, and kainate plus GW4869 treated slices. $P < 0.05$ was considered significant. #: significant difference compared to CONT group. *: significant difference compared to KA group.

Fig. 2. 4.

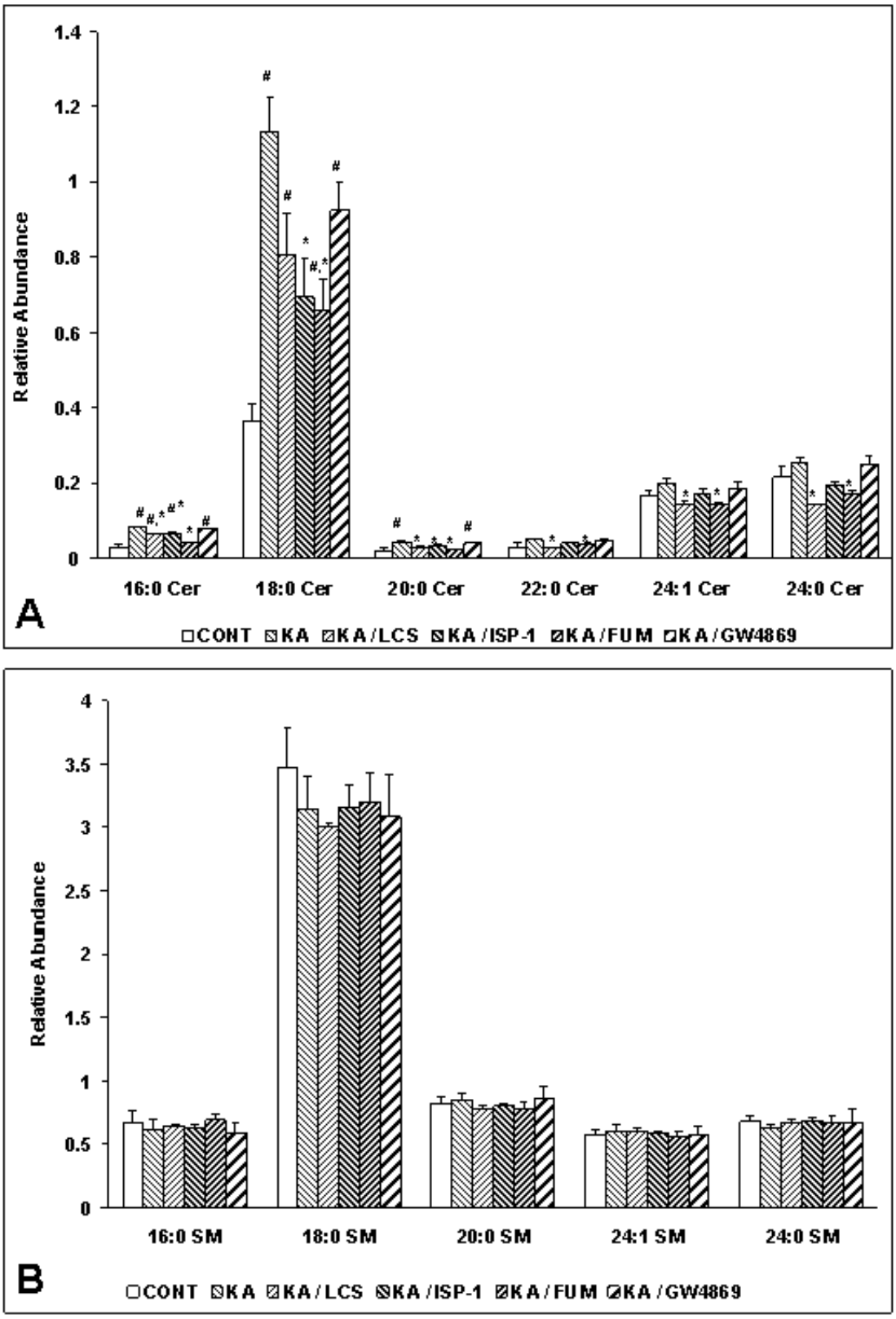
Relative Abundance
1.4
1.2
1
0.8
0.6
0.4
0.2
0
16:0 Cer
18:0 Cer
20:0 Cer
22:0 Cer
24:1 Cer
24:0 Cer
A
CONT KA KA/LCS KA/ISP-1 KA/FUM KA/GW4869
Relative Abundance
4
3.5
3
2.5
2
1.5
1
0.5
0
16:0 SM
18:0 SM
20:0 SM
24:1 SM
24:0 SM
B
CONT KA KA/LCS KA/ISP-1 KA/FUM KA/GW4869

Fig. 2. 5. Effect of SPT inhibitors on kainate-induced neuronal injury in hippocampal slice cultures. A,B: light micrographs (A) and cell counts (B) of MAP2 immunostained sections from untreated slices (CONT), kainate-treated slices (KA) or kainate plus ISP-1 treated slices (KA/ISP-1). Kainate treatment results in loss of labeling in neurons, and this loss was partially prevented by treatment with ISP-1. Arrows indicate uninjured neurons in fields CA1 and CA3. Scale = 300 μm. #: significant difference compared to CONT, *: Significant difference compared to KA ($P < 0.05$). C: cell counts of MAP2 immunostained sections from untreated slices (CONT), kainate-treated slices (KA) or kainate plus LCS treated slices (KA / LCS). Kainate treatment results in loss of labeling in neurons, and this loss was partially prevented by treatment with LCS. #: significant difference compared to CONT; *: significant difference compared to KA ($P < 0.05$).

Fig. 2. 5.

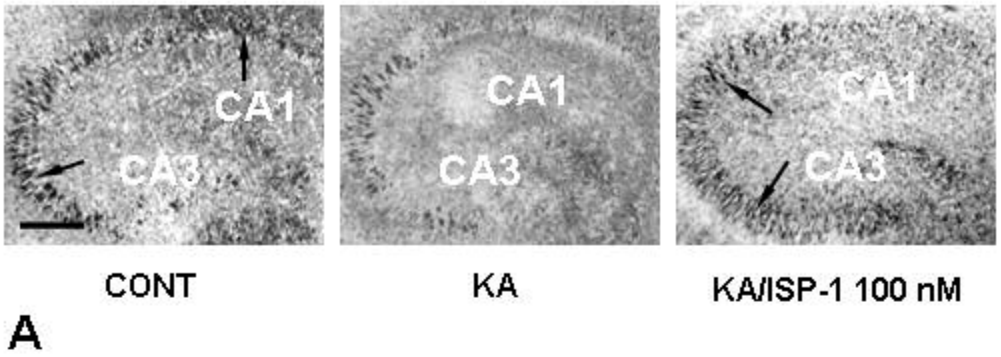
CA1
CA3
CA1
CA3
CA1
CA3
CONT
KA
KA/ISP-1 100 nM

A

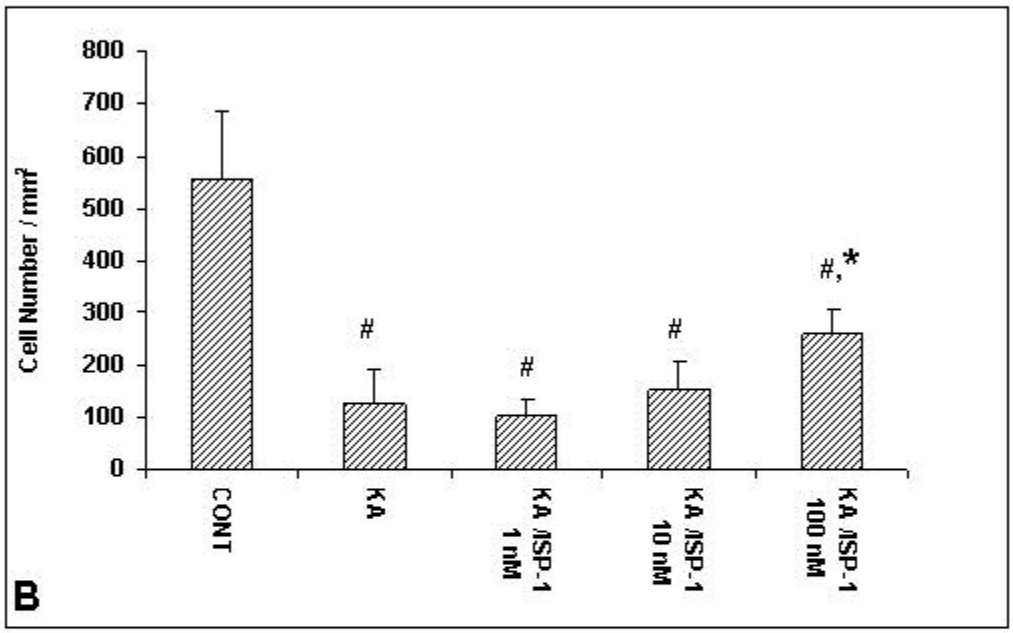
Cell Number / mm²
800
700
600
500
400
300
200
100
0
#
#
#
#,*
CONT
KA
KA /ISP-1 1 nM
KA /ISP-1 10 nM
KA /ISP-1 100 nM

B

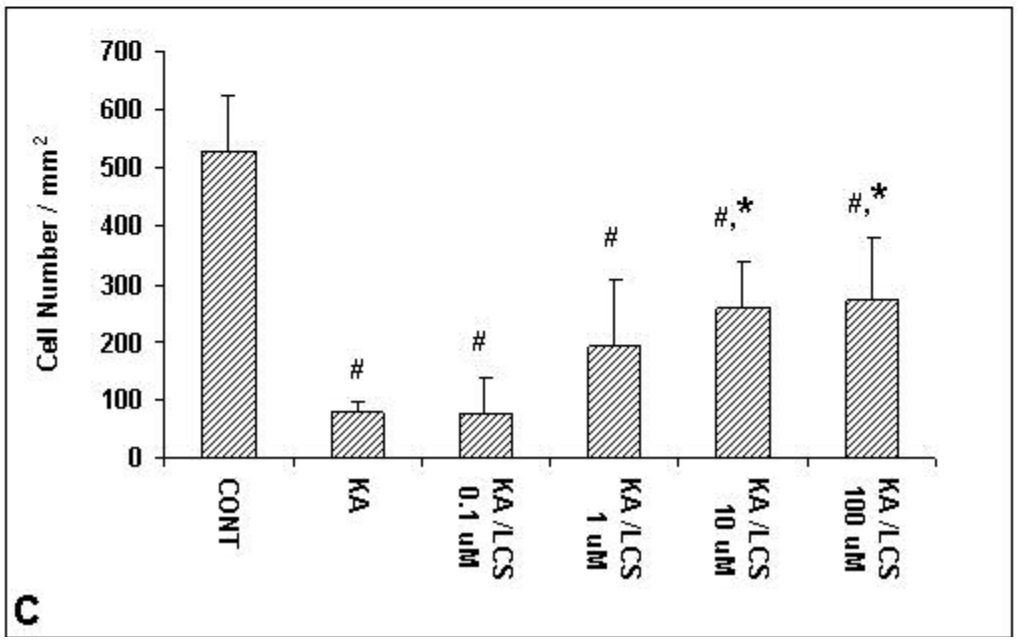
Cell Number / mm²
700
600
500
400
300
200
100
0
#
#
#
#,*
#,*
CONT
KA
KA /LCS 0.1 uM
KA /LCS 1 uM
KA /LCS 10 uM
KA /LCS 100 uM

C

Fig. 2. 6. Effect of SPT, ceramide synthase, and neutral sphingomyelinase inhibitors on kainate-induced neuronal injury in hippocampal slice cultures. Kainate treatment results in damage to neurons reflected by increased LDH activity in the culture medium, and this increase was partially prevented by treatment with ISP-1, LCS, and fumonisin B1. No significant effect was observed after treatment with GW4869. CONT, KA, KA/ISP-1, KA/LCS, KA/FUM and KA/GW4869 indicate untreated slices, kainate-treated, kainate plus ISP-1 treated, kainate plus L-cycloserine treated, kainate plus fumonisin treated, and kainate plus GW4869 treated slices. #: significant difference compared to CONT; *: significant difference compared to KA ($P < 0.05$).

Fig. 2. 6.

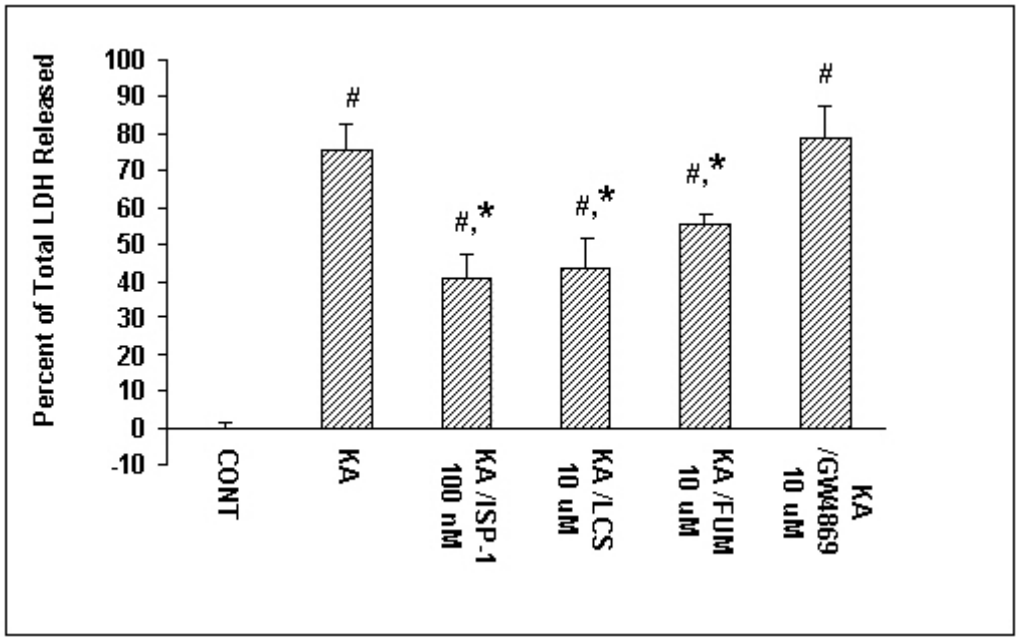
Percent of Total LDH Released
100
90
80
70
60
50
40
30
20
10
0
-10
#
#,*
#,*
#,*
#
CONT
KA
KA /ISP-1 100 nM
KA /LCS 10 uM
KA /FUM 10 uM
KA /GW4869 10 uM

Fig. 3. 1. The number of MAP2 labeled pyramidal neurons in CA field of cultured hippocampal slice. CONT, KA, 1, 5, 10 and 20 μg/ml apoD indicate untreated, kainate, and kainate plus 1, 5, 10 and 20 μg/ml final concentrations of apoD treated slices. The values are mean ± standard deviation of number of cells / mm^2 in CA field. Results were analyzed by 1-way ANOVA with Bonferroni's multiple comparison post-hoc test. $P < 0.05$ was considered significant. * Significant difference compared to CONT group; # Significant difference compared to KA group.

Fig. 3. 1.

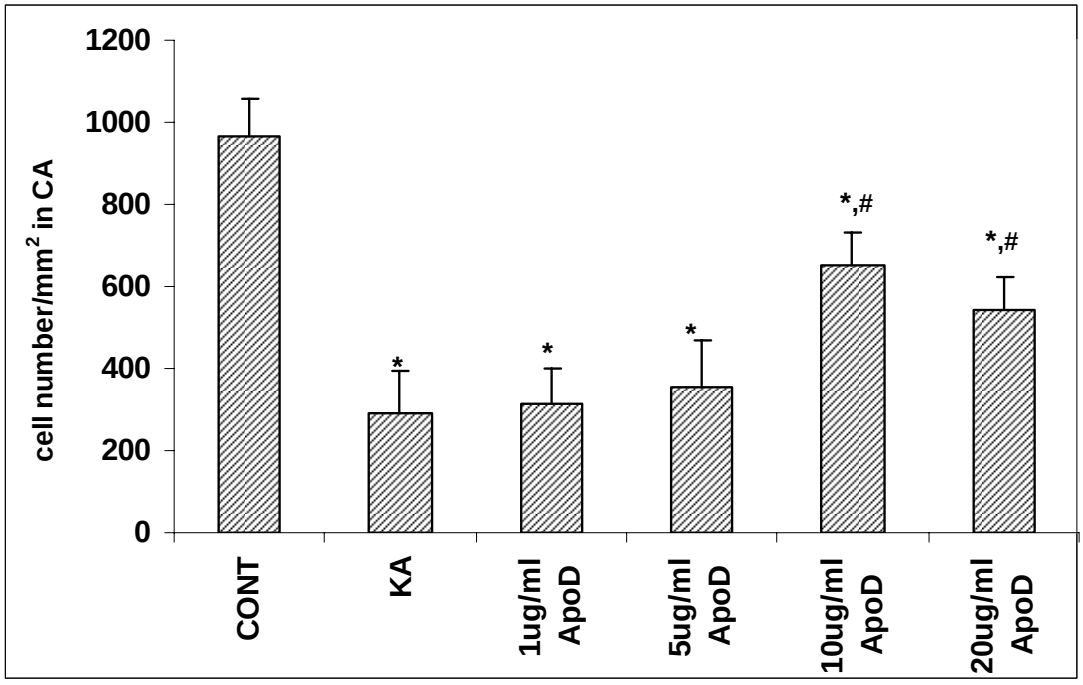
1200
1000
800
600
400
200
0
cell number/mm2 in CA
*
*
*
*,#
*,#
CONT
KA
1ug/ml ApoD
5ug/ml ApoD
10ug/ml ApoD
20ug/ml ApoD

Fig. 3. 2. A: effect of apoD on neuronal survival after addition of kainate to hippocampal slices. MAP2 immunostained sections from representative slices. Arrows indicate uninjured neurons in fields CA1 and CA3. CONT, KA and KA/apoD indicate untreated, kainate, kainate plus apoD treated slices. Scale = 300 μm. B: effect of apoD on LDH release in hippocampal slice cultures. CONT, KA and KA/apoD indicate untreated, kainate, and kainate plus apoD treated slices. The values are mean ± standard deviation of percentage of total LDH release. Results were analyzed by 1-way ANOVA with Bonferroni's multiple comparison post-hoc test. $P < 0.05$ was considered significant. * Significant difference compared to CONT group; # Significant difference compared to KA group.

Fig 3. 2.

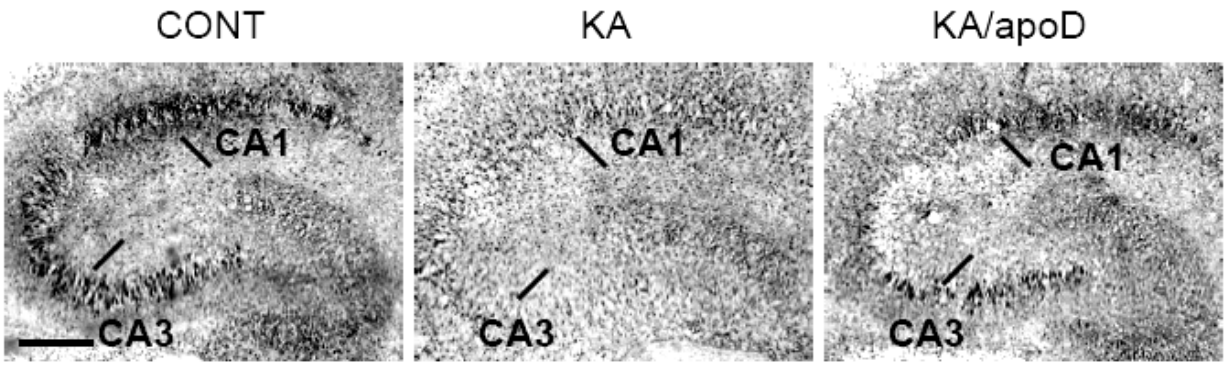
CONT
KA
KA/apoD
CA1
CA3
CA1
CA3
CA1
CA3

A

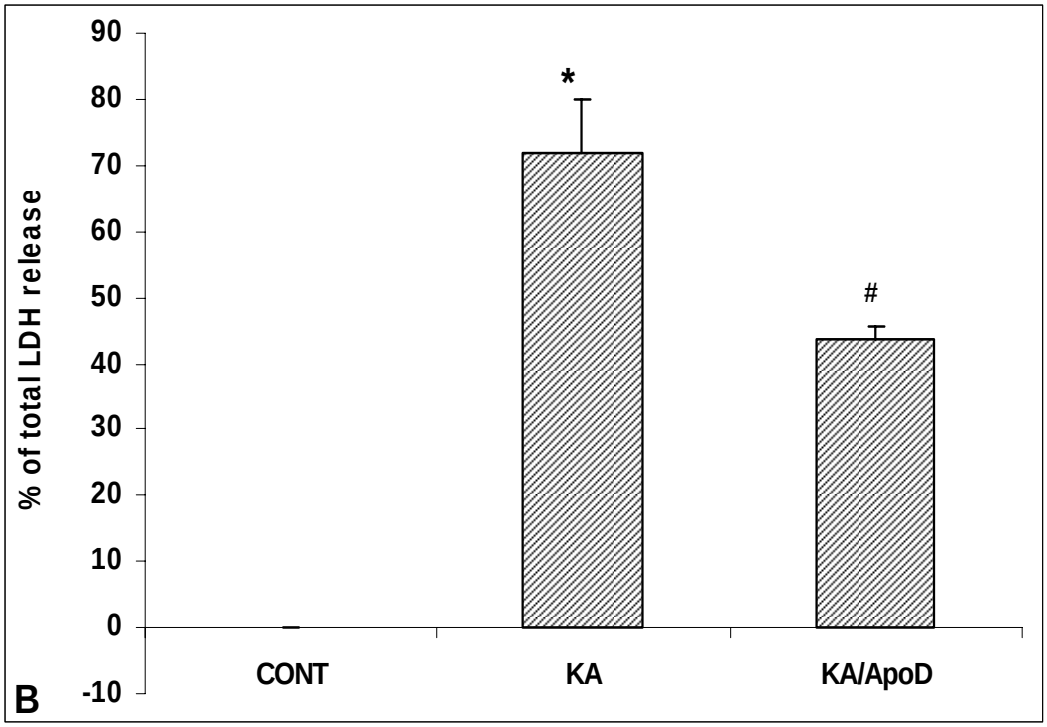
% of total LDH release
90
80
70
60
50
40
30
20
10
0
-10
*
#
CONT
KA
KA/ApoD
B

Fig. 3. 3. The number of MAP2 labeled pyramidal neurons in CA field of cultured hippocampal slice. CONT, KA, apoD, BLG and apoD/Ab indicate untreated, kainate, kainate plus apoD, kainate plus beta-lactoglobulin, kainate plus apoD and antibody to apoD treated slices. The values are mean ± standard deviation of number of cells / mm^2 in CA field. Results were analyzed by 1-way ANOVA with Bonferroni's multiple comparison post-hoc test. $P < 0.05$ was considered significant.

Fig. 3. 3.

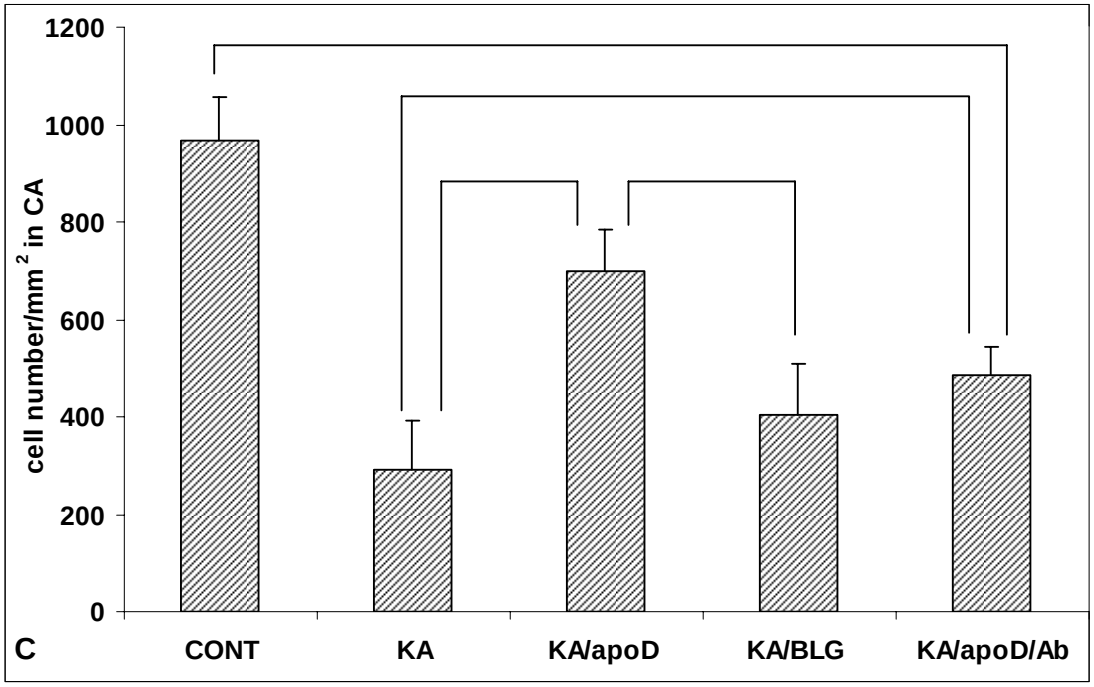
1200
1000
800
600
400
200
0
cell number/mm 2 in CA
C
CONT
KA
KA/apoD
KA/BLG
KA/apoD/Ab

Fig. 3. 4. Effect of apoD on F_2-isoprostanes (A), cholesterol (B), 7-ketocholesterol (C) and 24-hydroxycholesterol (D) levels in cultured hippocampal slices. CONT, KA and KA/apoD indicate untreated, kainate, and kainate plus apoD treated slices. Data was normalized to the weight of the slices and expressed as mean ± standard deviation of 3 experiments (12-16 slices were used in each treatment group per experiment). Results were analyzed by 1-way ANOVA with Bonferroni's multiple comparison post-hoc test. $P < 0.05$ was considered significant. * Significant difference compared to CONT group; # Significant difference compared to KA group.

Fig. 3. 4.

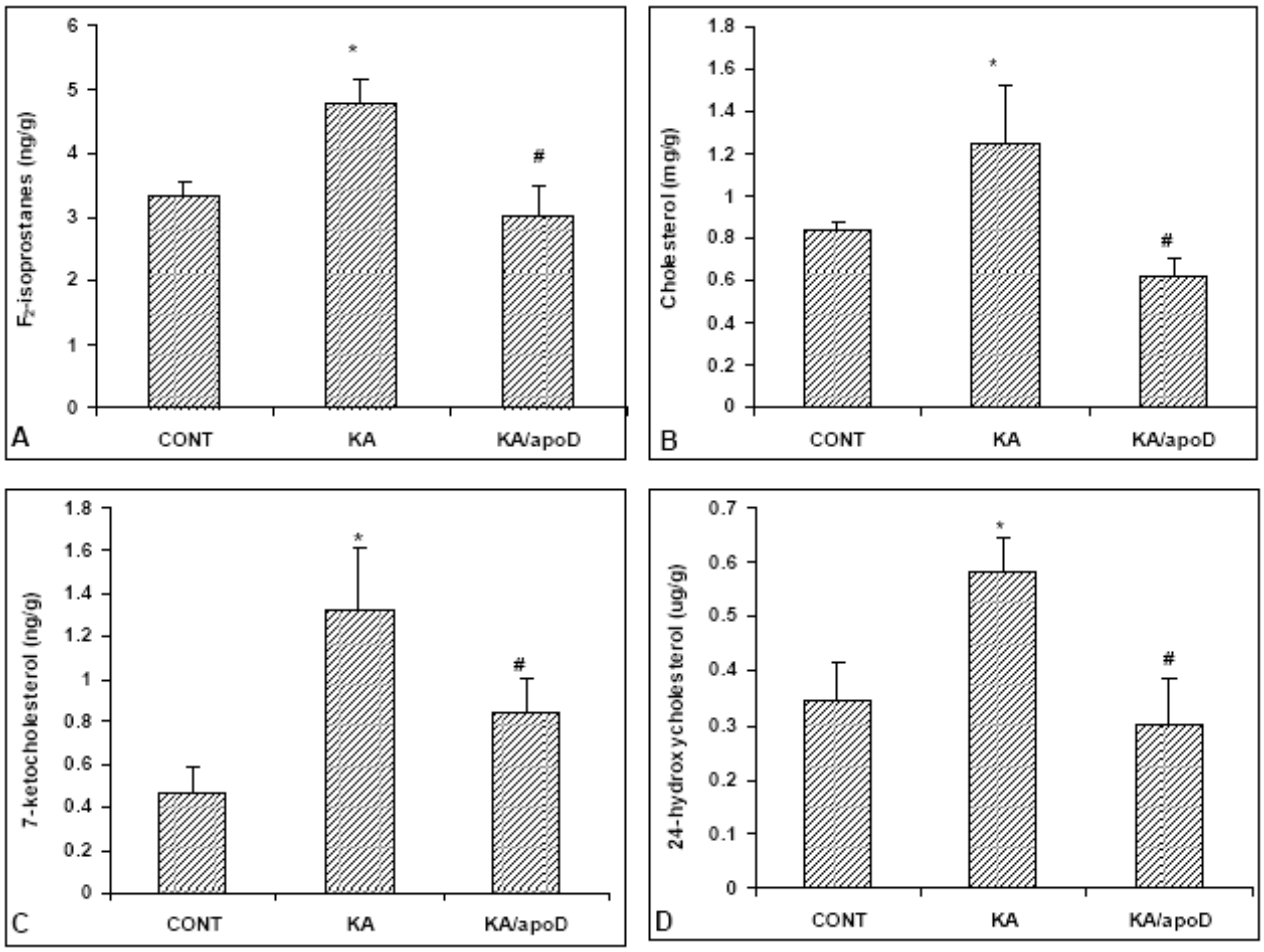
A
F2-isoprostanes (ng/g)
0
1
2
3
4
5
6
*
#
CONT
KA
KA/apoD
B
Cholesterol (mg/g)
0
0.2
0.4
0.6
0.8
1
1.2
1.4
1.6
1.8
*
#
CONT
KA
KA/apoD
C
7-ketocholesterol (ng/g)
0
0.2
0.4
0.6
0.8
1
1.2
1.4
1.6
1.8
*
#
CONT
KA
KA/apoD
D
24-hydroxycholesterol (ug/g)
0
0.1
0.2
0.3
0.4
0.5
0.6
0.7
*
#
CONT
KA
KA/apoD

Fig. 3. 5. Effect of hydrogen peroxide on F_2-isoprostanes (A), cholesterol (B), 7-ketocholesterol (C) and 24-hydroxycholesterol (D) levels in cultured fibroblasts from wild type and apoD knockout mice. CONT, WT and apoD KO indicate untreated control, cultured fibroblasts from wild type and apoD knockout mice. Data are expressed as mean ± standard error of concentrations per 1 x 10^6 cells. Results were analyzed by Student's t-test, $P < 0.05$ was considered significant. * Significant difference compared to WT group.

Fig. 3. 5.

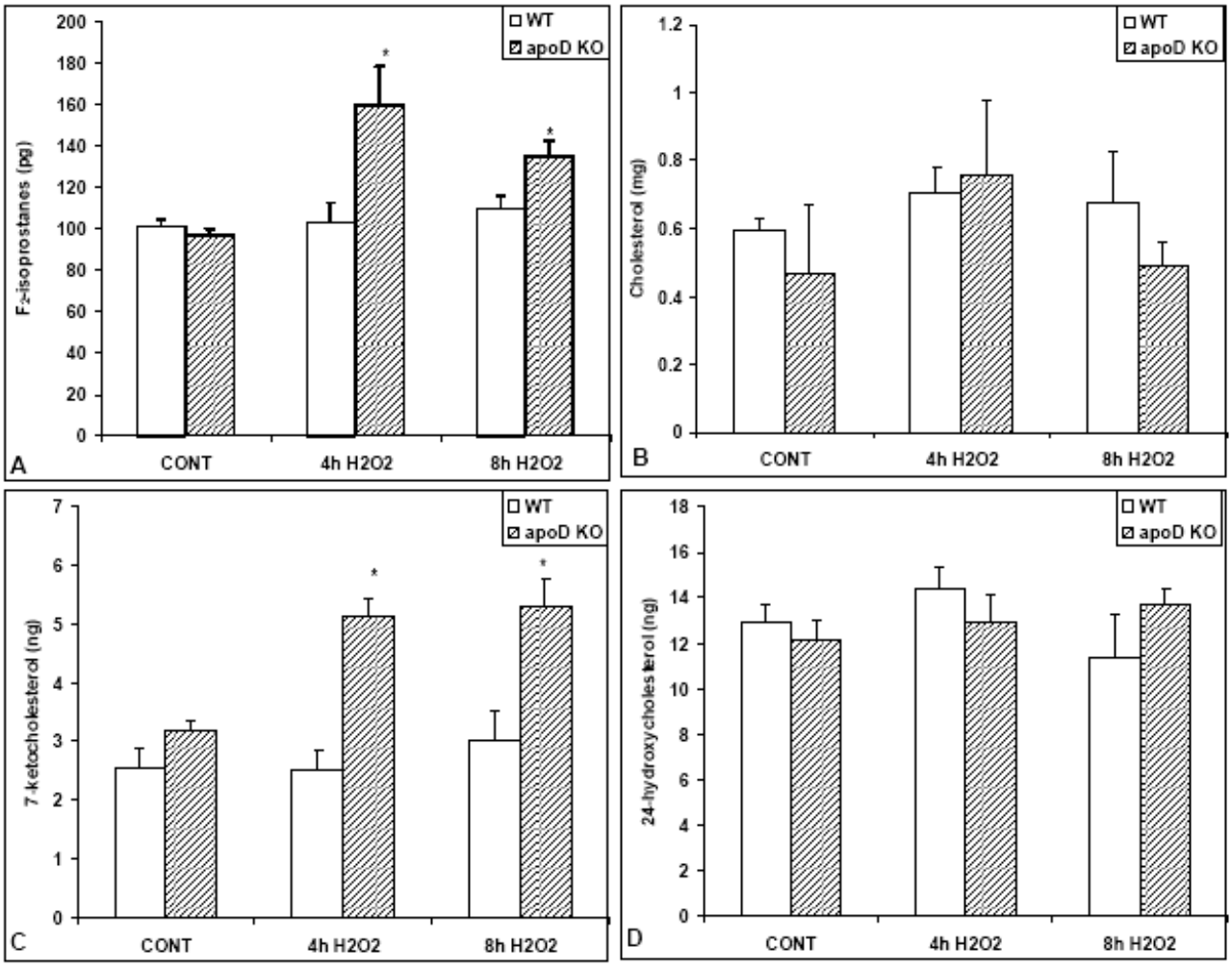
WT
apoD KO
F2-isoprostanes (pg)
A
CONT
4h H2O2
8h H2O2
Cholesterol (mg)
B
7-ketocholesterol (ng)
C
24-hydroxycholesterol (ng)
D